Progress in Energy and Combustion Science 87 (2021) 100953

Contents lists available at ScienceDirect

Progress in Energy and Combustion Science

journal homepage: www.elsevier.com/locate/pecs

Lithium Plating Mechanism, Detection, and Mitigation in Lithium-Ion Batteries

Xianke Lin [1,*], Kavian Khosravinia [1], Xiaosong Hu [2,*], Ju Li [3], Wei Lu [4]

[1] Department of Automotive and Mechatronics Engineering, Ontario Tech University, Oshawa, ON L1G 0C5, Canada
[2] State Key Laboratory of Mechanical Transmissions, Department of Automotive Engineering, Chongqing University, China
[3] Department of Nuclear Science and Engineering and Department of Materials Science and Engineering, MIT, Cambridge, MA 02139, USA
[4] Department of Mechanical Engineering and Department of Materials Science and Engineering, University of Michigan, Ann Arbor, MI 48109, USA

ARTICLE INFO

Keywords:
Lithium-ion battery
Degradation mechanisms
Lithium plating
Lithium plating mechanisms
Lithium plating detection and prevention
Fast charging strategies

ABSTRACT

The success of electric vehicles depends largely on energy storage systems. Lithium-ion batteries have many important properties to meet a wide range of requirements, especially for the development of electric mobility. However, there are still many issues facing lithium-ion batteries. One of the issues is the deposition of metallic lithium on the anode graphite surface under fast charging or low-temperature conditions. Lithium plating reduces the battery life drastically and limits the fast-charging capability. In severe cases, lithium plating forms lithium dendrite, which penetrates the separator and causes internal short. Significant research efforts have been made over the last two decades to understand the lithium plating mechanisms. However, the lithium plating mechanisms have not yet been fully elucidated. Meanwhile, another challenge in the development of fast charging technologies is to identify degradation mechanisms in real-time. This includes real-time detection of lithium plating while the battery is being charged. Accurate detection and prediction of lithium plating are critical for fast charging technologies. Many approaches have been proposed to mitigate lithium plating, such as adopting advanced material components and introducing hybrid and optimized charging protocols. Nevertheless, most detection techniques and mitigation strategies are only used for fundamental research with limited possibilities in large-scale applications. To date, there is still a lack of a comprehensive review of lithium plating, reflecting state of the art and elucidating potential future research directions. Therefore, in this article, we provide a snapshot of recent advances in lithium plating research in terms of mechanism, detection, and mitigation to fill this gap and incentivize more innovative thoughts and techniques. In the present study, the mechanisms of lithium plating and approaches used to characterize and detect it in different applications are carefully reviewed. This review also provides a summary of recent advances in model-based approaches to predict lithium plating. Based on the gathered information, the advantages and drawbacks of each model are compared. The mitigation strategies for suppressing lithium plating at different levels are studied. Finally, we highlighted some of the remaining technical challenges and potential solutions for future advancement.

Abbreviations: AU, Aluminum; BC, Boost charging; BMS, Battery management system; CC, Constant-current; CC-CV, Constant-current constant-voltage; CE, Coulombic efficiency; CPCV, Constant power constant voltage; C-rate, Current rate; DAE, Differential algebraic equation; DM, Degradation mode; DMC, Dimethyl carbonate; DOCV, Differential open-cell voltage; DV, Differential Voltage; DP, Dynamic Programming; EC, Electrochemical; ECM, Equivalent circuit model; EIS, electrochemical impedance spectroscopy; EPR, Electron paramagnetic resonance; EV, Electric vehicle; FTIR, Fourier transform infrared spectroscopy; GA, Genetic algorithm; GHG, Greenhouse gas; GPC, Generalized predictive control; IC, Incremental capacity; LAM, Loss of active materials; LCO, Lithium Cobalt Oxide; LFP, Lithium Iron Phosphate Battery; LiB, Lithium-ion battery; LLI, Loss of lithium inventory; LSTM, Long short-term memory; MCMB, Meso-carbon microbeads; ML, Machine learning; MPC, Model predictive control; MSCC, Multistage constant current; NMC, Lithium Nickel Cobalt Manganese Oxide; NMR, Nuclear magnetic response spectroscopy; OCV, Open circuit voltage; P2D, Pseudo-two-dimensional; PC, Pulse charging; PEV, Plug-in electric vehicle; RE, Reference electrode; ROM, Reduced-order model; SEM, Scanning electron microscopy; SEI, Solid electrolyte interphase; SOC, State of charge; SOH, State of health; STM, Scanning tunneling microscopy; TEM, Transmission electron microscopy; TOF, Time of flight; XFC, Extreme fast charging; XRD, X-ray diffraction; XPS, X-ray photoelectron spectroscopy.

* Corresponding authors.
E-mail addresses: xiankelin@ieee.org (X. Lin), xiaosonghu@ieee.org (X. Hu).

https://doi.org/10.1016/j.pecs.2021.100953
Received 30 September 2020; Received in revised form 24 July 2021; Accepted 26 July 2021
Available online 5 August 2021

1. Introduction

The transportation sector is one of the largest contributors to global greenhouse gas (GHG) emissions [1–3]. The negative effect of GHG on human life and the environment provides a strong driving force for reducing GHG emissions [4]. Transportation electrification is a promising solution to alleviate the growing concern about GHG emissions. More and more electric vehicles (EVs), hybrid electric vehicles (HEVs), and plug-in hybrid electric vehicles (PHEVs) have been developed and deployed as alternatives to traditional internal combustion engine (ICE) vehicles [4–6]. The success of transportation electrification depends largely on energy storage systems. As one of the most promising energy storage systems, lithium-ion batteries (LiBs) have many important properties to meet the wide range of requirements of electric mobility [7,8]. The challenging requirements for further development of the LiB system are longer life, fast charging, low-temperature charging, self-recovery capability, and safety performance. In fact, according to the literature, these requirements are related to the aging mechanisms of lithium plating and anode kinetics. Precise diagnosis, prognosis and understanding of the mechanisms and effects of lithium plating on the performance of cells and battery packs are critical to the optimal design and safe operation of LiB systems. However, due to the complex, nonlinear, and path-dependent nature of battery degradation [9,10], the aging mechanisms are not fully understood. As a result, as shown in Fig. 1, lithium plating has been the subject of several levels of research, ranging from understanding the mechanism of lithium plating to demonstrate why, where, when, and under what conditions this phenomenon occurs, to determining the most effective method to detect, predict, and prevent it. Therefore, the purpose of this article is to review the existing work in the literature and identify some of the fundamental knowledge gaps at each of these levels.

A typical lithium-ion battery cell, as shown in Fig. 2 (A), comprises a composite negative electrode, separator, electrolyte, composite positive electrode, and current collectors [11,12]. The composite negative electrode has a layered and planner crystal structure that is placed on the copper foil, which functions as a current collector. There are three types of carbonaceous materials: graphite, graphitizable carbon, and non-graphitizable carbon (hard carbon) [11,13]. Graphite is frequently used as a negative electrode because of its excellent performance, low cost, and non-toxicity [14]. The composite positive electrode (cathode) is a metal-oxide with a tunneled or layered structure that is coated with aluminum foil [15]. Aluminum acts as a current collector. The electrolyte plays a critical role in the lithium-ion diffusion process. The electrolyte allows lithium ions to move between electrodes [13,16]. The separator is a piece of thin microporous polymer film (10 to 30 μm) soaked in the electrolyte and sandwiched between the anode and cathode electrodes to prevent shorting of the two electrodes [11].

During the normal charging process, electrons are extracted from the cathode and moved to the anode through the external circuit by the charger. Meanwhile, Li^+ions are de-intercalated from the cathode and moved to the anode through electrolyte [14]. During discharge, the entire procedure is reversed. The lithium-ion intercalation process (during charging) has three major steps [17]: (i) the Li^+ions diffuse out of the cathode, (ii) the diffusion of solvated Li^+ions in the electrolyte, (iii) de-solvation Li^+ ions pass through the SEI and intercalate into the interlayer of graphite [18–20]. Step (iii), generally known as the charge-transfer process, is broken into three subprocesses [21,22]: 1) de-solvation of solvated Li^+ions (strip off their solvation shell), 2) naked Li^+passing through the SEI, and 3) solid-state lithium diffusion into graphite (Li^+ reaching the anode and receiving an electron, which could occur at the anode-SEI interface or the anode-electronic conductor-SEI interface [18]) (Fig. 2 (C)). These steps would be favored in an ideal battery working condition. Nonetheless, in real-world applications, LiBs are subjected to a variety of severe working conditions, which have a substantial impact on battery performance and longevity.

Battery degradation is a complicated issue involving numerous physical and chemical processes. Degradation is dependent on a number of complex mechanisms caused by a variety of factors (e.g., intrinsic and extrinsic) [23,24]. Intrinsic factors are classified into two categories: material properties and manufacturing procedures [25]. Extrinsic factors derive from the LiB operating conditions, such as charging at a high C-rate, high state of charge (SOC), or low temperature [23,24]. As shown in Fig. 3, the aging mechanisms affect not only the anode and cathode electrodes, but also other LiB components such as electrolyte, separator, binder, and current collector [25–27]. The most detrimental aging mechanisms impacting graphite anode electrodes are solid electrolyte interphase (SEI) film growth, binder decomposition, and lithium plating [28–30]. According to the literature, aging mechanisms can be divided into three main degradation modes (DMs): loss of lithium inventory (LLI), loss of active materials (LAM) [31], and loss of electrolyte [25,32]. In LLI, lithium ions are consumed by side reactions, such as SEI film formation and irreversible plating [33]. Since these lithium ions are

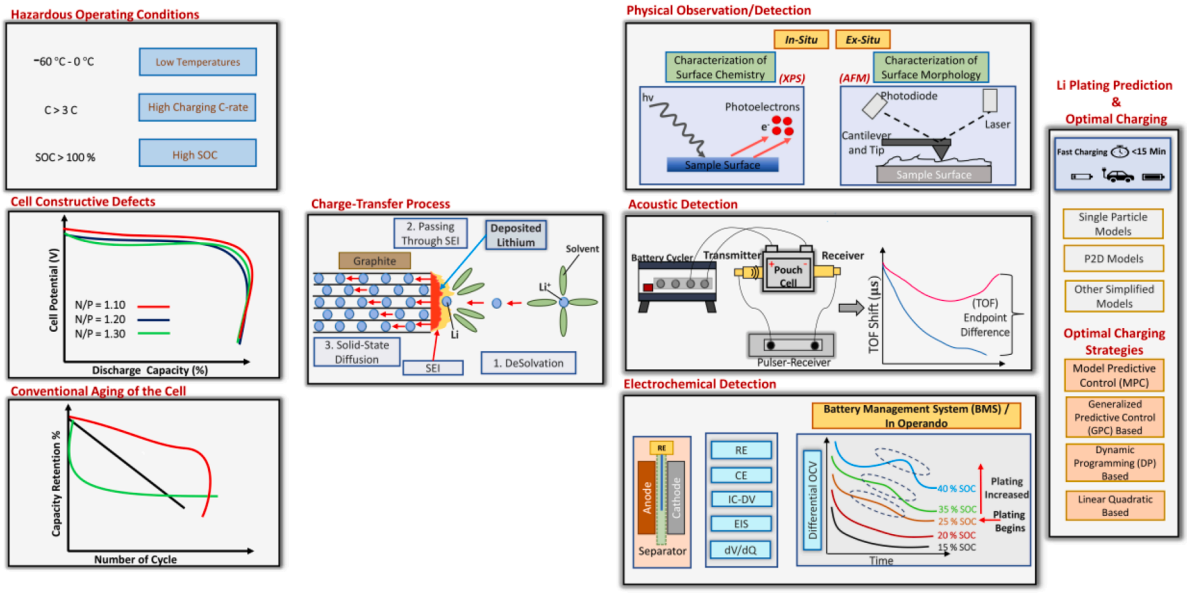

Figure 1. Lithium Plating Phenomena at Different Research Levels.

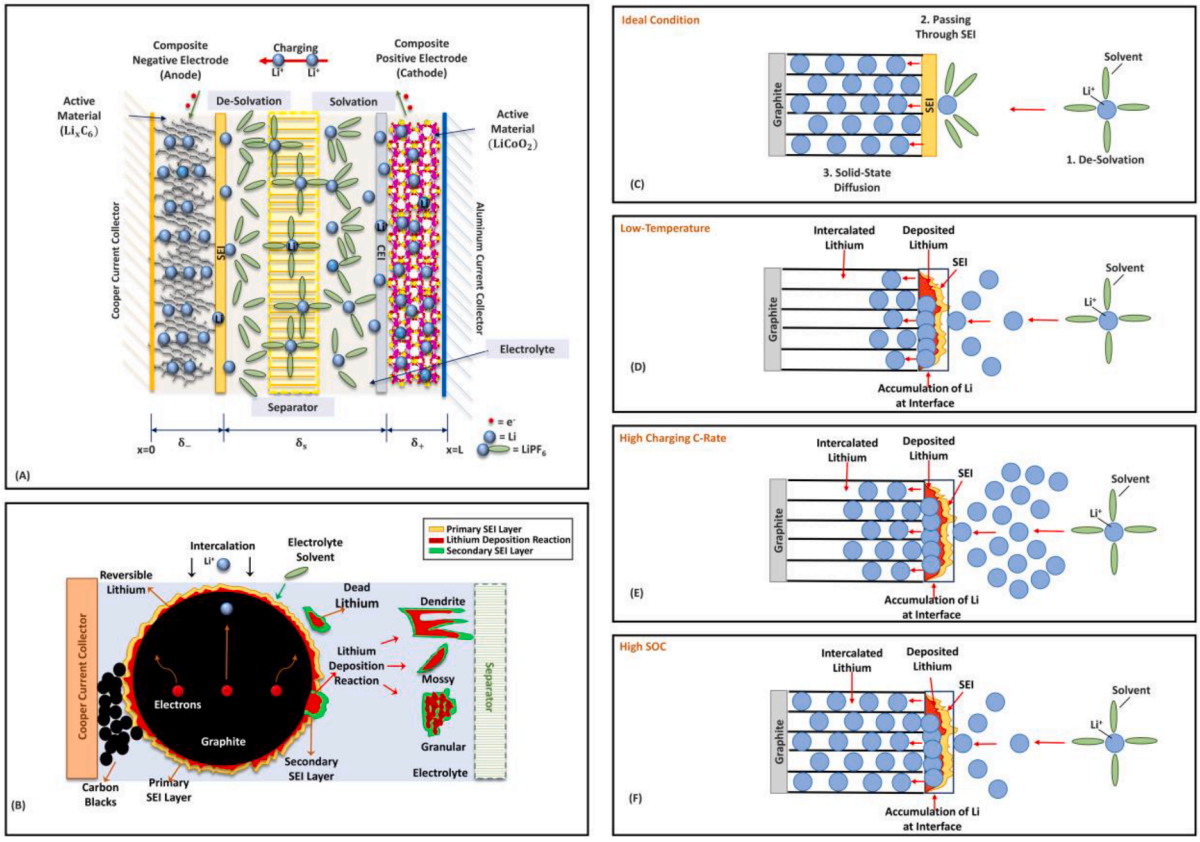

Figure 2. Schematic of a Battery Cell During Charging Process and Lithium Plating Behavior under Different Operational Conditions.
(**A**) In the intercalation/de-intercalation process, Li-ions intercalate into or de-intercalate from the active material between the two electrodes in a reversible manner. (**B**) Schematic of lithium plating-stripping on the graphite anode electrode. The primary SEI layer (yellow color) is formed at the anode surface during the first charge of the cell to protect the electrode. Because the primary SEI layer prevents electrons from making direct contact with the electrolyte, metallic lithium (red color) is deposited between the primary SEI layer and graphite particles. Mossy and dendritic deposition are two well-known morphologies of deposited lithium. When deposited lithium reacts with electrolyte solutions, the secondary SEI layer (green color) forms. (**C**) Under ideal conditions, the charge-transfer process consists of three steps: 1. de-solvation of solvated Li^+ions, 2. Li^+ions pass through the SEI, and 3. solid-state lithium diffusion into graphite particles. (**D**) At low temperature, Li^+ ions move slowly in graphite due to the low diffusivities of lithium ions and the sluggish charge transfer kinetics, resulting in lithium plating. (**E**) At high charging C-rate, Li^+ ions move fast and a large amount of Li^+ ions accumulate at the electrode interface due to the slow lithium solid diffusion, and lithium plating occurs. (**F**) Under high SOC conditions, Li^+ ions could accumulate at the surface due to fewer available sites in graphite under high SOC conditions.

no longer cyclable for the intercalation process, the cell capacity is reduced (capacity fade) [34,35]. LAM, on the other hand, is usually related with structural changes and material loss [23]. The active mass on the anode is reduced due to graphite exfoliation, electrode particle cracking, or dead lithium blocking the active site pathway. Furthermore, the active mass of the cathode is reduced due to transition metal dissolution, structural disordering, and electrode particle cracking [27,34,36,37]. The other significant cause of degradation is electrolyte loss; the deposited lithium on the anode interface reacts with the electrolyte, consuming the electrolyte [16,32]. The significant reduction in electrolyte content may result in capacity and power fading at the end of the battery's life.

Among the several aging mechanisms in LiBs, one of the most detrimental is the deposition of metallic lithium or lithium plating on the graphite anode surface. This is due to the fact that lithium plating may not only promote further degradation, but it may also have a negative impact on the safety of LiBs [38]. During fast charging, lithium-ions can be deposited on the surface of the graphite anode rather than being intercalated into the interstitial space between the graphite anode's atomic layers [39]. In general, the deposited lithium can be reversible or irreversible. The irreversible portion can react with the electrolyte to form a secondary SEI layer, or it can form a high-impedance "dead" lithium film that is electrically isolated from the graphite anode and remains irreversible, increasing internal resistance and decreasing energy density [29,40]. The irreversible portion causes capacity fade to be accelerated. In severe cases, the accumulated lithium might also form a dendrite. Dendrites can develop and pierce the separator [41]. The reversible portion describes the deposited lithium with an electrical contact on the anode interface, which can undergo charge transfer reaction into the electrolyte and subsequently re-intercalate into the anode, this process is known as lithium stripping. The stripping process occurs throughout the rest or discharge process following lithium plating [42,43]. One of the major limiting factors for fast charging is lithium plating. As a result, one of the major difficulties of fast charging technologies is to prevent or mitigate lithium plating during the charging process.

Several studies have been conducted, including investigations into lithium plating mechanisms at various charging conditions, the development of effective detection techniques, and the development of strategies for mitigating lithium plating. Fig. 4 (A) and (B) outline the various charging currents (C-rates), testing temperatures, and commercial cell types used in the literature to study lithium plating. The C-rate is the current value that discharges a battery within 1 h from a fully charged state to a fully discharged state [44]. It is generally known in battery testing as a current value equal to a cell's rated capacity (Ah). The test temperature varies from study to study and might range from -60 °C to 80 °C. According to our findings, the majority of the studies tested the cells at room temperature (25 °C) at 1 C. Some studies at

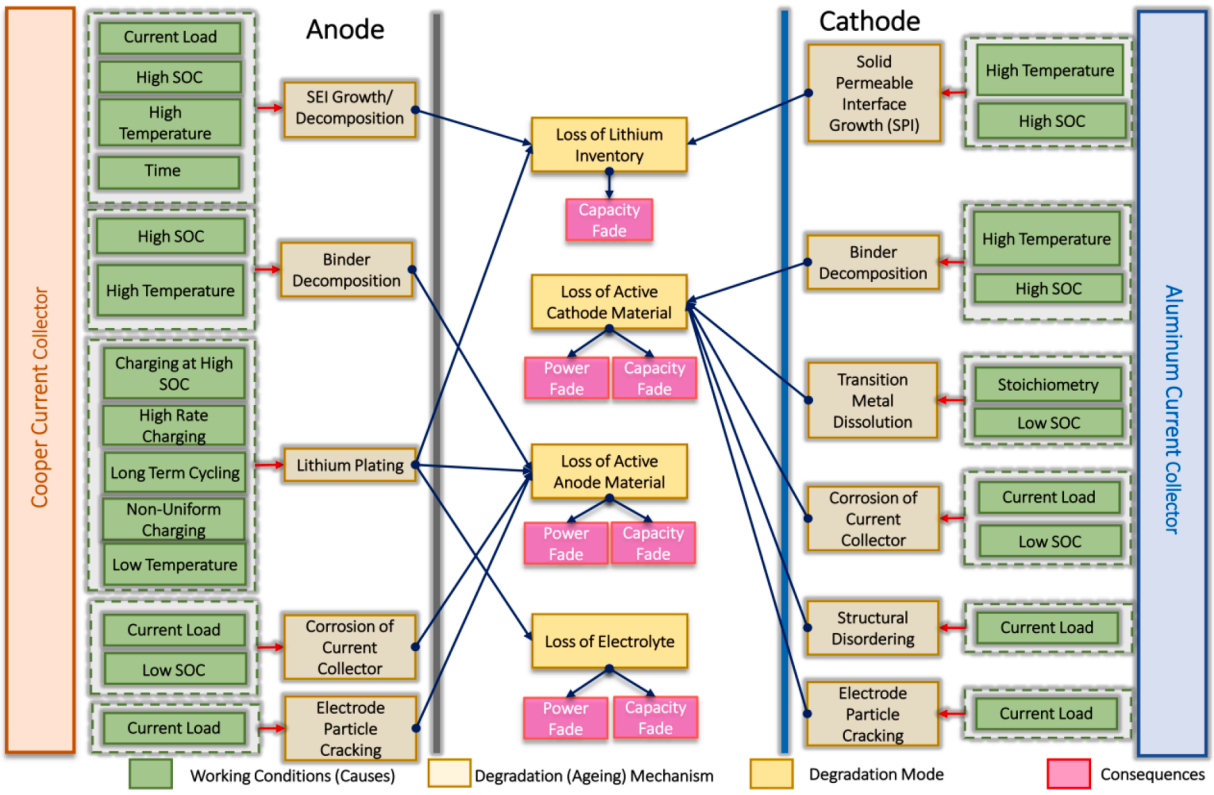

Figure 3. Degradation Modes, Aging Mechanisms and the Affected Components in Lithium-ion Batteries.
There are many different aging mechanisms, and they are generally divided into three different degradation modes (DMs): loss of lithium inventory (LLI), loss of active material (LAM) and loss of electrolyte. There is a general relationship between battery working conditions and the affected components with the corresponding aging mechanisms. Charging the battery at a high C-rate, a high state of charge (SOC), or at a low temperature can accelerate battery degradation [34].

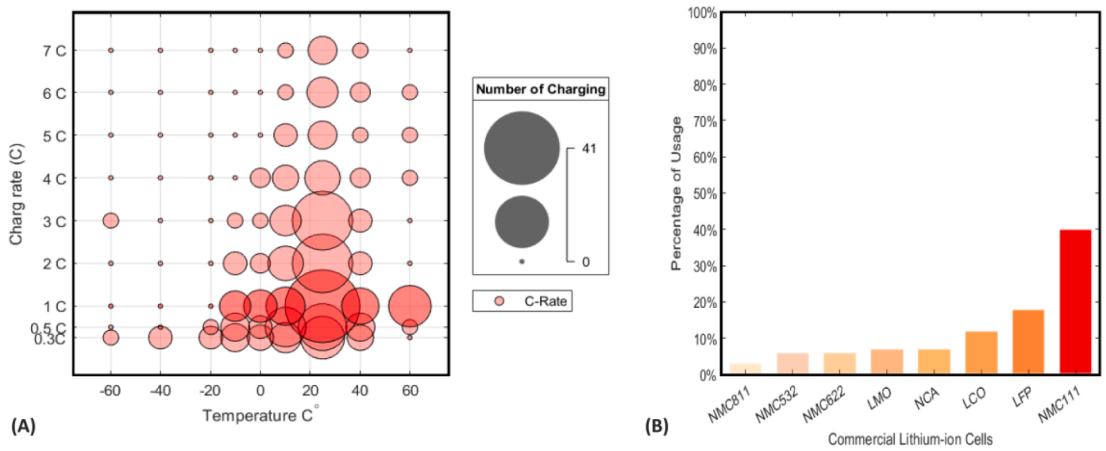

Figure 4. Lithium Plating C-rates/ Temperature Summary. (A) Analyzing the existing literature on lithium plating based on two common testing conditions: temperature and C-rate. Larger dots represent a greater number of publications that used the C-rate and temperature at those dots. (B) Commercial lithium-ion batteries cells that have been used for lithium plating studies in the literature.

higher C-rates and lower temperatures have also been conducted.

Several studies investigated lithium plating at lower charging rates (0.3 and 0.5 C-rate) and temperature ranges from (-20 °C to 40 °C). However, further research on lithium plating at lower temperatures and greater C-rates is still necessary. Various types of commercial cells were employed in the literature to study lithium plating, ranging from 18650 and 26650 types (1.5 Ah to 3.4 Ah) to large-scale pouch types (9.5 Ah to 16 Ah). In the literature, various battery cells are used for investigating lithium plating. Most of them use graphite as the anode and use different cathode materials, such as lithium nickel cobalt manganese oxide (NMC 111), lithium iron phosphate (LFP), and lithium cobalt oxide (LCO).

The overarching goal of this paper is to provide a timely, comprehensive review of the latest progress of lithium plating in the existing literature, to gain a better understanding of lithium plating. Since graphite has been widely used as the anode in commercial LiBs, this work is focused on studying lithium plating in batteries that use graphite as the anode. The most recent studies on lithium plating on graphite anode are thoroughly reviewed. The mechanisms of lithium plating and the chemical reactions that contribute to lithium plating under various conditions are discussed. Recent approaches for detecting lithium

plating are thoroughly explored and compared. Each detection method's applicability is also investigated. The existing electrochemical models used to simulate cell behavior in order to predict lithium plating are studied and explained. Additionally, optimal and common charging protocols are introduced. In conclusion, based on the literature, research gaps are identified, and suggestions for future research directions are provided.

2. Lithium Plating Reactions

Lithium plating is a parasitic process that goes along with the lithium intercalation process. Equation (1) shows the complete insertion of Li^+ions into the graphite anode electrode. Intercalation is a diffusion-limited process, meaning that a certain amount of Li^+ions can be embedded into the interlayer of graphite per unit time at a given temperature [37]. The potential range for Li^+ions insertion inside the graphite is 65-200 mV vs. Li^+/Li [29]. Equation (2) shows partial or full deposition of lithium on the anode surface. The charging current is divided into two parts: (i) intercalation current and (ii) lithium plating current [38]. Ideally, the charging current affects the pace at which Li^+ions are coming to the anode surface. However, there is a competition between the intercalation current and the lithium plating current. As the charging process continues, the vacancy sites in the graphite layer will decrease, and therefore the intercalation current is decreased while the lithium plating current is increased [19]. When the anode potential drops below 0 V, lithium plating is thermodynamically permitted and the rate of lithium deposition exceeds the rate of intercalation. The main contributors to the graphite electrode overpotential are i) charge transfer, ii) electrolyte concentration (mass transfer), and iii) lithium solid-phase in the negative electrode [39]. These are the kinetics cause for lithium plating. When the local potential at the negative electrode falls below 0 V (vs. Li^+/Li) due to high SOC, high charging C-rate, and low temperatures, all of which polarize the electrode, lithium plating can occur thermodynamically [7,45]. However, because the reaction enthalpy is more positive, lithium plating is not as favorable as intercalation from a thermodynamic standpoint. Kinetic arguments alone are insufficient to explain lithium plating. It should be noted that LiB charging is a dynamic process that is not in equilibrium, especially at high C-rates. In thermodynamic equilibrium, the cell voltage can be determined by the Nernst equation [40,41]. The equilibrium potential difference can be used as an indicator of the thermodynamic driving force of plating vs. intercalation, as plating and intercalation compete for electrons and lithium-ions [42]. The equilibrium electrode potential shifts with temperature, for both lithium plating and graphite intercalation. This temperature variation leads to a heterogeneous distribution of the equilibrium potential on the anode [41]. The heterogeneous equilibrium electrode potential leads to heterogeneous lithium plating [42]. It should be noted that the plated lithium will react with electrolyte and consume electrolyte, and due to the heterogeneity on the graphite electrode, lithium electroplating may occur locally [43].

$$x\mathrm{Li}^+ + \mathrm{Li}_\delta\mathrm{C}_6 + x\mathrm{e}^- \rightarrow \mathrm{Li}_{x+\delta}\mathrm{C}_6 \quad (1)$$

$$(1-X)\mathrm{Li}^+ + (1-X)\mathrm{e}^- \rightarrow (1-X)\mathrm{Li} \quad (2)$$

Lithium plating has three different outcomes, which are dead lithium, reversible lithium, and secondary SEI film, as shown in Fig. 2 (B) [46]. A portion of deposited lithium with lost electrical contact with the graphite is referred to as dead lithium [20]. Dead lithium may create a tortuous pathway for lithium-ion transport, reducing the active area for intercalation [46]. The secondary SEI film is the result of a reduction of solvent electrolyte (R) by the deposited lithium (Equation (4)). Both dead lithium and SEI film are irreversible [47] and lead to reduced lithium from the system and capacity loss over time [17]. Reversible lithium returns back to the system in the lithium stripping process (Equation (5)) during relaxation or resting time (Equation (3)) [48]. During relaxation, the reinsertion continues until all the reversible lithium is inserted into the anode. The lithium stripping process is an easier reaction than lithium deintercalation (Equation (3)). However, the reversible lithium in the lithium stripping process during discharge has two destinations, the intercalation into the graphite and transfer to the cathode to deliver output current [48].

$$\varepsilon\mathrm{Li} + \mathrm{Li}_{\delta+x}\mathrm{C}_6 \rightarrow \mathrm{Li}_{\delta+x+\varepsilon}\mathrm{C}_6 \quad (3)$$

$$\mathrm{R} + \mathrm{Li} \rightarrow \mathrm{R}-\mathrm{Li} \quad (4)$$

$$\mathrm{Li} \rightarrow \mathrm{Li}^+ + \mathrm{e}^- \quad (5)$$

Based on the working and charging conditions, the morphology of deposited lithium are different, which can be classified into three types, including mossy, granular (particle-like), and dendritic (needle-like deposits) [7,47]. Morphology is determined by the current rate. Mossy and granular lithium form at low current rates, whereas dendrites form at high current rates [49]. Dendritic growth can be particularly destructive to the cell because it can penetrate the separator and reach the cathode electrode, causing an internal short-circuit and rapid heating of the cell. The generated heat may first melt dendrite and disconnect the short, and later it may trigger other aging mechanisms, such as SEI formation and electrolyte decomposition [17,50]. In terms of safety, the dendritic structure is considerably less safe than the mossy and granular lithium forms. Internal short circuits can be classified into two types, soft shorts and hard shorts [20]. Soft shorts normally disappear after discharge and do not cause cells to fail catastrophically. A soft short may reduce the cell's current and voltage while simultaneously increasing the local temperature [51,52]. The heat generated by the soft short can cause an exothermic reaction with the electrolyte, causing the separator to melt. Hard shorts are characterized by slightly larger short circuit currents between the anode and the cathode due to their low resistance [52]. Due to a higher increase in local temperature, hard shorts are also more likely to contribute to thermal runaway [52]. It should be noted that lithium plating is a result of the actual operating conditions, poorly balanced cell, material properties, electrode design, and cell design [45].

3. Main Factors Affecting Lithium Plating

Many research efforts have been undertaken to understand how, where and why lithium plating occurs during both normal and fast charging conditions. However, the mechanisms of lithium plating have not been fully elucidated due to its complex nature [53]. According to numerous previous researches, lithium plating occurs as a result of three major factors, which include but are not limited to: (i) hazardous operating conditions, (ii) cell defects, and (iii) aging of the cell (Table 1) [54].

3.1. Hazardous Operating Conditions

Lithium plating occurs when batteries are subjected to harsh conditions, such as charging at high C-rates, charging at a high state of charge (SOC), and charging at low temperatures [55–59]. These harsh conditions can limit the charge transfer kinetics in the electrolyte and

Table 1
Factors Causing Lithium Plating

Factors	Causes and Conditions
Hazardous Operating Conditions	(a) Low temperatures (b) High charging C-rates (c) High SOCs
Cell Defects	(a) Cell properties and poor design, such as imbalanced negative to positive ratio
Aging of the Cell	(a) Leading to cell unbalance (b) Kinetic degradation (Capacity fade, energy fade, CE decrease, energy efficiency fade and resistance increase)

solid-state diffusion, causing anode potential to drop below the potential of lithium metal to make lithium plating happen [60,61]. Because hazardous operating conditions are considered to be one of the main factors affecting lithium plating, we will provide a comprehensive review of the main parameters that accelerate lithium plating under the aforementioned conditions in this section.

3.1.1. Low-Temperature Effects

Low temperature is one of the main obstacles to fast charging. Charging at high C-rates can result in a severe capacity fade. Charging a 7.5 Ah cell at 1 C-rate at 0 °C, for example, would result in a considerable capacity loss (3.6%) [59]. Generally, the power and energy densities of LiBs are reduced at low temperatures, particularly during the charging process, due to three major factors: 1. decreased ionic conductivity in the electrolyte; 2. poor solid diffusivity of lithium-ion in the electrode; 3. poor charge-transfer rate [62–64]. According to the Arrhenius equation, at low temperatures, the cell internal resistance increases due to decreasing ionic conductivity in the electrolyte; however, decreased ionic conductivity is not the main problem in low-temperature charging. Studies show that the poor Li^+diffusivity within the electrodes may be one of the main causes for lithium plating at low temperature, where lithium ions accumulate at the interface between carbon particles and electrolyte [46,47,59]. Lithium plating occurs when the surface concentration of lithium ions in the graphite particles reaches the maximum value. The other major limiting factor in low-temperature charging is sluggish charge transfer kinetics. As soon as the current is applied, a large overpotential is produced. As anode polarization increases, the anode potential falls below 0 V (vs. Li^+/Li), resulting in lithium plating, where Li^+ions accumulate at the anode interface rather than intercalation, as shown in Fig. 2 (D) [49,53]. In addition, the potential drop of the composite anode close to the separator is larger than that at other locations, indicating that the lithium plating begins on the anode close to the separator [46,54,65]. As a result, charging currents at low temperatures should be strictly controlled. The lithium deposition at low temperatures may be suppressed by applying a pre-heating strategy prior to charging the cell or by charging the cell at low rates [66]. Recently, Yang and coworkers developed a cell structure consisting of thin nickel (Ni) foils embedded within the cell. The Ni foil acts as an internal heating material, generating heat in less than 10 seconds. The structured cell can be charged to 80 % SOC without lithium plating in 15 minutes with high charging currents (3.5 C-rate) at temperatures as low as -50 °C [66]. The same group recently developed an asymmetric temperature modulation (ATM) method that charges a cell by elevating the cell temperature to 60°C during charging. They showed that lithium plating may be prevented by a short-time exposure to 60°C (10 minutes per cycle) [67]. It should be noted that, from an EV standpoint, most modern EVs have an effective thermal management system that prevents extreme operating temperatures. In addition, at low temperatures, electricity from the grid is often used to preheat the cells.

3.1.2. High Charging C-rates

Fast charging is becoming increasingly important for EVs and other types of applications. Fast charging, which is based on a high charging current (C-rate), has a significant impact on the battery's performance and cyclic life due to accelerated aging. The charging rate is more likely to exceed the intercalation rate during fast charging. At a high C-rate, the amount of Li^+ions moved from the cathode to the anode in the charge-transfer process per unit time increases [20]. Increased charging rates are often associated with higher polarization due to transport and kinetic overpotentials, making lithium plating favorable [68,69]. For example, to recharge a cell in 10 mins, a charge rate of 6 C is required. At this charge rate, Li^+ions start to accumulate at the anode surface (Fig. 2 (E)). As the high-rate charging continues, the accumulated Li^+ions result in a high concentration of Li^+ ions on the graphite surface. If the concentration at the anode surface is saturated, lithium plating occurs[16, 19]. Furthermore, because fast charging uses a high charge current, more heat is generated. Lithium plating and temperature rise are two well-known issues during the fast charging process [70].

3.1.3. High SOC

Each cell has an upper cutoff voltage predefined by the manufacturer. The failure of a battery management system (BMS) to stop charging beyond its upper cutoff voltage during the charging process is the main cause for overcharging (high SOC) of the cell. High SOC is a condition under which the LiB is already full, but the current keeps flowing to the LiB [71]. At high SOCs, as the charging continues, it is much easier for the concentration of Li^+ions on the anode surface to exceed the maximum allowable level and become saturated (Fig. 2 (F)). Lithium starts to deposit on the anode surface once the anode is saturated [19,49]. Juarez-robles et al. [72] studied the effect of high SOC on graphite/LCO 5 Ah pouch cells at the various cutoff voltages ranging from 4.2 V to 4.8 V. Cells charged beyond 4.5 V showed significant capacity fade, lithium plating, electrolyte decomposition, and volume expansion. Dendrite structures are observed in cells that were charged to 4.6 V, 4.7 V, and 4.8 V [72]. The dendrite penetrated the porous separator, resulting in a micro-internal short-circuit. Moreover, at high SOCs, the side reactions are not only limited to the anode electrode, and the decomposition of the electrolyte also occurs at the cathode electrode side.

3.2. Cell Defects

Many studies in the literature have emphasized the impact of the cell manufacturing process and cell properties on lithium plating. For example, Liu and coworkers showed that a cell with a negative to positive (N/P) ratio of 1.19 has a lower aging rate and less impedance rise than a cell with an N/P ratio of 1.06 [73]. The local cell defects can have an impact on lithium plating. For example, separator deformation (pore closure), which might occur during the cell manufacturing process or operation as a result of internal mechanical stress accumulation during charging or aging, could lead to lithium plating [74]. Furthermore, the kinetics at the material level can be characterized by the activation energy barrier. The kinetics of interfacial Li^+ion transfer is one of the important factors in charge transfer [22,49,75]. There is a correlation between the intercalation kinetics and the lithium plating behavior [20, 76]. Xu et al. [21] reported that desolvation is the most energy-consuming ($50 kJmol^{-1}$) step in the charge-transfer process while the overall activation energy barrier of the graphite/electrolyte is about ($60 - 70 kJmol^{-1}$) [77]. In another study, Yao et al. [78] found that due to the difference of the energy barrier for lithium de-solvation on the edge plane and the basal plane of graphite, the intercalation process prefers to occur at the edge plane of the graphite instead of the basal plane. It should be noted that during lithium plating, lithium-ions tend to continue deposition on the surface where lithium has been previously deposited.

3.3. Aging of the Cell

Even under normal operation conditions, lithium plating can still occur due to the aging of the cell. As mentioned earlier, the most common modes of degradation in the literature are LLI and LAM, where LAM can be further divided into four types based on the affected electrode and the degree of lithiation: loss of active material on the delithiated negative electrode (LAM_{deNE}), loss of active material on the delithiated positive electrode (LAM_{dePE}), loss of active material on the lithiated negative electrode (LAM_{liNE}), and loss of active material on the lithiated positive electrode (LAM_{liPE}) [31]. After the lithium plating occurs, the side reaction between the plated lithium and the electrolyte generates new SEI, resulting in capacity fading and increased impedance [17]. The changes in these degradation mechanisms can be used to study lithium plating. The analysis of capacity fade curve shapes will provide insight into the mechanism of aging and signs of lithium plating. These curve

shapes were classified into three types, linear capacity fade, decelerated capacity fade, and accelerated capacity fade, all of which can be expressed as a function of the number of cycles [20]. In commercial cells, generally, the batteries have a two-stage capacity fade. The capacity fade is fairly constant in the first stage, with a degradation mode related to LLI [31]. Accelerated capacity fade can be found in the second stage of degradation, usually after 500 cycles. The second stage is usually due to LAM_{deNE}. Ansean et al. [54] showed that LAM_{deNE} occurs at a pace four times faster than LLI, which causes cell imbalance and over-lithiation of the negative electrode and leads to lithium plating. They found that lithium deposition becomes irreversible at the turning point of sudden capacity loss (curve shape). The second stage usually does not occur due to changes in cell usage, but it may be a product of underlying silent degradation mechanisms from the beginning of life [54,79]. The type of silent degradation will be affected by the cell chemistry as well as its form factor (pouch and cylindrical cells). These silent degradations have a certain incubation period during which they do not cause any capacity loss [79]. Therefore, it is important to study the modes of degradation, particularly those that may lead to lithium plating. Besides the ratio of $LAM_{NE}$to the LLI, the plating threshold ($LAM_{NE,PT}$) is also a predictor of an accelerated degradation stage [80]. Cell design parameters (such as mass ratio), capacity loss, and the two degradation modes (LLI and LAM_{PE}) will affect this value. Values exceeding this threshold cause lithium plating [80]. In another study, Schuster et al. [81] found a significant decrease in capacity at moderate temperatures and charging rates due to lithium plating. They showed that the lithium plating occurred due to significantly decreased ionic kinetics of the graphite as a result of SEI growth and graphite active material loss. It should also be noted that in literature, the capacity curve is often plotted against temperature (Arrhenius plot), which is obtained from cycling experiments at various temperatures. Lithium plating leads to faster aging at lower temperatures, although without lithium plating, it typically ages faster at elevated temperatures [82].

4. Lithium Plating Detection Approaches

Detecting lithium plating in its early stages is often challenging. To understand the formation and growth of lithium plating, extensive efforts have been made in the past to characterize and observe the anode lithium plating morphology [83]. Many approaches (in-situ, ex-situ, non-destructive, and recently in-operando methods) have been proposed by researchers to investigate lithium plating mechanisms in LiBs. These detection methods are classified into three main categories: (i) physical characterization of surface morphologies, (ii) physical characterization of surface chemistry, and (iii) electrochemical methods. The first and second categories are based on physical properties of the plated lithium films, such as morphology, chemical composition, and surface chemistry, whereas the third technique is based on electrochemical reactions between the electrolyte and metal lithium [19]. These techniques enable ex-situ and in-situ investigations. To study lithium plating using ex-situ methods, post-mortem analysis is required, in which the cell is disassembled and opened with special tools, and then the desired specimen is transferred to microscopes or spectrometers for further investigation. In-situ approaches, on the other hand, require a complex spectroelectrochemical cell design [84]. In the following subsections, we have systematically classified the existing lithium plating detection approaches to highlight the technological status of this ever-evolving research field and current research gaps. Furthermore, we have classified each electrochemical approach based on its ability to be used on-board in real-time automotive applications. We briefly review the post-mortem analysis steps, including cell disassembly, specimen processing, and specimen analysis, as this is the basic procedure for the majority of the ex-situ approaches.

4.1. Post-Mortem Analysis for Lithium Plating Study

In literature, methodologies or procedures for post-mortem analysis of lithium plating have not been clearly explained. Research groups mainly carried out the procedures based on their own expertise and experiences [85,86]. Therefore, we provide a snapshot of the detailed steps for the disassembly process and post-mortem analysis (Fig. 4). The first stage, as illustrated in Fig. 5 (A), is to deep-discharge the cell (end of the discharge voltage 0 V) to reduce the potential risk of the short circuit during the cell opening process [87–89]. After that, since the electrode sample surfaces are reactive to the atmospheric gases (H_2OandO_2), the cell should be transferred to the controlled environment to decrease the risk of surface contamination during the disassembly process. In general, two types of controlled environments are used for this procedure: argon-filled glove boxes and fume hoods (Fig. 5 (B)). The choice of either option is dependent on the cell design and the goal of the investigation [86]. Choosing an appropriately controlled environment is not only important for safety, but it can also have an impact on the experimental outcomes [86]. The entire disassembling procedure takes place in a controlled environment. To avoid sample contamination, the H_2OandO_2 levels in the argon-filled glove box should be between 0.1 ppm and 10 ppm [87,90,91]. If the samples do not need to be protected from atmospheric gases, the disassembly procedure can be carried out in a fume hood. To avoid inhaling dangerous gases, the fume hood should evacuate the air at a rate of 60-100 feet per minute [86]. The final step of the disassembly process is cell opening. Non-conductive tools are recommended to prevent any short-circuiting between the cell terminals. The cell configuration will determine which cutting tool should be used in the disassembly process. Rotary tools, such as Dremel, are typically used for cylindrical cells; the isolated plier is used for prismatic cells; and the knife, along with a pair of scissors, can be used for pouch cells [85,86,92]. No heat or smoke will be produced if the disassembly procedure is successful. During the post-mortem analysis, the jelly cell is unrolled and the cell components are separated from one another to be studied individually. The separated components are then transferred to dimethyl carbonate (DMC) solvent for washing [92]. The appropriate components are immersed in the DMC liquid during the washing process to dissolve the electrolyte salt residues on the sample surface (Fig. 5 (C)). Some authors, however, suggested two washing steps, one minute each, to remove all electrolyte salt residues [85]. It should be noted that the post-mortem analysis takes place in a controlled environment. Following that, the samples are kept in the glove box to dry and prepared for further investigation. The cell components are now ready to be moved to the testing facility for physical characterization, and the samples must be transferred from the glove box to the testing facility in a vacuum-sealed container due to the possibility of air contamination of the cell component (Fig. 5 (D)) [86,93].

4.2. Physical Characterization of Surface Morphologies

Several efforts have been made in recent years to study the morphology of deposited lithium using physical characterization approaches to acquire a better understanding of the lithium plating-stripping mechanism. Physical characterization approaches are commonly employed to study the structure of the deposited lithium and the growth processes of the lithium dendrites on the anode surface in the laboratory [83]. The most commonly used approaches for the physical characterization of lithium plating are explained. In addition, Table 2 summarizes the advantages and disadvantages of each approach in order to highlight their effectiveness.

4.2.1. Optical Microscopy

High-resolution optical microscopy can be used both in-situ and ex-situ to observe lithium plating-stripping processes during cell operation [94]. In-situ optical microscopy can be used to directly observe the plating morphology. A custom-made optical in-situ cell is designed

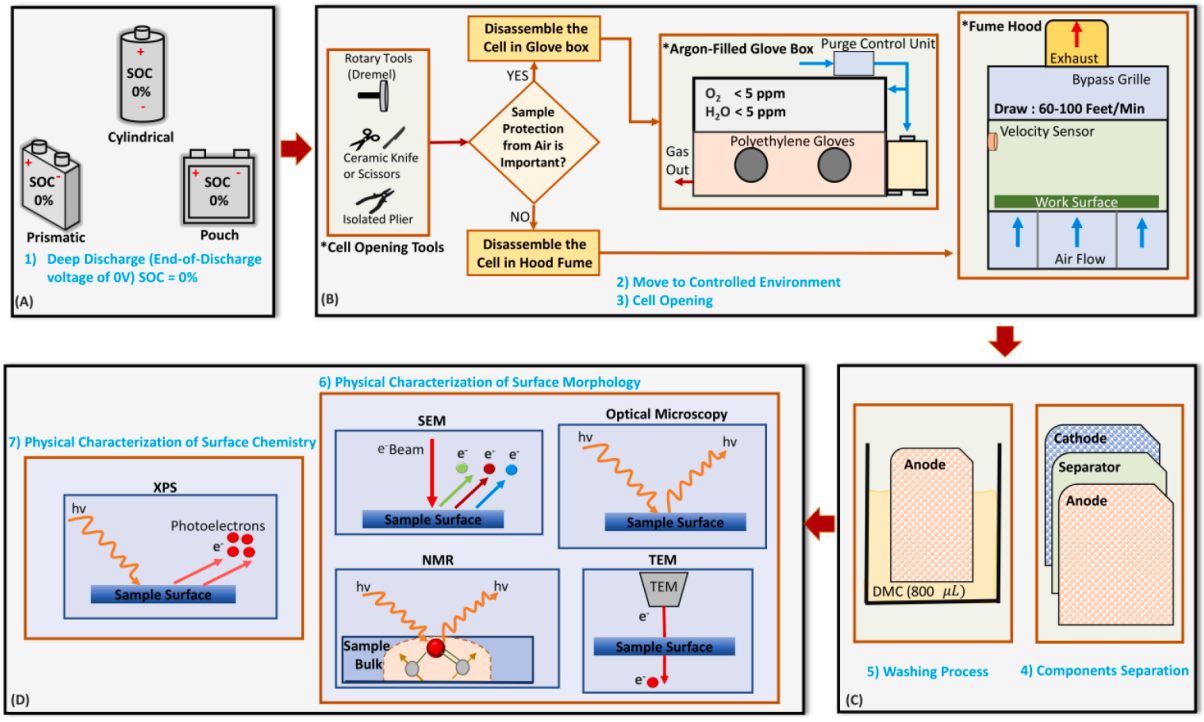

Figure 5. Overview of Post-Mortem Analysis for Lithium-Ion Cells. A) The test cell is required to be fully discharged before any further steps. B) The test cell is moved to the controlled environment for the opening procedure, where the controlled environment is chosen based on the study goals. Cell casing is removed. C) Cell components are separated and washed, and they are ready to be sent to the testing facilities. D) Cell components are subjected to further analysis in order to investigate lithium plating.

(Fig. 6 (A)) to study the penetration of lithium dendrite through the separator in order to find strategies to stop them (Fig. 6 (B) and (C)) [95]. The in-situ techniques can also be used to find the position and direction of the deposited lithium on the electrode surface [96]. In Ref. [77], in-situ optical microscopy is used to study the morphology of deposited lithium. At 10 °C, mushroom-like dendrites were seen, whereas needle-like and wound-ball morphologies were observed at 5 °C and 20 °C, respectively. During the lithium stripping process, dead lithium is observed, where it grows at the tips of the lithium and eventually loses electrical contact and separates from the graphite [96]. Lithium ions are extracted from the cathode compound and intercalate into the graphite structure. The color of the graphite changes depending on the stage of intercalation. Each stage has been associated with recognizable color, ranging from black to red to gold (as a function of lithium concentration x in Li_xC_6 (Fig. 6 (D)) [97,98]. As a result, the in-situ optical microscopy method based on color change can be useful for observing lithium plating. Thoma-Aleya et al. [99] designed a coin-type half-cell for in-situ optical microscopy to analyze color change at the graphite particles (Fig. 6 (E)). Using in-situ optical microscopy, Harris et al. [43] observed three stages on the meso-carbon microbeads (MCMB) electrode. In the beginning, the electrode was entirely in the blue stage (4L). The red-blue and gold-red boundaries then began at the edge of the electrode and sparsely departed from there until the voltage dropped to +2 mV (Fig. 6 (F)). Furthermore, they observed lithium plating on the (MCMB) electrode. The MCMB electrodes became golden (stage 1) after a voltage (+2 mV) was applied to the current collector, as shown in Fig. 6 (G) and (H). The edge of the electrode was free of lithium plating, whereas the rest of the electrode remained (stage 2) red graphite particles for many hours [43]. Moreover, they observed that lithium plating occurred when the anode potential was +0.002 V against Li^+/Li. However, thermodynamically lithium plating should occur when the anode potential drops below 0 V against Li^+/Li[43]. The change in the color associated with lithium concentration is dependent on the ambient lighting condition; thus, this technique is characterized as semi-quantitative.

4.2.2. *Scanning Electron Microscopy (SEM)*

Since 1988, SEM has been used to investigate the surface morphology of the lithium electrode, and it has a higher resolution than optical microscopy [100]. Many studies have employed both in-situ and ex-situ SEM to investigate the lithium plating-stripping process [101,102]. Yamaki et al. [103] used ex-situ SEM observation to characterize the lithium electrode surface morphologies during an extensive cycling test on a lithium coin cell for the first time. They identified two types of lithium deposits: particulate and dendritic. During discharge, the particulate lithium structure is reinserted into the anode graphite. The dendritic structure, on the other hand, remained on the anode surface. Rauhala et al. [88] investigated the lithium plating on the cell that was cycled at low temperatures using ex-situ SEM. A considerable amount of lithium plating was observed on the anode surface when the cell was cycled at -18 °C. Surface contamination is always a risk during ex-situ SEM investigations, especially for highly sensitive surfaces like graphite anode electrodes [83,96]. Using in-situ SEM to study lithium plating-stripping, on the other hand, requires unique cell and equipment designs. Many research groups have developed ultrahigh vacuum types of equipment to reduce the possible risk of lithium specimen contamination during the transfer process [100,102,104]. However, because ultra-high vacuum equipment is used in the examination process, in-situ SEM is only applicable to batteries that use solid polymer electrolytes and ionic liquids [102,105,106]. Uhlmann et al. [98] applied a high charging current of up to 10 C to three different half-cells to study lithium plating. They used SEM to observe changes in the surface morphology of the deposited lithium during both the charging and relaxation phases. Fig. 6 (I) and (J) show the surface structure of the anode sample with mossy grown lithium that is charged with a high charging current of 10 C. To avoid the relaxation period, this sample was disassembled in less than 5 minutes after charging. Another interesting approach was taken by Rong et al. [107] who developed an in-situ

Table 2
Advantages and Disadvantages Physical Characterization of Surface Morphologies for Lithium Plating Detection

Techniques	In-situ	Ex-situ	Advantages	Disadvantages	Refs
Scanning Electron Microscope (SEM)	✓	✓	(a) Suitable for large morphology change (b) Applicable to all types of cells (c) More effective to monitor the detrimental formation of dendrites directly	(a) Only applicable on batteries using solid polymer or inorganic SSE in in-situ condition (b) Risks of surface contamination were always present (c) Not applicable for quantitative studies in dynamic condition (d) The requirement of an extra high vacuum	[170,172,169, 174,7,105,83]
Optical Microscopy	✓	✓	(a) Instantly distinguish the surface change (b) Able to monitor lithium stripping/ plating during operation	(a) Resolution not as high as of SEM (b) Not applicable for quantitative studies in dynamic condition (c) Resolution is too low for most of the nanoscale materials (d) Required to design an optical cell for in-situ investigation	[7,43,83,175, 105]
Atomic Force Microscopy (AFM)	✓		(a) Imaging at the atomic level (b) Three-dimensional (3D) image (c) Visibility of Li surface including boundaries, ridgelines, flat areas	(a) Not suitable for inspection of dendrite formation (b) Not applicable for quantitative studies in dynamic condition (c) Destructive method (surface scratching needed in the contact mode) (d) Risks of surface contamination were always present	[176,7,130, 129]
Transmission Electron Microscope (TEM)	✓	✓	(a) Suitable for large morphology change (b) Dynamic evolution of interfaces at high tempo-spatial resolutions (c) Observation of SEI mechanisms and structures at the nanoscale (d) Observing microstructures in real-time (using open cell)	(a) The requirement of an extra high vacuum (b) Require solid-state electrolyte and ionic liquid (volatile organic electrolytes are incompatible with the high-vacuum environment) (c) Surface damage due to the beam effect (80/300keV) (d) Low spatial/energy resolution due to the presence of various stimuli along the beam path	[19,177,112, 7,178,101, 110]
Nuclear Magnetic Resonance Spectroscopy (NMR)	✓	✓	(a) Quantitative method (b) Provide a non-equilibrium state during charging/discharging (c) Processes in a non-invasive manner (d) Observe the change in intensity proportional to the lithium content of each stage	(a) Risks of surface contamination were always present on Ex-situ condition	[121,117,179, 102]

electrochemical scanning electron microscopy (EC-SEM) technique to observe the lithium plating-stripping process on Li/Cu electrode in liquid electrolyte LiTFSI/DOL/DME. They showed the significance and advantages of LiN_3 and Li_2S_8 as additives on lithium dendrite suppression.

Fig. 7 (A) shows lithium dendrites with a length of 18 μm after 350 seconds. During the stripping process, however, the majority of the lithium dendrites begin to dissolve into the electrolyte after 600 seconds, while the remainder tends to become dead lithium. Tallman et al. [108] reduced the amount of the deposited lithium up to 50 % by increasing the deposited overpotential through surface treatment. They deposited ultrathin (10 nm) Cu and Ni film on the graphite electrode surface. Ex-situ SEM results reveal that the deposited lithium was significantly decreased on the coated graphite with Cu and Ni compared to the uncoated graphite Fig. 7 (B).

4.2.3. Transmission Electron Microscopy (TEM)

One of the most promising observation methods for studying lithium dendrite growth at the nanoscale is transmission electron microscopy (TEM) [83]. In the literature, in-situ TEM setup is divided into two major types: a liquid cell system and an open-cell system [109,110]. In Ref. [111], a nanoscale LiB was built inside a TEM to investigate lithium plating in-operando using an ionic liquid as the electrolyte. They demonstrated how lithium ions nucleate at the anode-electrolyte interface and ultimately form fibers. The fundamental disadvantage of this approach is that volatile organic compounds (ionic liquids or solid-state electrolytes) are incompatible with the high-vacuum environment of TEM, hence it cannot be used to analyze lithium plating [112]. Mehdi et al. [113] recently used an in-situ liquid ec-TEM cell to study the dynamic volumetric changes at the electrolyte silicon nanowires interface during the charging and discharging process. They measured the thickness of the SEI layer of the anode electrode which was immersed in $LiClO_4$with (EC: DMC) as electrolytes during lithium plating-stripping. They confirmed that the SEI formation kinetics is greatly reduced by electron transport. Lithium plating-stripping in a $LiPF_6$-ethylene carbonate (EC)-diethyl carbonate (DEC) electrolyte was studied by Zeng et al. [114] to investigate the formation of dead lithium during cycling, as shown in Fig. 7 (C). Overall, in-situ TEM requires further development, particularly for liquid cell constructions due to electron scattering in the liquid layer [83]. The key issue is to find a suitable electrolyte for the TEM column [101].

4.2.4. Nuclear Magnetic Resonance Spectroscopy (NMR)

The key advantages of this technique over other approaches are its non-destructive nature and applicability to both crystalline and amorphous materials [115,116]. Ex-situ NMR can distinguish between different chemical states of lithium in the active material of the graphite electrode. Hao et al. [57] used an ex-situ NMR to measure the quantity of plated lithium while the cell was charged from 0 % to 60 % SOC (-25 °C), 80 % SOC (-25 °C), and 80 % SOC (-20 °C) with high currents (1.5 C). They found that the activation energy of lithium intercalation is higher than lithium plating even at low SOCs, resulting in lithium plating [57]. However, the use of the ex-situ method, like the ex-situ procedures discussed above, requires certain additional steps before the experiments, which may influence the experimental outcomes [117].

Several research groups have employed in-situ NMR to study carbon graphite electrodes, lithium metal oxide, and metal electrodes [117–120]. The hard carbon electrode as a negative electrode can consume more lithium during relaxation compared to the graphite electrode, Gotoh et al. [121] constructed full LiB cells with different materials including $LiCoO_2$, $LiNi_xCo_yAl_z$, and $LiMn_2O_4$ as the positive electrode, along with graphite and hard carbon as the negative electrodes to study relaxation effects in LiBs. They measured lithium spectra of cells at various SOCs, particularly after overcharging (2 C and 3 C) at 170 % SOC. They showed that the phenomenon of the "relaxation effect" occurs after overcharging based on the lithium metal signal measurement [121]. The lithium metal signal decreases with time as lithium atoms begin to reinsert into the graphite layer. Ota et al. [122] employed NMR spectroscopy to investigate the surface chemistry (surface film). They found that lithium cycling efficiency affects not only the

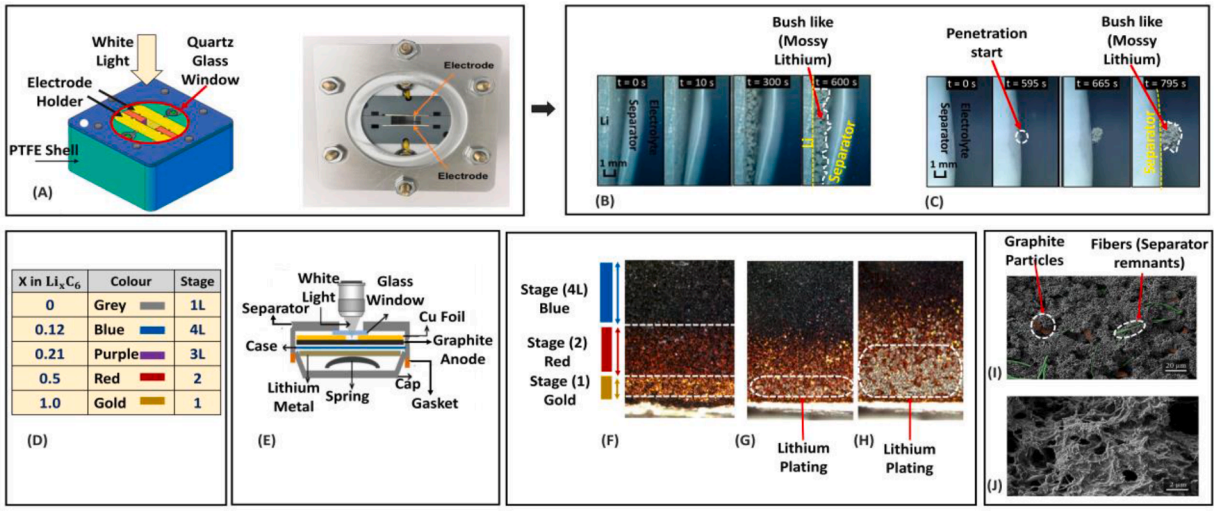

Figure 6. In-situ Cell Design and Results of Optical Microscopy and Ex-situ SEM for Lithium Plating Morphology Characterization.
(A) Schematic of the custom-made optical in-situ cell with a quartz glass window. **(B)** In-situ optical microscopy at a current density of 1 mA/cm^2 (t = 0 - 600 s). The gap between lithium metal and separator helps in the observation of the dendrite growth until it reaches the separator. **(C)** In-situ optical microscopy at a current density of 1 mA/cm^2 (t = 0 - 795 s). There is no gap between the separator and the lithium electrode. Penetration started at t = 595 s and quickly changed to the bush-like structure (Reprinted from Liu et al. [95] with permission of American Chemical Society Publications). **(D)** The color of graphite is affected by the concentration of lithium x in Li_xC_6 (data adapted from Ref. [123], the random occupation of all superlattices defined as 'liquid-like' or L stage). **(E)** Side-view schematic of a custom-made coin-type half-cell for in-situ optical microscopy (Reprinted from Thomas-Alyea et al. [99] with permission of Electrochemical Society). **(F)** The MCMB electrode surface inside an in-situ optical half-cell, three different graphite colors (stages) were observed over 3 hours. Lithium Plating on an MCMB electrode was observed when a voltage (+2 mV) is applied to the current collector, although according to bulk thermodynamics, lithium metal plating should not occur unless the voltage becomes negative. The image **(G)** is taken 8 h before **(H)** (Reprinted from Harris et al. [43] with permission of Elsevier). **(I)** and **(J)** Ex-situ SEM images show the morphology of an anode surface with mossy lithium plating. The anode is charged with a high current of 10 C and then instantly dismantled in less than 5 minutes to interrupt the relaxation phase, scale bars: 20 μm and 2 μm (Reprinted from Uhlmann et al. [98] with permission of Elsevier).

morphology of deposited lithium but also the chemical components of the surface film. Arai et al. [119] studied lithium metal deposition with in-situ solid-state Li NMR on a full cell consisting of $LiCoO_2$ (positive electrode), graphite (negative electrode), polypropylene (separator), and an organic liquid such as electrolyte (1 M $LiPF_6$, ethyl methyl carbonate 30:70 vol.%) during both continuous currents (CC) and pulses current (PC) mode operations. As shown in Fig. 7 (D), the deposited lithium metal became visible at approximately 265 ppm at -5 ^oC temperature for different cell cycles with a CC mode pattern. Simultaneously, no lithium metal deposition was detected at -5 ^oC with a PC mode pattern [119].

They also calculated the lithium deposition rate (k) using the slopes of the plots. The lithium deposition rate at -5 ^oC is approximately 12.4 ($10^3 mgmAh^{-1}$). Wandt et al. [124] employed electron paramagnetic resonance (EPR) spectroscopy to identify the onset of lithium plating in a graphite electrode under realistic cell conditions. EPR is more sensitive than NMR, making it excellent for analyzing lithium materials in-operando [125,126]. EPR spectroscopy, in addition to NMR, uses low-energy radiation that does not affect the chemical characteristics or morphology of the investigated species [125,127].

4.2.5. Atomic Force Microscopy (AFM)

AFM is one of the most effective tools for analyzing the surface morphology of electrodes at the nanoscale scale [128,129]. AFM scans the surface of a sample with a cantilever and a sharp probe. In comparison to SEM or optical microscopy, it can also provide significantly higher morphological resolution in three-dimensional (3D) format [83]. In-situ AFM was utilized by Mogi et al. [130] to investigate the surface morphology of deposited lithium on the Nickel substrate at elevated temperatures. At 40 °C, they discovered heterogeneous and massive deposits of lithium underneath the substrate's surface film, whereas, at 60 °C and 80 °C, they discovered a homogenous and thick surface film. The results, however, were inaccurate since the AFM observation was done in contact mode. During the investigation, the AFM probe (tip) scrapes the sample's surface in contact mode [130]. The image resolution is low in non-contact mode due to the large distance between the probe and the sample. As shown by in-situ AFM in Ref. [129], the structure of the lithium surface includes grain boundaries, ridge-lines, and flat areas. These lines were found to be critical in controlling the morphology of the deposited lithium. Aurbach et al. [131] studied lithium deposition on the copper electrode in a nonaqueous electrolyte system using in-situ AFM measurements. They found that although lithium metal is soft, utilizing AFM as a detection tool does not modify the surface morphology. In another approach, Shen et al. [132] used in-situ electrochemical atomic force microscopy (EC-AFM) to study lithium dendrite growth on a graphite electrode cycled in 1 M $LiPF_6$-EC-DMC and 1 M $LiPF_6$-FEC-DMC electrolytes. They confirmed the importance and advantages of FEC-based electrolytes on lithium dendrite detention, as the formed SEI is harder and denser compared to the SEI formed in the EC-based electrolyte. Overall, AFM is an accurate and powerful technique to study the morphology and topography changes of LiBs [133]. However, it is not recommended to use AFM for inspection of the dendrite formation as it has some limitations in the tip dimension and the usual vertical scanning range of instruments [134].

4.3. Physical Characterization of Surface Chemistry

One of the most common approaches in the field of LiBs is to analyze the chemical composition of the surface films on electrodes in non-aqueous solutions. The chemical composition of deposited lithium as well as the oxidation states of the elements can be examined using surface chemistry analysis techniques [135,136]. In the following part, the methodologies used to characterize the surface chemistry of the deposited lithium on the anode surface will be introduced. In addition, for a more in-depth understanding of the existing techniques, the advantages and disadvantages of each are listed in Table 3.

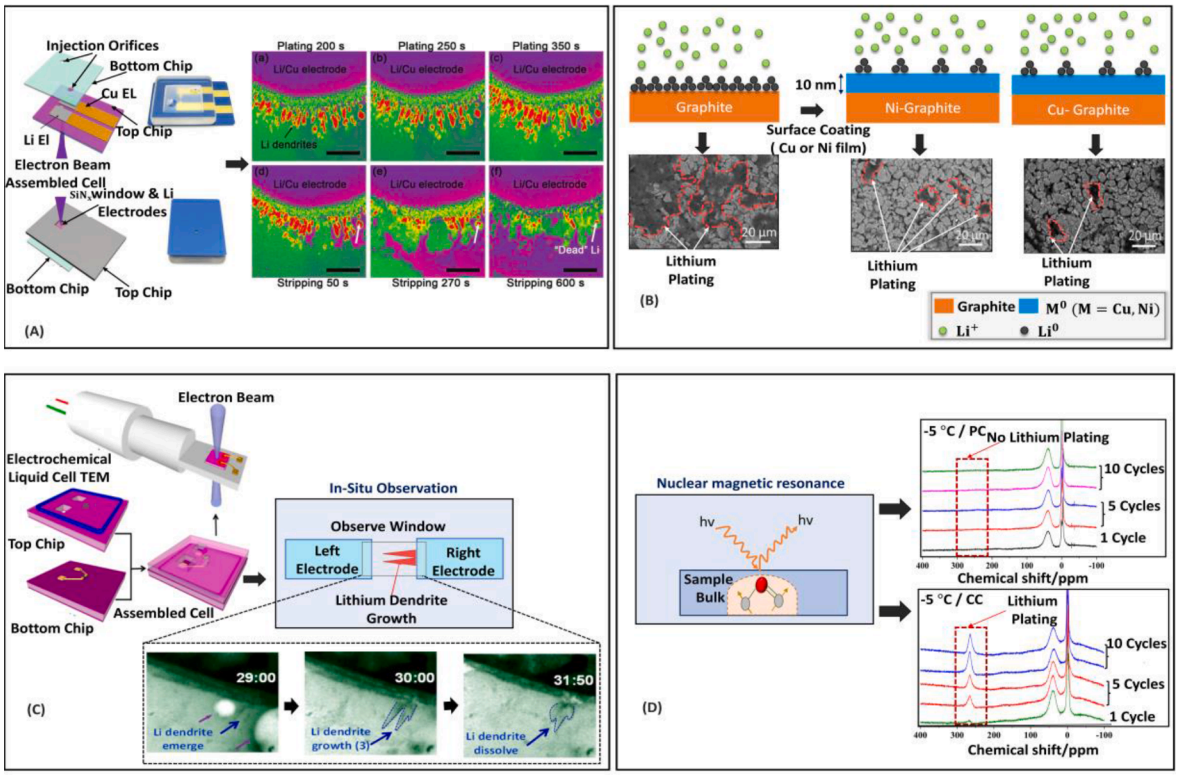

Figure 7. Different Physical Characterization Approaches for Lithium Plating investigation.
(A) Schematic of the in-situ SEM EC-liquid cell setup for direct observation of lithium plating, Li/Cu electrode during lithium plating for a)200 s, b)250 s, c)350 s, and d)50 s, e)270 s, f)600 s for stripping under 0.15 $mAcm^{-2}$. Scale bars: 20 μm, (Reprinted from Rong et al. [107] with permission of Advanced Materials). (B) Schematic of Li-metal nucleation on the uncoated graphite surface and coated graphite surface during high current charging, the nucleation is significantly decreased due to increased overpotential for Li-metal deposition, which was obtained by the nanoscale coating of Cu and Ni, backscatter SEM images of the deposited lithium metal on the uncoated graphite and coated graphite with Cu and Ni. Scale bar: 20 μm (Reprinted from Tallman et al. [108] with permission of American Chemical Society). (C) Schematic of in-situ TEM liquid cell for nanoscale observation of electrode-liquid electrolyte interfaces using lithium dendrite growth. Scale bars: 800 nm, (Reprinted from Zeng et al. [114] with permission of Nano Letters). (D) The stacked in-situ NMR spectroscopy for different cells at -5°C. These spectra were measured at the fully charged state in the latest cycle. Pulse current mode: cells were cycled with pulse current (PC) mode pattern, and no lithium plating was detected. Continuous current mode: cells were cycled with continuous current (CC) mode pattern and lithium plating observed at 265 ppm (Reprinted from Arai et al. [119] with permission of Electrochemical Society).

4.3.1. *X-ray Photoelectron Spectroscopy (XPS)*

X-ray photoelectron spectroscopy has been widely used for surface chemistry analysis (element analysis and oxidation state of elements) of lithium electrodes due to the relative simplicity in use and data interpretation [137]. Castro et al. [136] used XPS to investigate the aging mechanism of a $LiFePO_4$/graphite cell after 200 cycles at ambient temperature. They found that cyclable lithium can be consumed at each cycle due to the deposited lithium on the anode surface and the instability of the SEI (LAM). XPS may be a destructive method due to the usage of an argon ion sputter gun and an X-ray beam on the sample during the investigation [84]. However, Aurbach et al. [137] found that by working at low emission and balancing the quality of the spectra based on the shorter measurement duration, it is possible to collect reliable and reproducible findings with minimum damage to the material when using the XPS technique. The XPS method, like most other spectroscopic methods, requires a vacuum system and there is always the risk of surface contamination in highly sensitive electrodes. As a result, a special transfer arrangement is required [138,139]. X-ray tomography can provide a better understanding of the structure and material composition of the electrodes, as well as morphological changes [140–143]. X-ray beams with energy ranging from 10-100 keV may easily penetrate the plastic and metallic cell casing and directly visualize the inner LiB components in 3D [140,144]. Eastwood et al. [145] applied a synchrotron-based X-ray phase-contrast tomography technique to investigate the microstructures of the electrodeposited lithium, which is necessary for understanding the dendrite formation. Harry et al. [146] used synchrotron hard X-ray microtomography to investigate the lithium dendrite in a lithium/polymer/lithium cell. They discovered that the subsurface structure of the electrode is critical in facilitating dendritic formation in the polymer electrolyte.

4.3.2. *Fourier Transform Infrared Spectroscopy (FTIR)*

FTIR is a non-destructive method for analyzing the chemistry of the lithium surface [84]. Many researchers have used FTIR to investigate the surface chemistry of lithium in organic electrolytes [147–149]. To quantitatively describe liquid electrolyte solutions, Ellis et al. [150] combined FTIR spectra with machine learning (ML) techniques. The electrolyte concentration was reported to be reduced by 10–20% (Vol) in cells after 200 cycles at 55°C. This is a significant amount of salt loss, which contributes to cell failure. Morigaki [148] analyzed the impact of EC^+dimethyl carbonate (DMC) solution on lithium surface based on the locations and strengths of the peaks in DMFTIR spectra. They found a new reduction product of the solvent on lithium after 1 and 15 hours immersion with DMFTIR. In another approach, FTIR was used by Kramer et al. [149], who studied lithium plating in pristine cells of two different forms (cylindrical and pouch). The impacts of electrolyte solvent such as propylene carbonate (PC), ethylene carbonate (EC), dimethyl carbonate (DMC), and different salts ($LiAsF_6$,$LiBF_4$,$LiPF_6$)on the lithium surface were investigated with FTIR in [137]. The in-situ FTIR technique uses attenuated total reflectance (ATR) to examine the lithium sample in the nonaqueous system [151]. Therefore, using ATR crystal for each experiment would be prohibitively expensive due to the

Table 3
Advantages and Disadvantages Physical Characterization of surface chemistry for Lithium Plating

Techniques	In-situ	Ex-situ	Advantages	Disadvantages	Refs
Fourier Transform Infrared (FTIR)	✓	✓	(a) Non-destructive method (b) High surface sensitivity at the molecular level (c) Qualitative/quantitative analysis	(a) Only suitable for detecting the organic components (b) Low reflectance intensity and broad (c) Expensive material for in-situ experiments (d) Damages the electrode surface (in contact mode)	[83, 84, 151, 180]
X-ray Photoelectron Spectroscopy (XPS)	✓	✓	(a) Provide the 3D structure of surface films (b) Analysis of inorganic components (c) Study surface species (which are not too active in IR)	(a) Damages the electrode surface (b) Modify the oxidation states of elements (c) Requires a vacuum system	[181, 139, 136, 138, 137]

damage to the crystal surface during the investigation [84].

4.4. Electrochemical Methods

Electrochemical in-situ, ex-situ, and in-operando are the most effective methods for monitoring unsafe battery behavior, such as lithium plating. Voltage plateau after charging, anode potential, electrochemical impedance spectroscopy (EIS), differential voltage (DV), and incremental capacity (IC) can be used in in-situ or in-operando electrochemical methods [44]. These methods are based on electrochemical signals, which are available in any LIB. Using electrochemical techniques is convenient because they can be implemented in BMS [19]. The most common electrochemical approaches for detecting lithium plating in the context of possible BMS deployment are described briefly. Table 4 summarizes the benefits and drawbacks of each strategy for a more thorough comparison.

4.4.1. Voltage Plateau After Charging

Voltage plateau is a non-destructive and indirect method that has the potential to be used as an online tool for lithium plating detection in automotive applications [48]. Reversible lithium is reinserted into the graphite during the relaxation. This process affects the voltage plateau signal due to variations in the overall potential of the anode electrode during relaxation and discharging after a charging step [48,59,152]. Therefore, the presence and changes in the voltage plateau could provide indications of lithium plating [153,154]. Zinth et al. [155] combined the voltage plateau method with in situ neutron diffraction measurements to study lithium plating at -20 ^{o}C, where the degree of graphite lithiation can be used to estimate the amount of lithium plating. A quantitative detection method for lithium plating based on plotting the derivative of voltage over capacity (dV/dQ plot) was presented by Petzl et al. [153], who found that the voltage plateau appeared at the beginning of discharge. They proposed that the discharge capacity at the dV/dQ peak contributes to the total reversible part of the deposited lithium during charging. Recently, it has been reported by Campbell et al. [59] that the cell self-heating and concentration gradients during fast charging can increase the voltage plateau curve, which could be incorrectly detected as lithium plating. Also, they showed that the absence of stripping plateau does not mean that no lithium plating has taken place in the cell. However, a recent study showed that the relaxation process is much faster at a higher temperature and the voltage plateau is less visible at higher temperatures [156]. Therefore, the voltage plateau detection technique works better at lower temperatures (-20 ^{o}C) since the relaxation process is slower at subzero temperatures [98,157]. In another approach, Uhlmann et al. [98] detected a kink in the voltage curve during relaxation after the charging process rather than during discharging. They found that for the detection of lithium plating, flattening the voltage curve can be used. This technique was later expanded by plotting the derivative voltage over time (dV/dt), where the same dV/dt peak curve for lithium stripping is seen [154]. Yang et al. [48] studied the voltage plateau during relaxation and during discharge to determine the parameters affecting the voltage curves during lithium stripping. In this study, they used a 9.5 Ah pouch cell for a plug-in hybrid EV application. The dV/dt curve is plotted and shown in Fig. 8 (A), where it is shown that the dV/dt peaks appear sooner with a higher discharge rate compared to the dV/dQ analysis. They showed

Table 4
Advantages and Disadvantages of On-Line Electrochemical Lithium Plating Detection

Techniques	BMS	Advantages	Disadvantages	Refs
Measurement of Columbic Efficiency	-	(a) Applicable to all types of cell (b) Suitable for identification of side reactions in early stages	(a) Inaccurate results if another parasitic reaction happens (Oxidation, loss of active materials) (b) Expensive equipment	[170, 172, 169, 174]
Voltage Plateau after charging	✓	(a) Non-destructive method (b) Suitable for on-board implementation (c) No requirement for special and expensive equipment	(a) Needs slow discharge rate (b) Availability of abnormal exothermic peaks (c) The importance of the lithium deposited areas (d) Highly depends on internal cell characteristics	[17, 48,59, 98, 154, 195]
Third Lithium Reference Electrode	-	(a) Quantitative evaluation of different electrochemical aspects (b) Reliable method	(a) Safety (Short circuit) (b) Not applicable in Commercial cells (c) Require modifying cell design and fabrication (complicated implementation)	[49] [162, 196, 197, 163, 160]
Electrochemical impedance spectroscopy (EIS)	✓	(a) Suitable for study LiB characteristics (b) Non-destructive method which is suitable for on-board implementation (c) Fast analyzing period (25/min/cell)	(a) Reduction in cell performance after RE insertion (b) Require complicated computation (c) The cell must be in the equilibrium state	[183, 182, 23, 198, 199]
Incremental Capacity (IC) Differential Voltage (DV)	✓	(a) Non-destructive method (b) Suitable for on-board implementation (c) Ideal for identification and quantification of DM	(a) Required small currents for discharge curves (b) Slow analyzing period (10 h/cell)	[200, 31, 201, 44]

that the rate of lithium stripping is limited by the rate capability of intercalating Li^+ions into graphite, and that the duration of the voltage plateau is highly dependent on the rate of lithium stripping. Intercalation kinetics, graphite solid-state diffusivity, and cell temperature all have an effect on the voltage curves. Another interesting finding is represented in the schematic above Fig. 8 (A). Near the separator, lithium metal is deposited. The high degree of graphite lithiation limits the rate of Li^+ions insertion. Since the Li^+ions can not be inserted into the anode near the separator, they begin moving to the other part of the anode near the foil and are intercalated into the graphite along the path [48]. At the beginning of discharge, a dV/dQ peak occurs. Nevertheless, in the case of C/3 discharge, the dV/dQ peak seems earlier than that of 1 C Fig . 8 (B). Li^+ions intercalation still takes place in the anode in the discharge phase after charging, as long as the Li stripping reaction can support the discharge current.

4.4.2. Third Lithium Reference Electrode (RE)

As previously stated, lithium plating takes place when the anode potential drops below 0 V (vs. Li/Li^+). To directly measure the anode potential, a third reference electrode (RE) must be used [49]. Nonetheless, because commercial cells lack a third reference electrode, measuring the anode potential directly is not currently practicable. Anode potential may, however, be measured in the laboratory using a specific setup in which the RE is inserted into the cell (machinery). The RE materials (e.g., metallic Li, $FePO_4$/$LiFePO_4$, Li-Sn, Li-Al) and cell configurations are important factors in the insertion process. The location of the RE is chosen based on these factors [49,158,159]. Several studies have been conducted to demonstrate how to develop and implement the RE into LiBs, as well as where the ideal position for the RE is to reduce the ohmic drop while maximizing measurement accuracy [160–163]. An interesting approach was taken by Waldmann et al. [49],

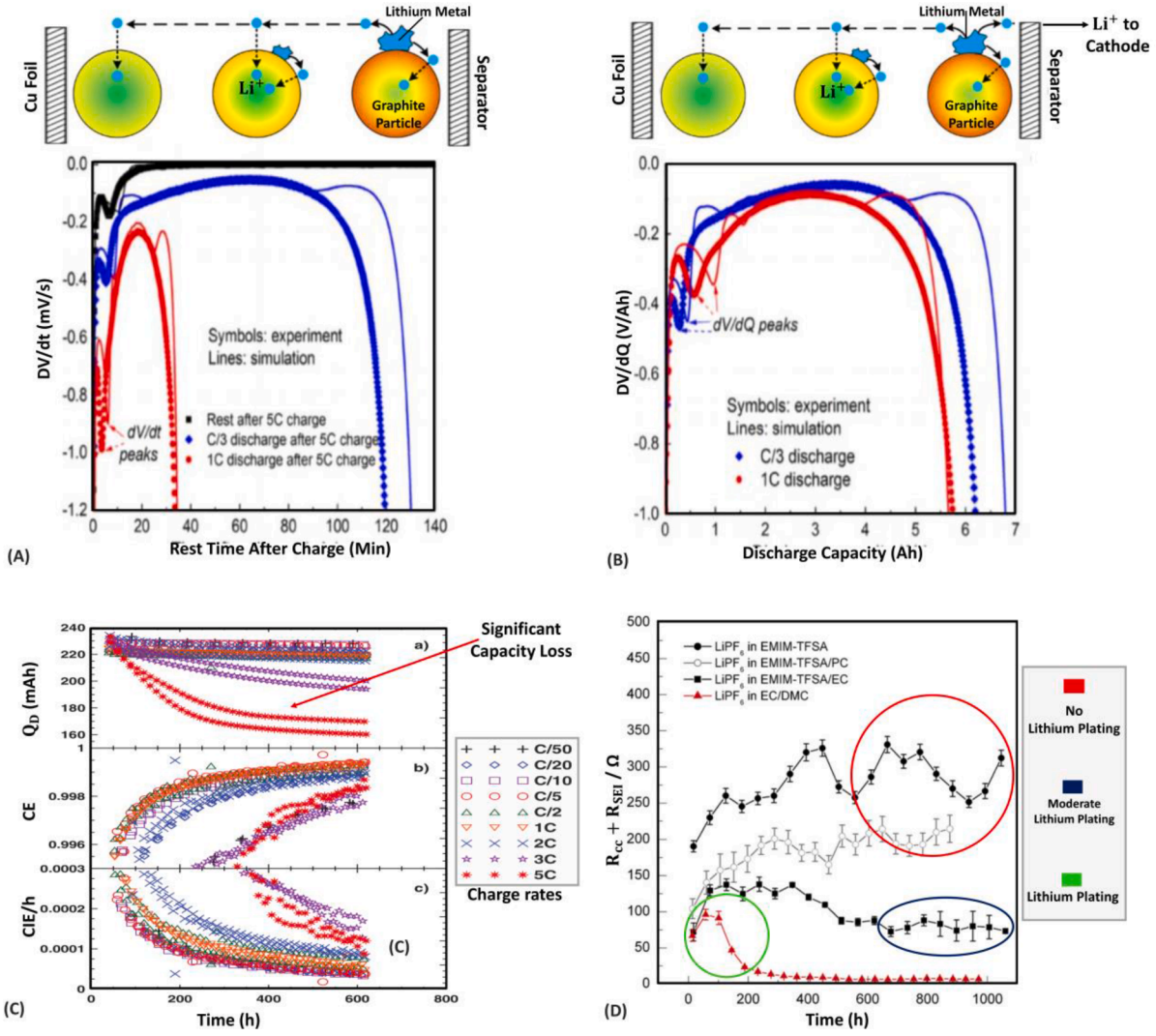

Figure 8. Electrochemical Methods.
(A) Differential voltage over time (dV/dt) for the two discharge cases and the 5C charge relaxation event, as well as a schematic diagram of the anode's internal characteristics at the start of relaxation. During relaxation, Li^+ions that are not consumable at the separator travel and diffuse through the electric field (migration) and concentration gradient (diffusion) towards the foil, where they are intercalated into graphite (Reprinted from Yang et al. [48] with permission of Elsevier). **(B)** Differential voltage over capacity (dV/dQ) in the discharge phase as a result of discharge capability and a schematic diagram of the anode's internal characteristics at the start of discharge. During discharge, Li^+ ions formed by Li stripping near the separator have three destinations: they are intercalated into graphite, they travel to the cathode to deliver output current, and they move under an electrical field (migration) and a concentration gradient (diffusion) towards the foil and are intercalated along the path into graphite (Reprinted from Yang et al. [48] with permission of Elsevier). **(C)** Cycling data versus time extracted by a high-precision charger. A two-stage charge process is applied on pouch cells at different rates from (C/50 to 5C) at 30 °C ((a) Capacity, (b) Coulombic efficiency, (c) Coulombic inefficiency per hour) (Reprinted from Burns et al. [170] with permission of Electrochemical Society). **(D)** Resistance values $R_{cc} + R_{SEI}$ as a function of time for various electrolyte solutions (Reprinted from Schweikert et al. [120] with permission of Elsevier).

who positioned the RE near the current collecting tab of the anode as this area has a higher current density. Due to the low diffusivity of lithium-ions in graphite at low temperatures and high SOC, they discovered that lithium-ions begin to accumulate at the anode interface. Rangarajan et al. [69] used a lithium titanate (LTO) electrode as a reference electrode in a pouch cell with a stable voltage over a range of SOC to detect and quantify lithium plating. To quantify the amount of lithium plating at each rate, the plating period, plating power, and plating energy were defined. They called lithium plating a non-linear process since it does not increase monotonically under varied working conditions. Low cost and reliable RE insertion methods have been introduced in Ref. [163], which require less equipment than existing procedures for commercial 18650 cells. Non-polarizability, reliability, and reproducibility are the key characteristics in the RE material selection process [164]. Lithium metal is the most common material for RE, but it cannot provide all these characteristics due to unstable potential (reliability) [165]. The potential of RE may vary due to mechanical treatment, the nature of the electrolyte, and the formation of the SEI layer [19,164]. Moreover, lithium metal is not a proper choice for high-temperature applications due to its low melting point (i.e., 180 °C) [49]. The accuracy of the RE method with alternative materials such as $Li_4Ti_5O_{12}$and$LiFePO_4$ has been studied by Mantia et al. [164]. They showed that these materials may be the most promising materials for RE since they exhibit a constant potential for $Li_4Ti_5O_{12}$ (1.567 ± 0.0025 V) and $LiFePO_4$(3.428 ± 0.0005 V) vs. Li/Li^+. These materials can also provide low polarizability under high current rates during the two-phase reactions. Overall, RE insertion may cause surface film modification and degradation by interfering with the battery's electrochemical process. Furthermore, due to safety concerns, RE has yet to be deployed in any commercial cells or real-time LiB applications for measuring electrochemical characteristics.

4.4.3. Incremental Capacity (IC) and Differential Voltage (DV)

IC-DV techniques are based on the rate of changes in the electrochemical equilibrium phase (EEP) [166]. The EEP changes are determined by the intercalation and de-intercalation processes that occur between the anode and cathode materials. The IC-DV curves are obtained by a constant battery charge curve, and the IC curve is mathematically estimated as the gradient of Q with respect to V ($dQ/dV = f(V)$) [166]. The DV curve is obtained by inversely computing the IC curve ($dV/dQ = f(Q)$). The researchers use prognostic/mechanistic models to directly clarify the aging mechanism by identifying model parameters [31,166,167]. Indeed, the mechanistic model is a backward-looking modeling approach in which the degradation is the input and the output is the cell's voltage and capacity [31]. Thus, when a cell is in equilibrium, the IC-DV approach can quantify its electrochemical properties as well as its various degradation modes (LLI, LAM) [31,167]. The IC and DV curves can be used to study the degradation mechanism both qualitatively and quantitatively [44]. Tanim et al. [68] recently investigated the lithiation voltage profile and demonstrated that reversible lithium stripping is dependent on the level of over-lithiation in the graphite electrode. Capacity fading was observed using IC analysis on 13 cells cycled at a low temperature (-10°C) under diverse conditions such as varying charge current rates, charge cut-off voltages, and charge cut-off current [24].

4.4.4. Coulombic Efficiency (CE)

Coulombic efficiency (CE) is defined as the ratio of energy (Q_d) a LiB outputs during discharge to the energy (Q_c) a LiB takes in during charge [168]. When lithium plating occurs on the anode surface during the charging cycles, the CE decreases [19]. As a result, CE can be recognized as a method for detecting lithium plating. Smith et al. [169] advised four important aspects to correctly measure the CE: (i) accuracy of the set current, (ii) precision of the voltage measurement, (iii) duration between voltage measurements, and (iv) precisely controlled cell temperature. Burns et al. [170] investigated lithium plating by plotting CE versus charging current rates. As shown in Fig. 8 (B), there is a considerable variation in the capacity loss rates of cells charged at room temperature above 2 C. Furthermore, with a charging rate of 1C at 12 °C, they found a considerable amount of lithium plating. The CE versus charging rate at various temperatures was recorded (Fig. 8 (C)), with a minor drop in CE occurring as the deposited lithium began to consume the active lithium. They also proved the presence of lithium plating on graphite electrodes for cells cycled at charging current rates of 2 C for 50 °C and 0.5 C for 12°C [170]. Liu et al. [171] measured the CE of four silicon-based electrode materials during cycling (condition: voltage cut off 1.5-0.02 V), and the resulting CE ranged from 95 % to 98 %. The measurement equipment used in this procedure must be highly precise to detect any variations in voltage and current. However, Tanim et al. [68] recently demonstrated that the CE approach could not be precise for detecting lithium plating in a full cell over extended cycling. When only small amounts of lithium are deposited, high precision coulombmeters are required. Otherwise, if the amount of deposited lithium is significant, conventional testers or measurement devices can be used [68,172]. Furthermore, the rest period has a considerable impact on the CE method, as it cannot distinguish stripping from the plating process [68,173].

4.4.5. Electrochemical Impedance Spectroscopy (EIS)

EIS is a quantitative approach for analyzing battery behavior and determining electrochemical kinetics throughout the lithium insertion-extraction process [165]. Lithium deposition has been studied in Li/L-i$_4$Ti$_5$O$_{12}$ battery cells based on ionic liquid electrolytes during several charging/discharging cycles by EIS [120]. In another study by the same author, a correlation between the surface area of the electrolyte and lithium metal (formation of lithium dendrites) with $R_{cc} + R_{SEI}$was introduced. They showed that a decrease in the $R_{cc} + R_{SEI}$value corresponds to an increase in the interfacial area between the electrolyte and lithium metal electrode [182]. As shown in Fig. 8 (D), using a conventional electrolyte ($LiPF_6$ in EC/DMC) resulted in the formation of lithium dendrites [120]. The $R_{cc} + R_{SEI}$ values of$LiPF_6$ in EMIM-TFSA/EC and $LiPF_6$ in EMIM-TFSA/PC do not show any decrease. However, there could be additional factors causing a drop in $R_{cc} + R_{SEI}$ values. EIS measurements are often conducted using laboratory equipment [120,182,183]. Nevertheless, Nazer et al. [184] proposed an online EIS technique for implementation in the BMS of HEVs and EVs. They measured electrochemical impedance using broadband excitation signals (pseudo-random binary sequences (PRBSs), random white noise, swept sine, swept square, and a square wave). The proposed system, however, was noisy and could result in an impedance error value at high frequencies [184].

4.5. Recent Non-Destructive Approaches for Detecting Lithium Plating

In addition to these electrochemical and physical detection methods, simpler techniques for studying lithium plating have been proposed. According to the literature, when transitioning from a completely unlithiated condition to lithiatedLiC_6 (intercalation of lithium), the total volume of the graphite anodes might increase by 10% [43,185]. The extra volume changes can also be caused by the deposited lithium on the graphite. As a result, detecting changes in cell thickness can be a useful strategy for detecting lithium plating [36,186,187]. There is a correlation between the volume change and lithium plating, which determines the expected extent of volume gain due to deposited lithium Fig. 9 (A) [185]. In Ref. [185], a customized setup was provided to measure the thickness of a 20Ah pouch cell during cycling with varied currents and temperatures, as illustrated in Fig. 9 (B). Due to the reversibility of lithium plating, it was shown that the cell thickness increases rapidly during the lithium plating condition and decreases during the rest time (Fig. 9(C)). This method is straightforward and valid, but it requires the use of an accurate device to measure cell thickness. Furthermore, this approach is only applicable to pouch cells. It should be also noted that it

is not possible to differentiate volume changes due to gassing reactions with lithium plating [188].

Ultrasonic acoustic approaches have recently been used to study LiB behavior [189–191]. The propagation and reflection of soundwaves is the fundamental working principle of the ultrasonic method. Hsieh et al. [192] used this approach to measure SOC and SOH in a pouch cell. The ultrasonic investigation can be divided into two modes [193]: (i) pulse-echo mode, which uses a transducer that can either be glued or pressed onto the cell casing. In this case, a voltage pulse is sent out towards the object (cell) and the pulse is reflected back to the transducers. (ii) Through-transmission mode, which employs two separate transducers, one of which serves as a transmitter and the other as a receiver; a voltage pulse is transmitted from the transceiver and travels through the object material (cell), arriving at the receiver, which is installed on the opposite side of the object. Gold et al. [191] proposed a linear model with ultrasonic pulse frequencies ranging from 200 kHz to 2.25 MHz, which is lower than the one used in prior studies to measure SOC in one cycle. Bommier et al. [189] recently employed the electrochemical acoustic (EA) technique to study SEI formation in NMC/SiGr pouch cells. Due to gassing reactions that occurred during the first SEI formation/lithiation of the silicon particles, the acoustic signal was lost during the first 40 hours of charging. They demonstrated that the acoustic signal is significantly attenuated in the presence of a gaseous environment. Moreover, they found a correlation between the passivation of the silicon particles and the acoustic time-of-flight (TOF) shift.

Bommier et al. [194] used the ultrasonic approach to detect lithium plating in a pouch cell. Commercial 210-mAh lithium-ion cells were ultrasonically tested in through-transmission mode. Fig. 9 (D), shows a schematic of the ultrasonic setup. In their study, they established a connection between the acoustic signal and lithium plating. When the cell was charged with 1C and discharged with C/10, the acoustic signal was quickly attenuated at the second cycle (t=20 h) and reappeared at the 18th cycle (t=195 h), as shown in Fig. 9(E) [194]. Meanwhile, the cell capacity was reduced from 0.210 Ah to 0.195 Ah, and they suspected that the loss of acoustic signal was due to lithium plating. However, the loss of the acoustic signal, according to the literature, is a strong sign of a gassing reaction in the cell, and because distinguishing between lithium plating and gas reaction is difficult, it cannot be utilized as an indication for lithium plating. As a result, they discovered that employing an acoustic signal alone is ineffective. In the second attempt, they decided to measure the shifts (time-of-light) in the full acoustic waveforms [194]. Cells were cycled twice at C/15 for both charge and discharge and then a CC charge with a fixed capacity of 0.210 Ah (no voltage cutoff) was applied to trigger lithium plating. As shown in Fig. 9 (F), they found a significant difference at the endpoints of the TOF shifts of the cells that were cycled with fixed-capacity charge (1 C) than the cells that were cycled with a C/15 charge. It was shown that there is a correlation between TOF endpoints differences and lithium plating. They proved the efficiency of this strategy using various ex-situ characterization methods, such as ex-situ SEM, as shown in Fig. 9 (G) [194].

5. Model-Based Investigation of Lithium Plating

In order to optimize the battery design and develop more practical charging protocols, model-based approaches are a good option [7,35,202]. There are several different approaches to model LiBs: electrochemical models, equivalent-circuit battery models (ECM), thermal models, electrical models, mechanical models, and molecular models [203]. Modeling provides us with the exact time of lithium plating and the location of the deposited lithium on the electrode surface. Newman [204] and co-workers introduced the first battery physics-based model. In the following, we review the recent results on lithium plating modeling, and based on the gathered information, the advantages and disadvantages of each model are compared in Table 5.

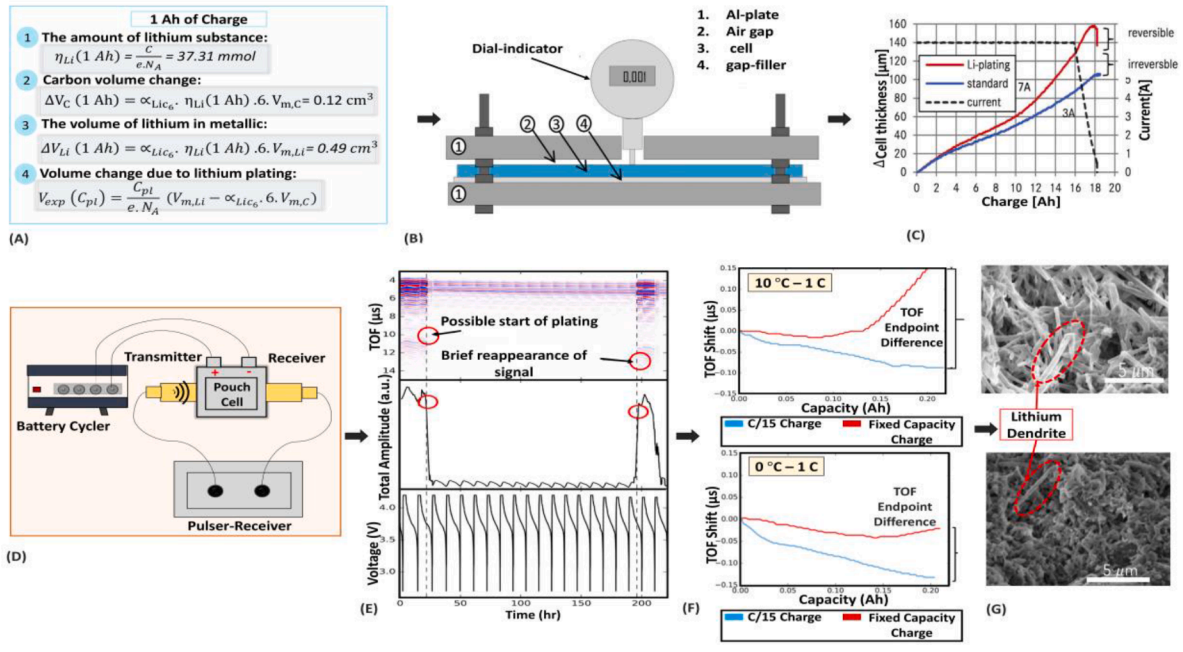

Figure 9. Non-Destructive Approaches for Detecting Lithium Plating.
(A) Theoretical relation between volume gain and lithium plating. (B) Schematic of the setup for in-operando measurements of pouch cell thickness during the lithium plating (resolution 1 μm). (C) Significant changes in the cell thickness at the charge current of 7 A due to lithium plating (Reprinted from Bitzer et al. [185] with permission of Elsevier). (D) Schematic of the in-operando acoustic detection setup for studying lithium plating. (E) Acoustic plots consist of three distinct panels, which are, from top to bottom, a heatmap of acoustic time of flight (s), total amplitude of waveforms in random components, and a voltage versus time curve corresponding to the adjoined waveforms. (F) The difference in acoustic TOF shifts during the C/15 charge and the fixed-capacity charge of 0.210 Ah at different temperatures was measured when the cell was cycled at 10°C with a fixed capacity charge of 1 C. The cell was cycled with a fixed capacity charge of 1 C at 0°C (G) Ex-situ SEM measurement: electrodes were washed in (DMC) and dried in an argon-filled box for 2 hours at 40°C. Scale bars: 5 μm (Reprinted from Bommier et al. [194] with permission of Cell Reports).

5.1. Electrochemical Models of Lithium Plating

Electrochemical models based on the porous electrode theory and lithium concentration solution have been widely used to study lithium plating in LiBs [7]. The electrochemical models cover both particle level and cell level dynamics. At the particle level, the mass conservation and diffusion dynamics at both electrodes are explained based on Fick's law [205]. At the cell level, it needs to describe the flow of lithium-ion in the electrolyte, the diffusion of lithium in the active material, and the electron charge transfer in the lithium-ion intercalation process at the surface of the active material. All of them are based on the porous-electrode model. The cell level and particle level dynamics are coupled through the local reaction current based on charge conservation. The properties of materials can be estimated based on the electrical measurements of the full cell [206]. The lithium plating criteria can be divided into two different kinds: (i) A saturation concentration at the interface; lithium plating would happen when the concentration of lithium-ions at the electrode interface reaches the saturation level [7, 57]. (ii) The interfacial overpotential; when the overpotential (η) is lower than 0 V against Li/Li^+, lithium plating would occur [7,57,98]. These criteria are applied in the electrochemical models to predict lithium plating. Arora et al. [38] made the first attempt to develop a physics-based mathematical model for investigating lithium plating on the negative electrode (graphite and coke) during charge and overcharge. This macro-homogeneous model was based on the work of Doyle and Newman [204]. Kinetic and thermodynamic parameters (e.g., transfer coefficient (α_a,α_c), exchange current density (i_0)) were adopted into the model to simulate the electrochemical reactions, mass transport, and other physical processes.

They assumed lithium plating is partially reversible. They found that the particle size and electrode thickness can influence the lithium plating phenomena [38]. As long as the electrode is thinner and has a smaller particle size, lithium plating is less favorable compared to thicker electrodes with larger particles [38]. However, many other features need to be added to this model to study lithium deposition in an overcharge reaction. Moreover, this model cannot capture the edge effects of the cell on the accumulation of the lithium-ions on the anode electrode during the charging process [207].

In another approach by Ge et al. [57], who used Newman's electrochemical model, also known as a pseudo-two-dimensional (P2D) model, to study lithium plating at low temperatures. They divided the total electrochemical reaction current density into two parts: the lithium intercalation current j_1 and the lithium deposition current j_2: [57],

$$j = j_1 + j_2 \tag{6}$$

Both of them can be described by the Butler-Volmer equation:

$$j_1 = j_{0,1}\left[\exp\left(\frac{\alpha_a F}{RT}\eta_1\right) - \exp\left(-\frac{\alpha_c F}{RT}\eta_1\right)\right] \tag{7}$$

where $j_{0,1}$ is the exchange intercalation current, α_a and α_c are the transfer coefficients which generally equal to 0.5, and η_1 is the overpotential for intercalation reaction.

$$j_2 = \min\left\{0,\ j_{0,2}\left[\exp\left(\frac{\alpha_{a,2} F}{RT}\eta_2\right) - \exp\left(-\frac{\alpha_{c,2} F}{RT}\eta_2\right)\right]\right\} \tag{8}$$

where $j_{0,2}$ is the exchange plating current, $\alpha_{a,2}$ and $\alpha_{c,2}$ are the transfer coefficients which are generally taken to be 0.3 and 0.7, respectively, and η_2 is the over-potential for lithium plating reaction. When the overpotential (η_2) is lower than 0 V against Li/Li^+, lithium plating would occur. They found that during low temperature charging when the overpotential (η_2) is minimum, lithium-ions start to accumulate at the anode-separator interface and then move into the anode electrode. This model also proposed a multi-step charging process that can charge the cell fast and safely without incurring lithium plating at low temperatures [57]. However, the model validation has been carried out with few data points.

Table 5
Advantages and Disadvantages of Lithium Plating Models in LiBs [7].

Criterion	Model	Advantages	Disadvantages
(i) The interfacial overpotential (ii) A saturation concentration at the interface.	Purushothaman et al. [212]	(a) Time-efficient calculation (b) Quickly iterate on cell design	(a)Only applicable at low C-rate and small electrode thickness (b) Not-accurate
	Arora et al. [38]	(a) Applicable to Predict the overall behavior of many systems. (b) High accuracy (c) Based on the internal electrochemical process	(a) Only focus on overcharging conditions. (b) Computationally expensive (b) Involve lots of manual tuning (c)Require deep understanding
	Tang et al. [207]	(a) Capture the edge effects (b) Easily iterate on cell design	(a). Long simulation time due to a large number of nonlinear equations (b) Extremely sensitive to the rate constant and charge rate
	Perkins et al. [209]	(a) Time-efficient calculation	(a) Only applicable at low C-rate and small electrode thickness

A P2D-modeling has been presented by Tang et al. [207] to study lithium plating during cell charging. They found that increasing the thickness of the negative electrode can hinder the deposition of lithium, specifically at the edge of the electrode. In another interesting approach by Tippmann et al. [206], a P2D electrochemical model was combined with a 0D thermal model to predict the aging at different temperatures (-25 °C to 40 °C) and currents (0.1 C to 6 C). They used COMSOL Multiphysics 4.2 to perform the simulation and compared the obtained results with EIS experiments. However, the implementation of this model into BMS is difficult due to the cost and time-consuming simulations while using the porous electrode theory.

Computational cost is also one of the challenges in lithium plating modeling due to a large number of governing equations (e.g., ten nonlinear and multidimensional partial differential in spatial directions x, r, t) that are required to be solved at the same time with the highly nonlinear algebraic expression for transport and kinetic parameters [208]. Liu et al. [50] developed a model that couples lithium plating with SEI growth, allowing simulating concurrent lithium dendrite growth, SEI growth, SEI penetration and regrowth. Their work highlights the effect of SEI in lithium plating. Boovaragavan et al. [208] proposed a reformulated physics-based model for real-time parameter estimation. Their model can simulate porous model equations in 15-45 ms with only 29-49 differential-algebraic equations (DAEs) while using the rigorous model, it takes 90-120s with at least 4800 DAEs. This model is suitable for predicting the capacity fade, but it has only been validated at the 2C rate of discharge [208]. A reduced-order model (ROM) was created by Perkins et al. [209], who defined five different assumptions, such as keeping the cell always in the quasi-equilibrium state for studying lithium plating during overcharge. This model is an optimized version of the Arora model to speed up the calculation of the governing equation in the ROM compared with the physical-based model. They could reduce the calculation time to 1/5000 by using ROM compared to the physical-based model. This ROM can only be implemented for short pulses (less than 10s) due to the quasi-equilibrium. Thus, it can recognize the time when lithium plating is about to occur in the charging

process [209]. A physics-based model by Wang et al. [210] studied the aging behaviors due to lithium plating and SEI growth of a plug-in electric vehicle (PEV) battery over a normal charge/discharge current at the ambient temperature. This model considered the SEI growth and lithium plating rate to explain linear and nonlinear behavior during cycling. The linear aging stage is linked to SEI growth. The transition from linear to nonlinear aging is associated with lithium plating. Recently, Lin [205] proposed a data-driven strategy that uses long short-term memory (LSTM) to monitor anode electrode potential in real-time to prevent lithium plating. Because physics-based model implementation is complex, time-consuming, and requires extensive manual tuning, real-time LSTM is far more computationally efficient and can be easily integrated into the BMS. The LSTM model can complete the entire test in 87 seconds, whereas the physics-based model takes 7 hours and 44 minutes.

6. Effect of Material Components and Charging Protocols on Lithium Plating

As shown in Fig. 10, developing high-performance fast-charging LiB without lithium plating requires a multidisciplinary approach. The previous sections have provided a comprehensive overview of the mechanisms, detection, and prediction of lithium plating. Extensive efforts have been made at multiple levels, including material component modification (electrode and electrolyte interfaces), cell and pack design optimization, charging protocol optimization, and the development of a battery management system to prevent the formation of lithium dendrites. The success of each approach can greatly improve the fast charging performance of lithium-ion batteries. As a result, we will review the existing literature on material components, cell design, and charging protocol approaches in terms of their strengths and weaknesses in the following sections.

6.1. Effects of Material Components on Lithium Plating

LiB material components, such as electrodes and electrolytes, have a significant impact on lithium plating. Many studies have been conducted from a material perspective to improve the lithium-ion cell for fast charging while suppressing lithium plating. The approaches proposed with an emphasis on material properties can be divided into two groups. As shown in Fig. 11 (A) [211], group A is focused on anode material modification, whereas group B is focused on advanced electrolyte adoption. In group A, the modification of anode martial can be further categorized into five groups in terms of their functions and effects on the charge transfer process. In group B, adopting advanced electrolytes could be further divided into three subgroups: (1) introduction of low viscosity co-solvents and esters, with improvement in ionic conductivity and electrolyte diffusion; (2) introduction of electrolyte additives to obtain desirable SEI properties; and (3) introduction of optimal Li^{+-} transfer number.

Based on the aforementioned classification, considerable efforts have been made to introduce a potential liquid electrolyte with enhanced transport as well as a fast-charging capable anode electrode that can prevent lithium dendrite formation. Recent advances in the improvement of the charge transfer process (rate performance) are discussed below. For a more precise comparison of the different strategies, the advantages and disadvantages of each strategy are summarized in Table 6.

Anode material modifications are necessary since it has a significant impact on the lithium plating in LiBs. The most practical anode material in the current market is graphite due to its low working potential, high capacity, and long cyclic life [12]. However, the activation energy of charge transfer, which is dependent on Li^{+}desolvation at the SEI layer and lithium diffusion in small graphite interlayer spaces (0.335 nm), limits the lithiation rate capability of graphite anode materials, resulting in lithium plating [213]. Hard carbon and soft carbon are two other carbonaceous-based compounds used as anode materials. Because of the larger interlayer space, these materials exhibit higher intercalation rates than graphite [214]. Nonetheless, due to low CE and high raw material costs, these materials are not widely used in today's market.

The size and structure of graphite particles, such as flake-like and spherical, can influence charge acceptance [7,215]. Park and his colleagues demonstrated that lithium plating occurs more frequently in graphite with flake-like particles than in graphite with spherical particles [216]. Graphite with flake-like particles is typically used in the market due to the low price. Cheng et al. [213] designed a multi-channel structure that significantly increased the intercalation sites by making holes on the graphite surface with KOH etching. A hybrid anode was developed which consists of an edge-plane activated graphite and Si nanolayer (SEAG), where the activated edge-plane increases the site reaction [217]. Nanoscale Si coating layer enhances the energy density while reducing the Li^{+} diffusion path by increasing accessible reaction

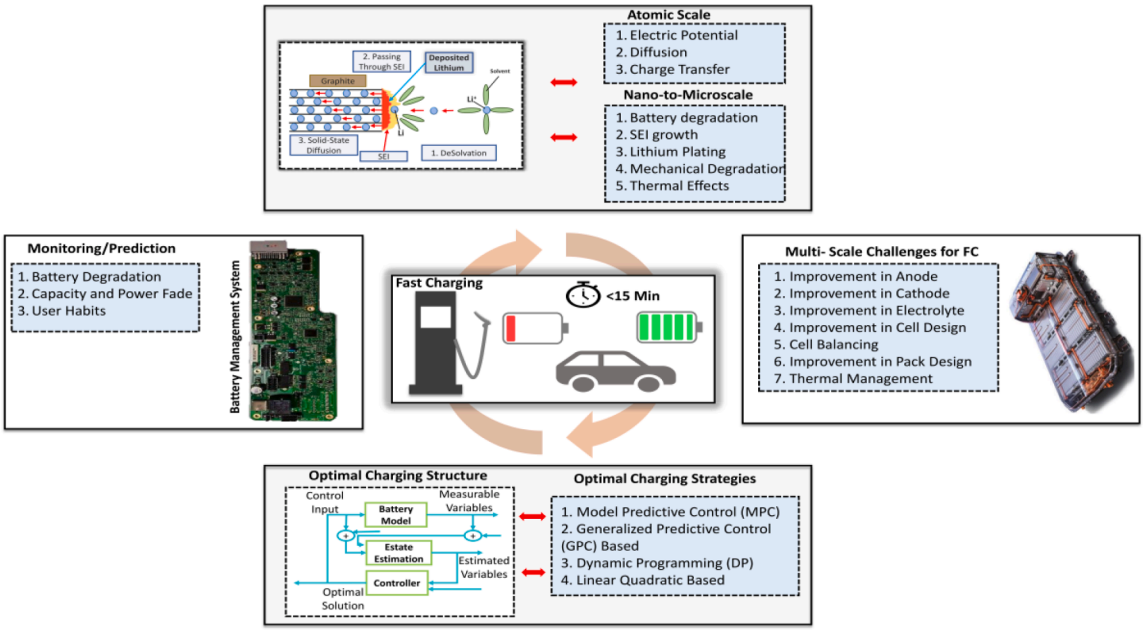

Figure 10. Fast Charging Process.

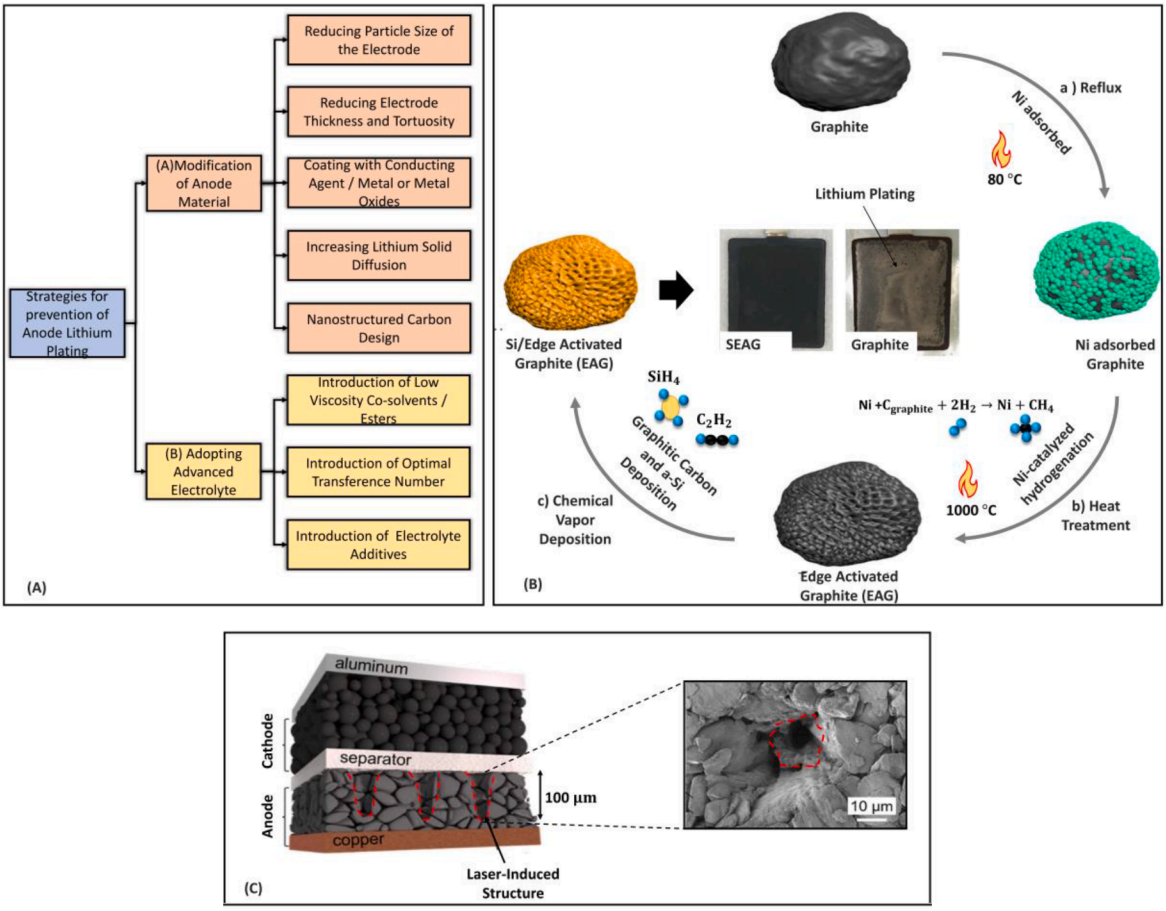

Figure 11. Electrode Modification and Mitigation Strategies.
A) Classification of existing mitigation strategies based on the material components**. B)** The procedures for the fabrication of SEAG composite. a) reflux: spherical nickel nanoparticles (size 500 nm) are adsorbed on the Mesocarbon Microbeads (MSMBs) with the use of reflux technique (80 ^{o}C), b) heat treatment: the holy structure of the sample is a result of two steps, first heating the sample at 1000 ^{o}C in a Hydrogen (H_2) environment, then the penetration of adsorbed Ni nanoparticles into the graphite with the methane (CH_4) gas evolution, c) Chemical vapor deposition: CVD method was used with C_2H_2 and SiH_4 gases to distribute graphitic carbon and a SiO nanolayer on the graphite with holy structure. As a result, no lithium plating was observed on the cell with the SEAG electrode after 50 cycles, while significant lithium plating was observed on the cell with a graphite electrode (Reprinted from Kim et al. [217] with permission of Nature Communication). **C)** Detailed illustration of a cell with the laser-structured graphite anode and unstructured NMC cathode and an SEM image (resolution 10 µm) of a structured hole with a lateral length of 100 µm (Reprinted from Habedank et al. [215] with permission of Electrochemical Society).

sites. The fabrication of SEAG composite includes simple steps which are: a) reflux, b) heat treatment, and c) chemical vapor deposition (CVD). The SEAG electrode showed improvement in capacity retention (99.3%) at a current density (1.75 mA/cm^2) for 50 cycles. Moreover, a stable CE (> 93.8%) is achieved with a high specific capacity (525 mAh/g) in the first cycle. Additionally, the effect of fast charging (> 3 C) on the SEAG electrode was examined, as shown in Fig. 11 (B), no lithium plating was observed on the SEAG electrode for the first 50 cycles, while a significant amount of the deposited lithium was observed on the graphite electrode [217].

The use of electrodes with reduced tortuosity is another approach, which is especially useful for thick electrodes to prevent lithium plating. The Li^+move in the electrolyte through the porous electrode, the diffusion rates of the Li^+ highly depends on the microstructure of the electrode, which is called tortuosity [215]. A lower tortuosity yields a higher rate capability and improvement in capacity retention, where a high tortuosity slows down Li^+ transport in the electrodes and increase the concentration gradients [218]. Reducing the tortuosity for thick and dense electrodes would be beneficial for developing materials for fast charging. Recently, Habedank and co-workers investigated the effects of anode tortuosity on lithium plating [215]. The tortuosity was reduced by using a laser structuring technique (pulse duration 150 ps/frequency 1.200 MHz) to remove a tiny fraction of the electrode material. As shown in Fig. 11 (C), many holes in a hexagonal pattern with a lateral length of 100 µm were made. They used OCV (after charging) as a detection technique. Lithium plating was significantly reduced in the cell at 2 C charge rate and 0 ^{o}C compared to the conventional cell. However, laser structuring of the graphite anode was not effective at -15 ^{o}C due to very slow lithium diffusion in the graphite particles. In another study, Kraft et al. [218] applied laser structuring to modify the pore morphology of the graphite anodes. Charging time was reduced by 15 % to 17 % for a 3 C charge, and almost no lithium plating was observed.

As mentioned earlier, strategies to prevent lithium plating are not only limited to the anode modifications. The electrolyte is the media in which Li^+ ions move between the cathode and anode electrodes, and the electrolyte also affects the properties of the SEI layer. Organic solvent blends for electrolyte is made of a mixture of ethyl methyl carbonate (EMC), ethylene carbonate (EC), dimethyl carbonate (DMC), and diethyl carbonate (DEC), where DEC, EMC, and DMC have a lower melting pointing and viscosity compared to the EC [219]. EC has a high dielectric constant and is traditionally included in the electrolyte as it can help form SEI on the graphite layer. Adding aliphatic esters alongside the linear carbonates, such as DMC and EMC, which have lower melting points and viscosity, would have a positive impact on the performance of the electrolyte [16]. Dahn et al. [219] have studied using the most typical type of solvents esters such as methyl acetate (MA),

Table 6
Advantages and Disadvantages of Material Based Strategies for Lithium Plating Mitigation

Material Based Strategies for Lithium Plating Mitigation	Material Components Modification	Advantages	Disadvantages	Refs.
	Reducing Particle Size of the Electrode	(a) Shortened lithium diffusion path (b) Enhance energy density	(a) Low electronic conductivity (b) Volumetric expansion	[215,213, 217]
	Reducing Electrode Thickness and Tortuosity	(a) Higher Li-ion diffusivity rate (b) Improvement in capacity retention	(a) Low performance at subzero temperatures	[215,218]
Modification of Anode Material	Coating with Conducting Agent / Metal or Metal Oxides	(a) Excellent electrical conductivity (b) Improve Electrode kinetics (c) Higher lithium-ion diffusivity	(a) Coulombic efficiency drops (b) Adverse effect on specific capacity	[108,215]
	Increasing Lithium Solid Diffusion	(a) Higher lithium-ion diffusivity (b) Improve high-rate charge (c) Improve low-temperature performance	(a) Coulombic efficiency drops (b) Severe parasitic reactions	[19,20]
	Nanostructured Carbon Design	(a) Increased energy (b) Shortened lithium diffusion path	(a) Costly process (b) Not applicable for large scale	[215,232]
Adopting Advanced Electrolyte	Introduction of Low Viscosity Co-solvents / Esters	(a) Improve high-rate charge (b) Increase in ionic conductivity (c) Improve low-temperature performance	(a) Failure in properly SEI layer formation (b) Negative impact on calendar life (c) Gas generation (d) Coulombic efficiency drops	[219-221]
	Introduction of Optimal Transference Number	(a) Increased power densities (b) Improve high-rate charge (c) Improvement in capacity retention	(a) Corrosion of the current collector	[222-226]
	Introduction of Electrolyte Additives	(a) Improve low-temperature performance (b) Forming effective SEI (c) Reduce anode interface resistance are	(a) Prone to lithium plating (b) Increase polarization at the anode	[228-231]

ethyl acetate (EA), methyl propionate (MP), and methyl butyrate (MB) in the electrolyte to improve the charging speed of lithium-ion cells. They found that MA is the most suitable co-solvent as it has the lowest viscosity compared to the EMC and DMC (Fig. 12 (A)). Therefore, esters (MA) were added at a fraction of 20 % and 40 % to the (NMC532)/graphite cells that were cycled at 1 C, 1.5 C, and 2 C charge rates, leading to a 50 % increase in ionic conductivity. As shown in Fig. 12 (B), significant capacity fade at 2 C charging occurred due to lithium plating in the cells without MA. However, cells with 20 % and 40 % MA did not show any capacity fade. Other research groups also investigated the effects of esters such as MA or EA as co-solvents in LiB electrolytes, where all of them agree that using esters can significantly improve low-temperature performance and rate capability of cells. They also found the negative effect of using esters. The SEI layer can not be formed properly, and the cell cycle life is reduced because esters cause other side reactions, such as gassing and CE drops [220,221].

Transference number (t_+) is defined as the fraction of the ionic conductivity contributed by the Li^+ions [16,222]. The importance of the transference number, especially at rates above 2 C, is highlighted in Fig. 12 (C). The optimal transference number should be close to 1. Even when the electrolyte has a low conductivity, a high transference number can still provide good power densities and enable high-rate charging [222]. However, due to the formation of large solvation shells around the Li^+, the transference number in existing liquid electrolytes ranges between 0.30 and 0.40. Approaches to increase transference number can be divided into two groups: (a) immobilizing the anions (using salts with bulky anions) [223,224], (b) increasing electrolyte concentration (nonaqueous polyelectrolytes) [225,226]. Du and colleagues investigated the effects of the lithium bis(fluorosulfonyl)imide (LiFSI), as an alternative to the typical salt hexafluorophosphate ($LiPF_6$) in the graphite - $LiNi_{0.8}Co_{0.1}Mn_{0.1}O_2$ pouch cells [227]. Cell capacity retention and fast charging capability have been significantly improved, as the LiFSI have a higher transference number ($t_+ = 0.495$) and ionic conductivity compared to the $LiPF_6$($t_+ = 0.382$). Additionally, a smaller amount of lithium plating was observed on the graphite electrode in the LiFSI electrolyte after 500 cycles compared to the $LiPF_6$ electrolyte (Fig. 12 (D)). In fact, Li^+ can move faster in LiFSI, as LiFSI have bulky anions (FSI^-95 $Å^3$) compared with $LiPF_6$ (PF_6^-69 $Å^3$). However, using LiFSI may cause anodic corrosion of the aluminum cathode current collector.

The effects of electrolyte additives on the performance of LiBs have been extensively investigated over the last decade. Electrolyte additives play a critical role in forming the SEI layer. To improve the fast charging capability, the desirable SEI layer should be thin, compact, and less resistive with high ionic conductivity [228,229]. Using electrolyte additives, such as vinylene carbonate (VC), lithium bis (oxalato) borate (LiBOB), fluoroethylene carbonate (FEC), showed significant improvement in terms of performance and lifetime at a lower charge rate [230, 231]. However, it may also increase the chance of lithium plating due to the formation of a highly resistive SEI layer by adding the above additives. Adding LiSFI as an electrolyte additive in (1.0 M $LiPF_6$ in EC + EMC + MP (20: 20: 60 vol%) can improve the low temperature performance and reduce lithium plating [230]. A comprehensive review of recent advances in electrolyte composite for fast-charging can be found in Ref. [16].

Besides the material selection and microstructure modification discussed in the previous section, the selection of electrode and cell geometrical parameters (cell and pack design) and the design of advanced battery thermal management systems (high-temperature homogenization) are also important. Approaches such as increasing the porosity and the width of the anode are widely used in literature as a method to prevent lithium plating. However, they may also lead to a reduction in capacity [231]. The negative to positive ratio (N/P) is closely related to lithium plating, where values greater than 1 are typically used for commercial cells. Mechanical stresses on the anode are reduced with the higher N/P ratios, resulting in a decrease in SEI

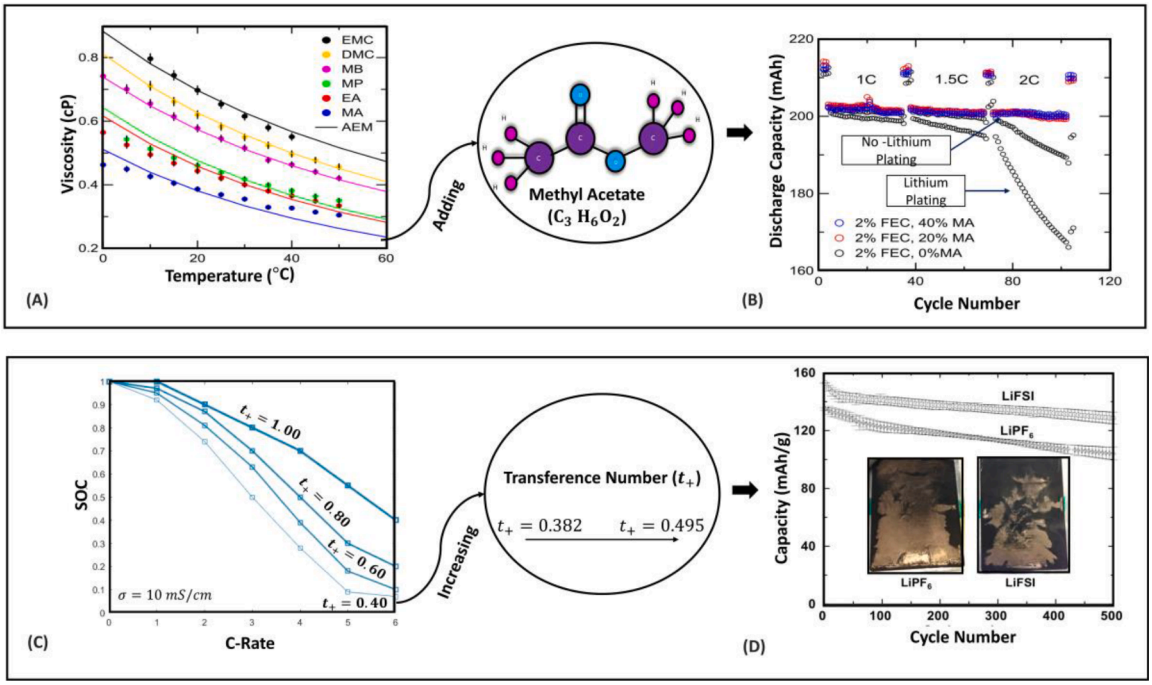

Figure 12. Electrolyte Adaptation and Mitigation Strategies.
A) The viscosity of different esters and carbonated co-solvents was measured as a function of temperature (-25 °C to 40 °C), solid lines show the viscosities that measured from the advanced electrolyte mode (AEM). **B**) Discharge capacity against cycle number; after adding 20 % and 40 % of MA, two similar cells were designed and evaluated. All cells were charged at 1 C, 1.5 C, and 2 C rates at 20 °C, cells without MA showed significant capacity fade due to lithium plating (Reprinted from Dahn et al. [219] with permission of Electrochemical Society). **C**) Attainable SOC against C-rate for electrolyte with a constant ionic conductivity (10 mS/cm), the positive impacts of high transference number is highlighted at 2 C charge rate and above (Adopted from Diederichsen et al. [222]). **D**) long term cycling (500 cycles) performance for two cells with $LiPF_6$($t_+ = 0.382$)and LiFSI ($t_+ = 0.495$), both cells were charged at 5 C rate for 12 minutes. Capacity fade for the cell with LiFSI at the first cycle was about 153.2 mAh/g, which was 134.3 mAh/g for the same cell after 500 cycles (84 % retention). Capacity fade for the cell with $LiPF_6$ at the first cycle was about 135.4 mAh/g, which was 110.6 mAh/g for the same cell after 500 cycles (77 % retention) (Reprinted from Du et al. [227] with permission of Elsevier).

formation and associated LLI. Kim and colleagues investigated the effect of various N/P ratios on 1.4 Ah pouch cells. In cells with N/P ratios greater than 1.10, no lithium plating was observed at 0.85 C and 25°C. They demonstrated that designing the anode capacity at least 20% bigger than the cathode capacity is an effective strategy to suppress lithium plating [233].

However, the optimal ratio may also be affected by other parameters in the battery, such as the electrode material and battery form parameters. Especially for large cells, the battery form parameters affect the current and temperature distribution. In large cells, the current distribution is very important, because a uniform current distribution can reduce the risk of lithium plating. Details of cell and pack design and their impacts on lithium plating can be seen in reference [61].

6.2. *Effects of Charging Protocols on Lithium Plating*

Several mitigation strategies were discussed in the previous section from a material standpoint. Although they show promising results, most of them are complicated and time-consuming to execute and are not compatible with large-scale manufacturing. As a result, many researchers have focused more on cell and pack-level solutions, such as charging strategies, which can usually be implemented in actual systems. Charging protocols determine how the current changes during the charging process. The improvement of the charging protocols would be beneficial for mitigating the formation of lithium dendrite on the graphite surface [19,70,234]. Conventional charging protocols include constant-current constant-voltage (CC-CV), multistage constant current (MSCC), pulse charging (PC), and boost charging (BC). These methods are based on predetermined charging parameters with constant voltage, current, or power (Fig. 13) [235]. These techniques are simple and ignore the detailed battery response in each stage. Optimizing the charging protocols according to the battery dynamics could be useful. In the following subsections, we review different charging protocols and their characteristics, along with a discussion of strategies that can reduce the charging time without sacrificing battery health. Table 7 highlights the advantages and disadvantages of each charging protocol.

6.2.1. *Constant Current Constant Voltage (CC-CV) Charging*

The standard constant current-constant voltage (CC-CV) is a combination of the constant current (CC) and constant voltage (CV) methods, which is the most commonly-used technique for charging the LiBs [70, 236]. The CC-CV charging profile starts with the (CC) phase until the cell voltage reaches a predefined voltage (cut-off voltage). Then the process switches to CV phase, maintaining the constant cell voltage. The charging process stops when the charging current drops below a predetermined low value(I_{end})(Fig. 13 (A)). The CC-CV technique is simple and useful for various battery types. However, the charging time is usually long due to CV phase [234]. One of the main reasons for battery degradation in CC-CV high-rate charging is lithium plating because the high charge rate triggers favourable conditions for lithium plating [237]. Some researchers proposed some methods that may reduce lithium plating during the charging process, such as modifying the electrode thickness, adding electrolyte additives, and using smaller active material particles in the negative electrode [37,214,238]. Tippmann et al. [206] performed a charging experiment in which, CC phase continued until it reached 4.2 V (cut-off-voltage) followed by CV phase to investigate CC-CV charging parameters for LiBs to prevent anode lithium plating at sub-zero temperatures. Ref. [239] studied the effect of high charge current rate and high charge voltage on the cycle life of a 900-mAh wound prismatic cell, and found that a cut-off voltage higher

than 4.2 V, a long charge period at 4.2 V, and a high charge rate above 1 C will significantly reduce the cell cycle life. Zhang et al. [240] studied the effect of charging currents and temperatures on the electrode's potential during the CC-CV charging and showed that the anode potential is decreased at high charging rates and low ambient temperature. Lithium plating could occur at the end of the CC phase and continue until the charge current reaches the predetermined value.

6.2.2. Multistage Constant Current (MSCC) Charging

The multistage constant current (MSCC) method can be a suitable alternative to the CC-CV charging protocol [7]. MSCC is designed to charge LiB through a series of decreasing currents ($I_{ch1} > I_{ch2} > I_{ch3} \ldots > I_{chn}$) [70]. The MSCC consists of several CC steps. At each stage, the charging current has a predefined value. Charging continues until the voltage reaches its upper limit. Then the charge current is reduced to the next level accordingly and the charging process continues until all the stages are completed (Fig. 13 (B)) [70]. The decreasing charging rate over time can help reduce the chance of lithium plating on the anode surface. MSCC fast charging technique was introduced in Ref. [241] for charging a high-power LFP cell. The charging pattern was divided into three stages to recharge a cell in 20 min. No cell overheating was observed during the charging process. MSCC optimization technique was proposed in Ref. [242] based on Taguchi's method to calculate the magnitude of each current step in the MSCC charging pattern. They charged a cell up to 75% capacity in 40 min. This method can be easily implemented into the battery charging and testing equipment. Tanim et al. [53] proposed an MSCC charging protocol to examine XFC cycling behavior in different cells. In the proposed MSCC charging protocol, they maximized the magnitude of CC charging by minimizing the cell overpotential (< 0.25V). Zhang et al. [243] studied the effect of three charging protocols (MSCC, CC-CV, and constant power-constant voltage (CP-CV)) on the capacity fade of commercial 18650 cells. They found that the rate of capacity degradation is minimum when using CP-CV at 1 C rate compared with other charging protocols.

6.2.3. Pulse Charging (PC)

Pulse charging is a fast-charging method [212,244]. In PC, the charging current to a LiB consists of pulses characterized by frequency, duty cycle, pulse current peak, and pulse width. In order to control these parameters, the internal states of LiBs are needed (Fig. 13 (C)). PC improves the charging performance due to the short relaxation times or discharge pulses which reduce the concentration gradients and anode overpotential. Therefore, this technique can reduce the risk of lithium plating. Another useful approach was proposed by Purushothaman et al. [212]. They developed a macro-homogeneous lithium diffusion model for conventional and pulse charging protocols. They determine the charging current waveform based on the lithium concentration. The charging pulse width and the rest pulse width were determined. Their pulse charging method is 2.6 times faster than the typical method. Hasan et al. [245] presented an electrochemical thermal coupled model to study the impact of different temperatures and charging rates on PC, CC-CV, and BC protocols. They found that the pulse charging protocol is the fastest one among others and has maximum efficiency. Monte Carlo simulation was used by Aryanfar et al. [246] to study the dendrite growth during the pulse charging process. They showed that using shorter pulses (1 ms) with 3 ms relaxation time can hinder lithium dendrite growth. However, they did not study the impact of ambient temperature during their experiments. PC technique requires a good understanding of LiB internal states. Also, implementing PC into chargers requires a complicated control algorithm.

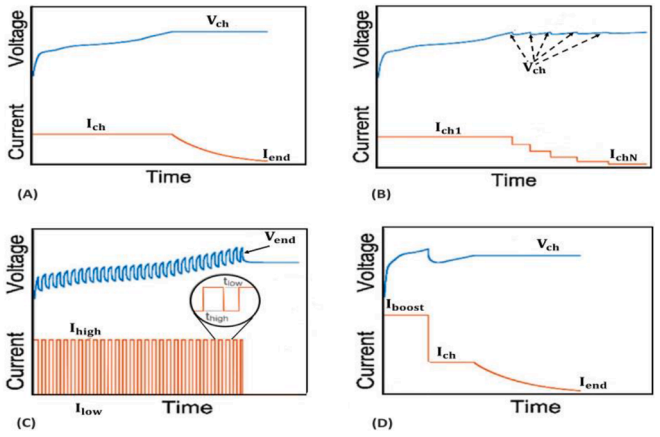

Figure 13. Schematic of General Fast Charging Protocols. A) Constant Current-Constant Voltage, B) Multi-stage Constant Current, C) Pulse Charging, D) Boost charging (Reprinted from Keil et al. [70] with permission of Elsevier).

Table 7
Advantages and Disadvantages of Charging Protocols

Charging Protocols	Advantages	Disadvantages	Consider lithium plating	Refs.
Constant Current – Constant Voltage (CC-CV)	(a) Simplicity (b) Ease of implementation (c) Reliable at mid to low charging rates (d) Chargeable up to max. capacity	(a) It is not suitable for rapid charging (b) Not time-oriented due to the long CV stage (c) Impedes overcharging the battery (d) Reduces the cyclic life of the battery	By choosing appropriate constant current and voltage	[70, 236, 262]
Multi Constant Current – Constant Voltage	(a) Prolonged cycling life (b) Improve energy transfer efficiency (c) Improve cell capacity retention	(a) Limited in application to pouch cell (b) Needs to estimate the SOC accurately during the process. (c) Increases the implementation costs	Limited effect on lithium plating	[70, 242, 241, 235]
Pulse Charging	(a) Shortening charging time (b) Reduce the impedance accumulation of anode electrode (c) Reduce the polarization	(a) Pulverization of the electrode particle due to informal cycling performance (b) Increase heat generation in the connected parallel pack (c) It is so complicated and costly (d) Require an accurate estimation for selecting the appropriate parameter for pulse sequence.	The pauses during charging can prevent lithium plating	[263, 236, 246, 235]
Boost Charging	(a) Shorter charging time (b) Ease of implementation (c) Reduce the degradation effects	(a) Temperature is not considered (b) The charge rate is not optimized	–	[70, 235, 247, 235]

6.2.4. Boost Charging (BC)

The boost charging method is another form of MSCC. The cell is charged using a high current (I_{boost}) at the beginning of the charging

process for a short period which is called the boost-charge period, and is then followed by a conventional CC-CV method (Fig. 13 (D)) [70]. The boost-charge period is terminated based on a predefined maximum voltage $V^{max}$and time value t_b. Notten et al.[247] proposed the BC protocol on the cylindrical (US18500, Sony) and prismatic (LP423048, Philips) cells. They compared BC with the conventional CC-CV in terms of charging time and cyclic life performance. Both cells can be charged to 30% of the cell capacity in 5 mins for 700 times without any degradation. Keil et al. [70] studied different charging protocols and the effect of charging currents and charging voltages on the cycle life of three high-power 18650 cell types. They showed that the cell cycle life could be reduced in BC protocol at high charging rates and high or low SOCs. However, in both above studies, the impact of temperature on the charging process was not considered.

6.2.5. Charging of Electric Vehicles

EV companies try to address the issue of 'range anxiety,' which is one of the primary market barriers for EVs [248,249]. Depending on the ambient temperature, charging a Nissan LEAF with a typical 50 kW charger can take anywhere from 30 minutes to 90 minutes to reach 80 % SOC [250]. Among EV manufacturers, Tesla was the first to offer superchargers with a recharge rate of 120 kW [251]. They also just upgraded the supercharger's charging rate to 225 kW [252]. Last year, Porsche developed an ultra-rapid charger rated at 350 kW (800 V) in Berlin for the new Taycan model released to the market in 2020 [253, 254]. The Tycan ultra-rapid charger with a maximum charging capacity (peak) of 270 kW can charge the battery from 5 % to 80 % in just 22 minutes [254]. Despite the recent development, the current charging solutions are still far from what EV consumers expect. Charging up to 80% SoC in 15 minutes by 2023 is a goal set by the U.S. advanced battery consortium [255]. To achieve the 15-minutes refueling for a large battery pack size (for example, >90 kWh), at least 300 kW charging power is required [214].

Various charging standards have been developed around the world. IEC 62196 is a global standard issued by the International Electrotechnical Commission (IEC) that acts as an umbrella standard for many charging standards. The umbrella standard addresses the fundamentals of power and communication interfaces, whereas other charging standards address the mechanical and electrical requirements for plug and socket assemblies [256]. Charging standards are classified into four categories [256]: (i) SAE J1772, which is used in North America for ac and dc charging, (ii) VDE-AR-E 2623-2-2, which is used in Europe for single-phase and three-phase ac charging, (iii) JEVS G105-1993 (also known as CHAdeMo), which is developed in Japan and used globally for high-power dc charging, (iv) Charging standard provided by Tesla [251]. Tanim et al. performed pack-level evaluations using two Nissan Leaf battery packs (2012 model year) [257]. They evaluated the effect of 50 kW (approximately 2C) direct current rapid charging on a full-size electric vehicle's battery pack compared with a pack charged at 3.3 kW (the standard alternating current level 2 charging). They investigated various aging modes using IC analysis. The primary aging modes in the cells tested with AC Level 2 and DCFC charging protocols were found to be LLI and LLM in the negative electrode. Lithium plating was not observed at any stage of the test at any of the three temperatures (20°C, 30°C, and 40°C) [257].

6.2.6. Optimization Methods for Fast Charging

The current standard fast-charging protocols are mostly model-free strategies, which means they are based on charging profiles with fixed values and do not use any mathematical models. The existing protocols cannot achieve optimal charging performance in terms of charging efficiency and charging time. Therefore, developing optimal charging algorithms is essential to meet the requirements. The LiB charging structure is shown in Fig. 10, which includes the battery model, state estimator and model-based controller [235]. In general, optimal charging strategies are formulated based on battery models. Zou et al. [258] divided optimal charging strategies into two categories based on the type of battery model used in the development process: (I) ECMs, which fit the electrical and thermal behavior using an equivalent circuit consisting of a voltage source, several resistors, and capacitors. This model is known for its simplicity. The results of ECMs are less accurate due to the simple structure of the model. (II) Electrochemical-based model, which is based on the ion diffusion dynamics, intercalation kinetics, and electrochemical potentials [235,259,260]. Based on the state estimator and reduced-order battery model, an optimal charging algorithm is developed [235]. Many optimal control algorithms were developed, such as (i) model predictive control (MPC)-based, (ii) generalized predictive control (GPC)-based, (iii) dynamic programming (DP)-based, and (iv) linear quadratic-based. MPC, as one of the most powerful and advanced control techniques, has been widely used in industrial process control. For the multiple objectives during the charging process, MPC is one of the most promising techniques to meet these objectives [235,261]. MPC can be implemented in BMS due to its simple structure and computational efficiency.

7. Challenges and Future Trends

Lithium plating has been widely investigated in the last decade. However, some problems remain, such as accurate and reliable detection methods, mechanisms, prediction, and prevention. In this section, challenges and prospects are introduced in the aspects of mechanisms, detection methods, modeling, material components, and optimized charging protocols.

7.1. Mechanisms Study

Understanding the lithium plating mechanism is the key to advancing fast charging technology. Most of the current studies are conducted in the laboratory, which is useful to understand lithium plating mechanisms [45]. However, the results obtained from laboratory experiments cannot be easily validated in large-scale engineering applications [45]. Considering electric vehicles equipped with a large battery pack, electrical contacts between different parts of the system, mechanical forces, and vibrations may affect the behavior of lithium plating in the cell [264]. Therefore, the results from the lab may become inaccurate when applied in the actual vehicle [265]. Taylor et al. [266] showed that even the laboratory experiments on the same battery cell could have a 4% error. They divided the errors into two types: procedural and environmental. Procedural errors occur during the experiments, such as set-up variations. Environmental errors include room temperature, humidity, and measurement accuracy [266]. For example, a recent study by Tanim et al. [53] showed that lithium plating behavior could be different between two same cells (NMC532 pouch cell) cycled under the same XFC conditions. Therefore, a major challenge in studying lithium plating mechanisms in laboratories and large-scale applications is how to ensure accurate and reliable results at different charging conditions.

The impact of vibration on the electrochemical performance of a single cell or an EV battery pack has not been investigated. Based on the previous study, the pouch cell does not experience any degradation under vibration [267]. However, when going through the z-vibration, the cylindrical cells appear to show an increase in the internal resistance, which may cause power capability decline [268]. Vibration could cause the SEI layer to break [269] and SEI has been shown to interact with lithium plating [50]. Moreover, it is well-known that temperature plays a vital role in the performance of LiB. During low-temperature charging, the resistance of charge transfer increases, and lithium plating may occur, which leads to significant battery capacity fade. Thus, accurate measurement of internal temperature would be helpful for a deeper understanding of the lithium plating mechanism. In the literature, the cell temperature can be adjusted in a thermal chamber. However, battery cells in electric vehicles are located in a battery pack

where the temperature can decrease slowly and the internal temperature and heat generation of cells cannot be monitored easily [270]. There are methods in the literature to measure cell temperature based on the thermal models [64]. These methods are computationally costly and challenging to implement. Besides, accurate measurement of battery core temperature is still challenging in real-time applications. A method for internal temperature estimation is proposed in [271]. The authors proposed an internal temperature estimation approach using a recurrent neural network which was trained based on the temperature signal measured by a thermocouple inserted into a cylindrical cell. However, the method was only tested on a single cell, not a battery pack. Two important questions remain: what is the core temperature of the cells in the automotive battery packs, how does it affect the lithium plating. Unfortunately, there are limited studies on lithium plating mechanisms under real-world EV operation conditions. A better understanding of the relationship between battery testing environment and local electrochemistry is needed. Further research on lithium plating mechanisms under actual EV operation conditions is needed.

Another important aspect of studying lithium plating at the cell level is related to overall safety. It is necessary to understand the negative impact of lithium plating on safety. According to the literature, internal short circuits caused by lithium dendrites are safety concerns. The thermal runaway caused by lithium plating on the anode surface has been studied, and most of the studies have theoretically explained the possibility of thermal runaway due to lithium plating. Recently, Li et al. [272] explained that the reaction between plated lithium and electrolyte could release enough heat after fast charging to activate the thermal runaway, and the temperature rise rate decreases as the plated lithium is completely consumed. Commercial battery cells with a considerable amount of lithium plating can still be cycled hundreds of times without any explosion, short circuit, or other safety hazards [54]. Therefore, an important question is whether lithium plating is really a dangerous safety issue.

It is still difficult to understand the lithium plating mechanism at the atomic level, as lithium plating is a reversible/irreversible reaction. If all the lithium deposited on the surface of the anode is reversible, the cell will not lose capacity. Therefore, another important question is what variables affect the reversibility. There is an urgent need to study the factors that affect the reversibility of lithium plating, which can mitigate lithium plating in various applications.

7.2. Detection Methods

Since lithium plating significantly affects the capacity of LiBs, much research has been conducted to design and develop methods for detecting lithium plating. Characterization methods for analyzing the morphology and material composition are available. TEM, SEM, FTIR, XPS, and acoustic methods have been used in many studies to observe and quantify the deposited lithium on the anode surface. Physical characterization approaches for both surface morphologies and chemistry are commonly used for fundamental studies to gain a deep understanding of the lithium plating process in the laboratory. However, they can not be used for real-time lithium plating detection in actual engineering applications. In ex-situ studies, sample transfer while avoiding contamination is required. Due to the difficulty of quantifying the lithium plating process during cycling, ex-situ techniques cannot provide enough dynamic information [156]. Techniques such as X-ray diffraction (XRD) are known as techniques that can characterize the local lithium plating in fully assembled cells [53]. It is challenging to study ex-situ lithium plating, because the deposited lithium is partially reversible and most of the reversible lithium plating could be gone after sample transfer [155]. Several non-destructive electrochemical methods have been developed. Some of them require specialized instrumentation such as high precision coulombmeters, while others, such as RE technique, require special cell design. In-situ electrochemical methods rely on electrochemical parameters such as voltage, current, and capacity [153,154]. In the literature, analyzing voltage plateau after discharging or relaxation and analyzing IC curves are some of the most promising methods for detecting lithium plating [54]. However, new studies show that when the amount of deposited lithium is small, the voltage plateau technique could provide incorrect results [60]. Fear et al. [60] showed that battery capacity fade could be prevented by detecting lithium plating when graphite starts lithiation. However, none of the existing techniques can detect and quantify lithium plating in real-time when the battery is in the charging process. Recently, Konz et al. [195] developed an in-situ method for detecting lithium plating using differential open-circuit voltage (dOCV) analysis. Knowing the starting point of lithium plating is very useful for charging protocols to prevent lithium plating. However, it is not clear how much lithium must be deposited on the anode surface to detect the dOCV plating signal. In another interesting approach, Carter et al. [273] introduced a new in-operando technique for detecting lithium plating. They detected the onset of lithium plating under two transient thermal conditions (transient 10 to 0 ^{o}C and 40 to 0 ^{o}C). The deposited lithium was increased by charging the battery under transient thermal conditions, and a negative differential voltage occurs. They mentioned that the negative differential voltage in the charge voltage could be used as a signal to detect the onset of lithium plating in the BMS algorithm. Several in-situ electrochemical lithium plating detection techniques based on the reversible part of lithium plating have been proposed. However, only a few of them can measure or estimate the irreversible part via online measurements. Therefore, further research should develop a better in-operando method that can distinguish and evaluate the ratio of reversible and irreversible lithium plating and stripping during the fast charging.

7.3. Lithium Plating Modeling

Electrochemical models are usually used to simulate lithium plating. They can be used to study the long-term behaviors of LiBs. One of the problems for electrochemical models is the difficult parameterization due to a large number of parameters [206]. Developing sophisticated models that capture the interaction of lithium plating with other side reactions, such as SEI growth, can help understand the lithium plating mechanisms and battery degradation [50]. The models need to be simplified so that they can be implemented in the BMS for real-time monitoring. The charging strategy can use the feedback from electrochemical models to adjust the charging current to prevent lithium plating and extend battery cycle life. With machine learning algorithms, data-driven methods can become a promising solution and are expected to play an important role in predictions, especially for lithium plating predictions. However, they require a huge amount of training data. Recently, Dubarry et al. [274] proposed a mechanistic framework that works backward compared with the conventional battery model, which means the model input is the degradation and the model's output is the voltage and capacity of the cell. This makes the technique ideal for producing training data. They produced the first synthetic dataset to train diagnosis and prognosis algorithms.

7.4. Material Components and Optimized Charging Methods

Many research groups have investigated each LiB component separately to prevent lithium plating on the anode electrode. Some of the important approaches for suppressing lithium plating are: adopting advanced electrolytes, reducing the lithium-ion path by changing the structure of the anode electrode, and introducing hybrid and optimized charging protocols. However, any changes in internal components may adversely affect other battery components [214]. Moreover, most of the existing strategies are only focusing on suppressing lithium plating, but other factors, including final production cost and the requirement of new manufacturing techniques, need to be considered because the cost is a very important factor in large-scale applications.

Most existing charging protocols are only validated for specific types

of cells at fixed temperatures. However, under fast charging conditions, each type of cell has a different response. Validating charging protocols for each type of cell is a time-consuming process. Therefore, developing reliable cell and battery pack models is important to speed up the development of fast charging protocols. The charging protocols need to be optimized to effectively control lithium plating. The optimization of the charging protocols requires a balance between charging time and battery degradation [261]. The disadvantages associated with the existing optimized charging protocols, such as complexity, implementation cost as well as harsh duty cycle cell tests, need to be addressed before implementation [265]. Rynne and coworkers tried to address the challenge of a large number of testing in battery research by using Design of Experiments (DoE) and statistical techniques, which made it possible to minimize the number of experiments and obtain meaningful parameters [275]. Overall, the development of fast and smart optimal charging protocols based on machine learning techniques is a promising direction for future research.

8. Conclusions

In this paper, the current literature on lithium plating was reviewed. Degradation of LiBs during operation is one of the most complicated and critical issues that involve the variety of electrochemical side reactions in all the LiB components. Lithium plating is one of the most important degradation mechanisms of the anode electrode. The main impact of lithium plating is severe capacity fade. It occurs under three main working conditions: low-temperature charging, high C-rate charging, and high SOC charging. It's a challenging but important task to understand the lithium plating mechanisms and how to prevent them. Therefore, in this paper, we comprehensively reviewed the recent progress on investigating the lithium plating mechanisms, existing detection techniques, and mitigation strategies. Detection techniques can be divided into two main categories: (i) Physical characterization of the deposited lithium morphology and anode surface characterization. These techniques are more suitable for fundamental studies. (ii) Electrochemical techniques based on the charging voltage and currents are more useful for real-time applications. Although many studies have been done for lithium plating detection, there is still no promising and real-time method for lithium plating detection in engineering applications. Prediction of lithium plating is also a complicated task. The current electrochemical models for lithium plating have been reviewed. These models are too complicated and computationally costly for implementation in BMS. Many approaches have been studied that could potentially prevent lithium plating, especially the formation of lithium dendrite, including modification of material components (adopting advanced electrolyte and modifying the graphite surface structure) and optimization of charging protocols. More progress needs to be made in developing methods to avoid lithium plating during charging. We can significantly reduce the degradation during fast charging and achieve long cycle life through a deep understanding of lithium plating mechanisms under different operating conditions and advanced detection methods that can be easily implemented in engineering applications.

Declaration of Competing Interest

The authors declare that they have no known competing financial interests or personal relationships that could have appeared to influence the work reported in this paper.

Acknowledgements

XL acknowledges support by the Natural Sciences and Engineering Research Council of Canada (NSERC) through the NSERC Early Career Researcher Supplement & Discovery Grant Program (RGPIN-2018-05471) and Ontario Tech University Startup Fund. XH acknowledges support by the National Natural Science Foundation of China (Grant no. 51875054 and Grant no. U1864212). JL acknowledges support by Wuxi Weifu High-Technology Group Co., Ltd.

References

[1] Petroleum British. BP Energy Outlook 2019 edition The Energy Outlook explores the forces shaping the global energy transition out to 2040 and the key uncertainties surrounding that. BP Energy Outlook 2019 2019. 22–4, 72–6, 144-118.
[2] Popham K. Transportation electrification. Smart Cities Appl Technol Stand Driv Factors 2017:109–22. https://doi.org/10.1007/978-3-319-59381-4-7.
[3] Zhang R, Fujimori S. The role of transport electrification in global climate change mitigation scenarios. Environ Res Lett 2020;15. https://doi.org/10.1088/1748-9326/ab6658.
[4] IRENA. Global Renewables Outlook: Energy transformation 2050. 2020th ed. 2020.
[5] Latulippe É, Mo K. Outlook for Electric Vehicles and Implications for the Oil Market. 2019.
[6] National Resources Canada. Electric Vehicle Technology Roadmap for Canada: A strategic vision for highway-capable battery-electric, plug-in and other hybrid-electric vehicles. Nat Resour Canada 2010;1:1–71.
[7] Li Z, Huang J, Yann Liaw B, Metzler V, Zhang J. A review of lithium deposition in lithium-ion and lithium metal secondary batteries. J Power Sources 2014;254:168–82. https://doi.org/10.1016/j.jpowsour.2013.12.099.
[8] Pistoia G, Liaw B. Green Energy and Technology Behaviour of Lithium-Ion Batteries in Electric Vehicles; Battery Health, Performance, Safety, and Cost. Springer International Publishing AG; 2017. https://doi.org/https://doi.org/10.1007/978-3-319-69950-9.
[9] Dubarry M, Baure G, Devie A. Durability and reliability of EV batteries under electric utility grid operations: Path dependence of battery degradation. J Electrochem Soc 2018;165:A773–83. https://doi.org/10.1149/2.0421805jes.
[10] Ma Z, Jiang J, Shi W, Zhang W, Mi CC. Investigation of path dependence in commercial lithium-ion cells for pure electric bus applications: Aging mechanism identification. J Power Sources 2015;274:29–40. https://doi.org/10.1016/j.jpowsour.2014.10.006.
[11] Nitta N, Wu F, Lee JT, Yushin G. Li-ion battery materials: Present and future. Mater Today 2015;18:252–64. https://doi.org/10.1016/j.mattod.2014.10.040.
[12] Pistoia G, Boston A, et al. Lithium-Ion Batteries Advances and Applications. Elsevier B.V; 2014. https://doi.org/https://doi.org/10.1016/B978-0-444-59513-3.00001-7.
[13] Mishra A, Mehta A, Basu S, Malode SJ, Shetti NP, Shukla SS, et al. Electrode materials for lithium-ion batteries. Mater Sci Energy Technol 2018;1:182–7. https://doi.org/10.1016/j.mset.2018.08.001.
[14] Goriparti S, Miele E, De Angelis F, Di Fabrizio E, Proietti Zaccaria R, Capiglia C. Review on recent progress of nanostructured anode materials for Li-ion batteries. J Power Sources 2014;257:421–43. https://doi.org/10.1016/j.jpowsour.2013.11.103.
[15] Xu B, Qian D, Wang Z, Meng YS. Recent progress in cathode materials research for advanced lithium ion batteries. Mater Sci Eng R Reports 2012;73:51–65. https://doi.org/10.1016/j.mser.2012.05.003.
[16] Logan ER, Dahn JR. Electrolyte Design for Fast-Charging Li-Ion Batteries. Trends Chem 2020;2:354–66. https://doi.org/10.1016/j.trechm.2020.01.011.
[17] Tomaszewska A, Chu Z, Feng X, O'Kane S, Liu X, Chen J, et al. Lithium-ion battery fast charging: A review. ETransportation 2019;1:100011. https://doi.org/10.1016/j.etran.2019.100011.
[18] Jow TR, Delp SA, Allen JL, Jones J-P, Smart MC. Factors Limiting Li + Charge Transfer Kinetics in Li-Ion Batteries. J Electrochem Soc 2018;165:A361–7. https://doi.org/10.1149/2.1221802jes.
[19] Liu Q, Du C, Shen B, Zuo P, Cheng X, Ma Y, et al. Understanding undesirable anode lithium plating issues in lithium-ion batteries. RSC Adv 2016;6:88683–700. https://doi.org/10.1039/c6ra19482f.
[20] Waldmann T, Hogg B. Wohlfahrt-mehrens M. Li plating as unwanted side reaction in commercial Li-ion cells – A review. J Power Sources 2018;384:107–24. https://doi.org/10.1016/j.jpowsour.2018.02.063.
[21] Xu K, Von Cresce A, Lee U. Differentiating contributions to "ion transfer" barrier from interphasial resistance and Li+ desolvation at electrolyte/graphite interface. Langmuir 2010;26:11538–43. https://doi.org/10.1021/la1009994.
[22] Yamada Y, Iriyama Y, Abe T, Ogumi Z. Kinetics of lithium ion transfer at the interface between graphite and liquid electrolytes: effects of solvent and surface film. Langmuir 2009;25:12766–70. https://doi.org/10.1021/la901829v.
[23] Pastor-Fernández C, Uddin K, Chouchelamane GH, Widanage WD, Marco J. A Comparison between Electrochemical Impedance Spectroscopy and Incremental Capacity-Differential Voltage as Li-ion Diagnostic Techniques to Identify and Quantify the Effects of Degradation Modes within Battery Management Systems. J Power Sources 2017;360:301–18. https://doi.org/10.1016/j.jpowsour.2017.03.042.
[24] Ouyang M, Chu Z, Lu L, Li J, Han X, Feng X, et al. Low temperature aging mechanism identification and lithium deposition in a large format lithium iron phosphate battery for different charge profiles. J Power Sources 2015;286:309–20. https://doi.org/10.1016/j.jpowsour.2015.03.178.
[25] Vetter J, Novák P, Wagner MR, Veit C, Möller KC, Besenhard JO, et al. Ageing mechanisms in lithium-ion batteries. J Power Sources 2005;147:269–81. https://doi.org/10.1016/j.jpowsour.2005.01.006.
[26] Agubra V, Fergus J. Lithium ion battery anode aging mechanisms. Materials (Basel) 2013;6:1310–25. https://doi.org/10.3390/ma6041310.

[27] Tanim TR, Dufek EJ, Evans M, Dickerson C, Jansen AN, Polzin BJ, et al. Extreme Fast Charge Challenges for Lithium-Ion Battery: Variability and Positive Electrode Issues. J Electrochem Soc 2019;166:A1926–38. https://doi.org/10.1149/2.0731910jes.

[28] Birkenmaier C, Bitzer B, Harzheim M, Hintennach A, Schleid T. Lithium plating on graphite negative electrodes: Innovative qualitative and quantitative investigation methods. J Electrochem Soc 2015;162:A2646–50. https://doi.org/10.1149/2.0451514jes.

[29] Legrand N, Knosp B, Desprez P, Lapicque F, Raël S. Physical characterization of the charging process of a Li-ion battery and prediction of Li plating by electrochemical modelling. J Power Sources 2014;245:208–16. https://doi.org/10.1016/j.jpowsour.2013.06.130.

[30] Pastor-Fernández C, Bruen T, Widanage WD, Gama-Valdez MA, Marco J. A Study of Cell-to-Cell Interactions and Degradation in Parallel Strings: Implications for the Battery Management System. J Power Sources 2016;329:574–85. https://doi.org/10.1016/j.jpowsour.2016.07.121.

[31] Dubarry M, Truchot C, Liaw BY. Synthesize battery degradation modes via a diagnostic and prognostic model. J Power Sources 2012;219:204–16. https://doi.org/10.1016/j.jpowsour.2012.07.016.

[32] Edge JS, O'Kane S, Prosser R, Kirkaldy ND, Patel AN, Hales A, et al. Lithium ion battery degradation: what you need to know. Phys Chem Chem Phys 2021;23:8200–21. https://doi.org/10.1039/d1cp00359c.

[33] Ratnakumar BV, Smart MC. Lithium plating behavior in lithium-ion cells. ECS Trans 2010;25:241–52. https://doi.org/10.1149/1.3393860.

[34] Birkl CR, Roberts MR, McTurk E, Bruce PG, Howey DA. Degradation diagnostics for lithium ion cells. J Power Sources 2017;341:373–86. https://doi.org/10.1016/j.jpowsour.2016.12.011.

[35] Lin X, Park J, Liu L, Lee Y, Lu W, Sastry AM. A Comprehensive Capacity Fade Model and Analysis for Li-Ion Batteries. J Electrochem Soc 2013;160:A1701–10. https://doi.org/10.1149/2.040310jes.

[36] Grimsmann F, Brauchle F, Gerbert T, Gruhle A, Parisi J, Knipper M. Impact of different aging mechanisms on the thickness change and the quick-charge capability of lithium-ion cells. J Energy Storage 2017;14:158–62. https://doi.org/10.1016/j.est.2017.10.010.

[37] Ahmed S, Bloom I, Jansen AN, Tanim T, Dufek EJ, Pesaran A, et al. Enabling fast charging – A battery technology gap assessment. J Power Sources 2017;367:250–62. https://doi.org/10.1016/j.jpowsour.2017.06.055.

[38] Arora P, Doyle M, White RE. Mathematical Modeling of the Lithium Deposition Overcharge Reaction in Lithium-Ion Batteries Using Carbon-Based Negative Electrodes 1988;146.

[39] Chandrasekaran R. Quantification of bottlenecks to fast charging of lithium-ion-insertion cells for electric vehicles. J Power Sources 2014;271:622–32. https://doi.org/10.1016/j.jpowsour.2014.07.106.

[40] Hein S, Latz A. Influence of local lithium metal deposition in 3D microstructures on local and global behavior of Lithium-ion batteries. Electrochim Acta 2016;201:354–65. https://doi.org/10.1016/j.electacta.2016.01.220.

[41] Hein S, Danner T, Latz A. An Electrochemical Model of Lithium Plating and Stripping in Lithium Ion Batteries. ACS Appl Energy Mater 2020;3:8519–31. https://doi.org/10.1021/acsaem.0c01155.

[42] Wang H, Zhu Y, Kim SC, Pei A, Li Y, Boyle DT, et al. Underpotential lithium plating on graphite anodes caused by temperature heterogeneity. Proc Natl Acad Sci U S A 2020;117:29453–61. https://doi.org/10.1073/pnas.2009221117.

[43] Harris SJ, Timmons A, Baker DR, Monroe C. Direct in situ measurements of Li transport in Li-ion battery negative electrodes. Chem Phys Lett 2010;485:265–74. https://doi.org/10.1016/j.cplett.2009.12.033.

[44] Barai A, Uddin K, Dubarry M, Somerville L, McGordon A, Jennings P, et al. A comparison of methodologies for the non-invasive characterisation of commercial Li-ion cells. Prog Energy Combust Sci 2019;72:1–31. https://doi.org/10.1016/j.pecs.2019.01.001.

[45] Ecker M, Shafiei Sabet P, Sauer DU. Influence of operational condition on lithium plating for commercial lithium-ion batteries – Electrochemical experiments and post-mortem-analysis. Appl Energy 2017;206:934–46. https://doi.org/10.1016/j.apenergy.2017.08.034.

[46] Zhao X, Yin Y, Hu Y, Choe SY. Electrochemical-thermal modeling of lithium plating/stripping of Li(Ni0.6Mn0.2Co0.2)O2/Carbon lithium-ion batteries at subzero ambient temperatures. J Power Sources 2019;418:61–73. https://doi.org/10.1016/j.jpowsour.2019.02.001.

[47] Ren D, Smith K, Guo D, Han X, Feng X, Lu L, et al. Investigation of Lithium Plating-Stripping Process in Li-Ion Batteries at Low Temperature Using an Electrochemical Model. J Electrochem Soc 2018;165:A2167–78. https://doi.org/10.1149/2.0661810jes.

[48] Yang XG, Ge S, Liu T, Leng Y, Wang CY. A look into the voltage plateau signal for detection and quantification of lithium plating in lithium-ion cells. J Power Sources 2018;395:251–61. https://doi.org/10.1016/j.jpowsour.2018.05.073.

[49] Waldmann T, Hogg BI, Kasper M, Grolleau S, Couceiro CG, Trad K, et al. Interplay of operational parameters on lithium deposition in lithium-ion cells: Systematic measurements with reconstructed 3-electrode pouch full cells. J Electrochem Soc 2016;163:A1232–8. https://doi.org/10.1149/2.0591607jes.

[50] Liu G, Lu W. A model of concurrent lithium dendrite growth, SEI growth, SEI penetration and regrowth. J Electrochem Soc 2017;164:A1826–33. https://doi.org/10.1149/2.0381709jes.

[51] Sahraei E, Meier J, Wierzbicki T. Characterizing and modeling mechanical properties and onset of short circuit for three types of lithium-ion pouch cells. J Power Sources 2014;247:503–16. https://doi.org/10.1016/j.jpowsour.2013.08.056.

[52] Orendorff CJ, Roth EP, Nagasubramanian G. Experimental triggers for internal short circuits in lithium-ion cells. J Power Sources 2011;196:6554–8. https://doi.org/10.1016/j.jpowsour.2011.03.035.

[53] Tanim TR, Paul PP, Thampy V, Bryant J, Dunlop AR, Trask SE, et al. Article Heterogeneous Behavior of Lithium Plating during Extreme Fast Charging Heterogeneous Behavior of Lithium Plating during Extreme Fast Charging 2020. https://doi.org/10.1016/j.xcrp.2020.100114.

[54] Anseán D, Dubarry M, Devie A, Liaw BY, García VM, Viera JC, et al. Operando lithium plating quantification and early detection of a commercial LiFePO4 cell cycled under dynamic driving schedule. J Power Sources 2017;356:36–46. https://doi.org/10.1016/j.jpowsour.2017.04.072.

[55] Guan T, Sun S, Yu F, Gao Y, Fan P, Zuo P, et al. The degradation of LiCoO2/graphite batteries at different rates. Electrochim Acta 2018;279:204–12. https://doi.org/10.1016/j.electacta.2018.04.197.

[56] Gireaud L, Grugeon S, Laruelle S, Yrieix B, Tarascon JM. Lithium metal stripping/plating mechanisms studies: A metallurgical approach. Electrochem Commun 2006;8:1639–49. https://doi.org/10.1016/j.elecom.2006.07.037.

[57] Ge H, Aoki T, Ikeda N, Suga S, Isobe T, Li Z, et al. Investigating lithium plating in lithium-ion batteries at low temperatures using electrochemical model with NMR assisted parameterization. J Electrochem Soc 2017;164:A1050–60. https://doi.org/10.1149/2.0461706jes.

[58] Petzl M, Kasper M, Danzer MA. Lithium plating in a commercial lithium-ion battery - A low-temperature aging study. J Power Sources 2015;275:799–807. https://doi.org/10.1016/j.jpowsour.2014.11.065.

[59] Campbell ID, Marzook M, Marinescu M, Offer GJ. How observable is lithium plating? differential voltage analysis to identify and quantify lithium plating following fast charging of cold lithium-ion batteries. J Electrochem Soc 2019;166:A725–39. https://doi.org/10.1149/2.0821904jes.

[60] Fear C, Adhikary T, Carter RE, Mistry AN, Love CT, Mukherjee PP. In Operando Detection of the Onset and Mapping of Lithium Plating Regimes during Fast Charging of Lithium-ion Batteries. ACS Appl Mater Interfaces 2020. https://doi.org/10.1021/acsami.0c07803.

[61] Ringbeck F, Rahe C, Fuchs G, Sauer DU. Identification of Lithium Plating in Lithium-Ion Batteries by Electrical and Optical Methods. J Electrochem Soc 2020;167:090536. https://doi.org/10.1149/1945-7111/ab8f5a.

[62] Ouyang D, He Y, Weng J, Liu J, Chen M, Wang J. Influence of low temperature conditions on lithium-ion batteries and the application of an insulation material. RSC Adv 2019;9:9053–66. https://doi.org/10.1039/c9ra00490d.

[63] Jaguemont J, Boulon L, Dubé Y. A comprehensive review of lithium-ion batteries used in hybrid and electric vehicles at cold temperatures. Appl Energy 2016;164:99–114. https://doi.org/10.1016/j.apenergy.2015.11.034.

[64] Ma S, Jiang M, Tao P, Song C, Wu J, Wang J, et al. Temperature effect and thermal impact in lithium-ion batteries: A review. Prog Nat Sci Mater Int 2018;28:653–66. https://doi.org/10.1016/j.pnsc.2018.11.002.

[65] Börner M, Horsthemke F, Kollmer F, Haseloff S, Friesen A, Niehoff P, et al. Degradation effects on the surface of commercial LiNi0.5Co0.2Mn0.3O2 electrodes. J Power Sources 2016;335:45–55. https://doi.org/10.1016/j.jpowsour.2016.09.071.

[66] Yang XG, Zhang G, Ge S, Wang CY. Fast charging of lithium-ion batteries at all temperatures. Proc Natl Acad Sci U S A 2018;115:7266–71. https://doi.org/10.1073/pnas.1807115115.

[67] Yang XG, Liu T, Gao Y, Ge S, Leng Y, Wang D, et al. Asymmetric Temperature Modulation for Extreme Fast Charging of Lithium-Ion Batteries. Joule 2019;3:3002–19. https://doi.org/10.1016/j.joule.2019.09.021.

[68] Tanim TR, Dufek EJ, Dickerson CC, Wood SM. Electrochemical Quantification of Lithium Plating: Challenges and Considerations. J Electrochem Soc 2019;166:A2689–96. https://doi.org/10.1149/2.1581912jes.

[69] Rangarajan SP, Barsukov Y, Mukherjee PP. In operando signature and quantification of lithium plating. J Mater Chem A 2019;7:20683–95. https://doi.org/10.1039/c9ta07314k.

[70] Keil P, Jossen A. Charging protocols for lithium-ion batteries and their impact on cycle life-An experimental study with different 18650 high-power cells. J Energy Storage 2016;6:125–41. https://doi.org/10.1016/j.est.2016.02.005.

[71] Zhang L, Zhang Z, Redfern PC, Curtiss LA, Amine K. Molecular engineering towards safer lithium-ion batteries: A highly stable and compatible redox shuttle for overcharge protection. Energy Environ Sci 2012;5:8204–7. https://doi.org/10.1039/c2ee21977h.

[72] Juarez-Robles D, Vyas AA, Fear C, Jeevarajan JA, Mukherjee PP. Overcharge and Aging Analytics of Li-Ion Cells. J Electrochem Soc 2020;167:090547. https://doi.org/10.1149/1945-7111/ab9569.

[73] Liu S, Xiong L, He C. Long cycle life lithium ion battery with lithium nickel cobalt manganese oxide (NCM) cathode. J Power Sources 2014;261:285–91. https://doi.org/10.1016/j.jpowsour.2014.03.083.

[74] Cannarella J, Arnold CB. The Effects of Defects on Localized Plating in Lithium-Ion Batteries. J Electrochem Soc 2015;162:A1365–73. https://doi.org/10.1149/2.1051507jes.

[75] Abe T, Fukuda H, Iriyama Y, Ogumi Z. Solvated Li-ion transfer at interface between graphite and electrolyte. J Electrochem Soc 2004;151. https://doi.org/10.1149/1.1763141.

[76] Smart MC, Ratnakumar BV. Effects of electrolyte composition on lithium plating in lithium-ion cells. J Electrochem Soc 2011;158. https://doi.org/10.1149/1.3544439.

[77] Love CT, Baturina OA, Swider-Lyons KE. Observation of lithium dendrites at ambient temperature and below. ECS Electrochem Lett 2014;4:A24–7. https://doi.org/10.1149/2.0041502eel.

[78] Yao F, Güneş F, Ta HQ, Lee SM, Chae SJ, Sheem KY, et al. Diffusion mechanism of lithium ion through basal plane of layered graphene. J Am Chem Soc 2012;134:8646–54. https://doi.org/10.1021/ja301586m.

[79] Dubarry M, Baure G, Anseán D. Perspective on State-of-Health Determination in Lithium-Ion Batteries. J Electrochem Energy Convers Storage 2020;17:1–8. https://doi.org/10.1115/1.4045008.

[80] Baure G, Dubarry M. Synthetic vs. Real driving cycles: A comparison of electric vehicle battery degradation. Batteries 2019;5. https://doi.org/10.3390/batteries5020042.

[81] Schuster SF, Bach T, Fleder E, Müller J, Brand M, Sextl G, et al. Nonlinear aging characteristics of lithium-ion cells under different operational conditions. J Energy Storage 2015;1:44–53. https://doi.org/10.1016/j.est.2015.05.003.

[82] Waldmann T, Wilka M, Kasper M, Fleischhammer M, Wohlfahrt-Mehrens M. Temperature dependent ageing mechanisms in Lithium-ion batteries - A Post-Mortem study. J Power Sources 2014;262:129–35. https://doi.org/10.1016/j.jpowsour.2014.03.112.

[83] Zhang J-G, Xu W, Henderson WA. Lithium Metal Anodes and Rechargeable Lithium Metal Batteries. Springer Series in Materials Science; 2017. https://doi.org/DOI 10.1007/978-3-319-44054-5.

[84] Perla BB, Yixuan W. Lithium-Ion Batteries - Solid-Electrolyte Interphase. Imperial College Press; 2010. https://doi.org/10.1142/9781860946448.

[85] Waldmann T, Iturrondobeitia A, Kasper M, Ghanbari N, Aguesse F, Bekaert E, et al. Review—Post-Mortem Analysis of Aged Lithium-Ion Batteries: Disassembly Methodology and Physico-Chemical Analysis Techniques. J Electrochem Soc 2016;163:A2149–64. https://doi.org/10.1149/2.1211609jes.

[86] Williard N, Sood B, Osterman M, Pecht M. Disassembly methodology for conducting failure analysis on lithium-ion batteries. J Mater Sci Mater Electron 2011;22:1616–30. https://doi.org/10.1007/s10854-011-0452-4.

[87] Friesen A, Horsthemke F, Mönnighoff X, Brunklaus G, Krafft R, Börner M, et al. Impact of cycling at low temperatures on the safety behavior of 18650-type lithium ion cells: Combined study of mechanical and thermal abuse testing accompanied by post-mortem analysis. J Power Sources 2016;334:1–11. https://doi.org/10.1016/j.jpowsour.2016.09.120.

[88] Rauhala T, Jalkanen K, Romann T, Lust E, Omar N, Kallio T. Low-temperature aging mechanisms of commercial graphite/LiFePO4 cells cycled with a simulated electric vehicle load profile—A post-mortem study. J Energy Storage 2018;20:344–56. https://doi.org/10.1016/j.est.2018.10.007.

[89] Iturrondobeitia A, Aguesse F, Genies S, Waldmann T, Kasper M, Ghanbari N, et al. Post-Mortem Analysis of Calendar-Aged 16 Ah NMC/Graphite Pouch Cells for EV Application. J Phys Chem C 2017;121:21865–76. https://doi.org/10.1021/acs.jpcc.7b05416.

[90] Kassem M, Delacourt C. Postmortem analysis of calendar-aged graphite/LiFePO4 cells. J Power Sources 2013;235:159–71. https://doi.org/10.1016/j.jpowsour.2013.01.147.

[91] Lang M, Darma MSD, Kleiner K, Riekehr L, Mereacre L, Ávila Pérez M, et al. Post mortem analysis of fatigue mechanisms in LiNi0.8Co0.15Al0.05O2 – LiNi0.5Co0.2Mn0.3O2 – LiMn2O4/graphite lithium ion batteries. J Power Sources 2016;326:397–409. https://doi.org/10.1016/j.jpowsour.2016.07.010.

[92] Storch M, Hahn SL, Stadler J, Swaminathan R, Vrankovic D, Krupp C, et al. Post-mortem analysis of calendar aged large-format lithium-ion cells: Investigation of the solid electrolyte interphase. J Power Sources 2019;443:227243. https://doi.org/10.1016/j.jpowsour.2019.227243.

[93] Cohen Y, Aurbach D. The use of a special work station for in situ measurements of highly reactive electrochemical systems by atomic force and scanning tunneling microscopes. Rev Sci Instrum 1999;70:4668–75. https://doi.org/10.1063/1.1150130.

[94] Steiger J, Kramer D, Mönig R. Mechanisms of dendritic growth investigated by in situ light microscopy during electrodeposition and dissolution of lithium. J Power Sources 2014;261:112–9. https://doi.org/10.1016/j.jpowsour.2014.03.029.

[95] Liu G, Wang D, Zhang J, Kim A, Lu W. Preventing Dendrite Growth by a Soft Piezoelectric Material 2019. https://doi.org/10.1021/acsmaterialslett.9b00289.

[96] Steiger J, Kramer D, Mönig R. Microscopic observations of the formation, growth and shrinkage of lithium moss during electrodeposition and dissolution. Electrochim Acta 2014;136:529–36. https://doi.org/10.1016/j.electacta.2014.05.120.

[97] Persson K, Sethuraman VA, Hardwick LJ, Hinuma Y, Meng YS, Van Der Ven A, et al. Lithium diffusion in graphitic carbon. J Phys Chem Lett 2010;1:1176–80. https://doi.org/10.1021/jz100188d.

[98] Uhlmann C, Illig J, Ender M, Schuster R, Ivers-Tiffée E. In situ detection of lithium metal plating on graphite in experimental cells. J Power Sources 2015;279:428–38. https://doi.org/10.1016/j.jpowsour.2015.01.046.

[99] Thomas-Alyea KE, Jung C, Smith RB, Bazant MZ. In situ observation and mathematical modeling of lithium distribution within graphite. J Electrochem Soc 2017;164:E3063–72. https://doi.org/10.1149/2.0061711jes.

[100] Baudry P, Armand M, Gauthier M, Masounave J. In situ observation by SEM of positive composite electrodes during discharge of polymer lithium batteries. Solid State Ionics 1988. https://doi.org/10.1016/0167-2738(88)90421-3. 28-30:1567-71.

[101] Shao M. In situ microscopic studies on the structural and chemical behaviors of lithium-ion battery materials. J Power Sources 2014;270:475–86. https://doi.org/10.1016/j.jpowsour.2014.07.123.

[102] Chang HJ, Trease NM, Ilott AJ, Zeng D, Du LS, Jerschow A, et al. Investigating Li Microstructure Formation on Li Anodes for Lithium Batteries by in Situ ^{6}Li/^{7}Li NMR and SEM. J Phys Chem C 2015;119:16443–51. https://doi.org/10.1021/acs.jpcc.5b03396.

[103] Yoshimatsu I, Hirai T, Yamaki J ichi. Lithium Electrode Morphology during Cycling in Lithium Cells. J Electrochem Soc 1988;135:2422–7. https://doi.org/10.1149/1.2095351.

[104] Nagao M, Hayashi A, Tatsumisago M, Kanetsuku T, Tsuda T, Kuwabata S. In situ SEM study of a lithium deposition and dissolution mechanism in a bulk-type solid-state cell with a Li2S-P2S5 solid electrolyte. Phys Chem Chem Phys 2013;15:18600–6. https://doi.org/10.1039/c3cp51059j.

[105] Chen D, Indris S, Schulz M, Gamer B, Mönig R. In situ scanning electron microscopy on lithium-ion battery electrodes using an ionic liquid. J Power Sources 2011;196:6382–7. https://doi.org/10.1016/j.jpowsour.2011.04.009.

[106] Sagane F, Shimokawa R, Sano H, Sakaebe H, Iriyama Y. In-situ scanning electron microscopy observations of Li plating and stripping reactions at the lithium phosphorus oxynitride glass electrolyte/Cu interface. J Power Sources 2013;225:245–50. https://doi.org/10.1016/j.jpowsour.2012.10.026.

[107] Rong G, Zhang X, Zhao W, Qiu Y, Liu M, Ye F, et al. Liquid-Phase Electrochemical Scanning Electron Microscopy for In Situ Investigation of Lithium Dendrite Growth and Dissolution. Adv Mater 2017;29. https://doi.org/10.1002/adma.201606187.

[108] Tallman KR, Zhang B, Wang L, Yan S, Thompson K, Tong X, et al. Anode Overpotential Control via Interfacial Modification: Inhibition of Lithium Plating on Graphite Anodes. ACS Appl Mater Interfaces 2019;11:46864–74. https://doi.org/10.1021/acsami.9b16794.

[109] Wu Y, Liu N. Visualizing Battery Reactions and Processes by Using In Situ and In Operando Microscopies. Chem 2018;4:438–65. https://doi.org/10.1016/j.chempr.2017.12.022.

[110] Yuan Y, Amine K, Lu J, Shahbazian-Yassar R. Understanding materials challenges for rechargeable ion batteries with in situ transmission electron microscopy. Nat Commun 2017;8:1–14. https://doi.org/10.1038/ncomms15806.

[111] Ghassemi H, Au M, Chen N, Heiden PA, Yassar RS. Real-time observation of lithium fibers growth inside a nanoscale lithium-ion battery. Appl Phys Lett 2011;99:1–4. https://doi.org/10.1063/1.3643035.

[112] Liu XH, Liu Y, Kushima A, Zhang S, Zhu T, Li J, et al. In situ TEM experiments of electrochemical lithiation and delithiation of individual nanostructures. Adv Energy Mater 2012;2:722–41. https://doi.org/10.1002/aenm.201200024.

[113] Mehdi BL, Gu M, Parent LR, Xu W, Nasybulin EN, Chen X, et al. In-situ electrochemical transmission electron microscopy for battery research. Microsc Microanal 2014;20:484–92. https://doi.org/10.1017/S1431927614000488.

[114] Zeng Z, Liang WI, Liao HG, Xin HL, Chu YH, Zheng H. Visualization of electrode-electrolyte interfaces in LiPF 6/EC/DEC electrolyte for lithium ion batteries via in situ TEM. Nano Lett 2014;14:1745–50. https://doi.org/10.1021/nl403922u.

[115] Krachkovskiy S, Trudeau ML, Zaghib K. Application of magnetic resonance techniques to the in situ characterization of Li-ion batteries: A review. Materials (Basel) 2020;13. https://doi.org/10.3390/ma13071694.

[116] Arai J, Okada Y, Sugiyama T, Izuka M, Gotoh K, In Takeda K. Situ Solid State 7 Li NMR Observations of Lithium Metal Deposition during Overcharge in Lithium Ion Batteries. J Electrochem Soc 2015;162:A952–8. https://doi.org/10.1149/2.0411506jes.

[117] Chevallier F, Poli F, Montigny B, Letellier M. In situ7Li nuclear magnetic resonance observation of the electrochemical intercalation of lithium in graphite: Second cycle analysis. Carbon N Y 2013;61:140–53. https://doi.org/10.1016/j.carbon.2013.04.078.

[118] Letellier M, Chevallier F, Béguin F, Frackowiak E, Rouzaud JN. The first in situ 7Li NMR study of the reversible lithium insertion mechanism in disorganised carbons. J Phys Chem Solids 2004;65:245–51. https://doi.org/10.1016/j.jpcs.2003.10.022.

[119] Arai J, Nakahigashi R. Study of Li metal deposition in lithium ion battery during low-temperature cycle using in situ solid-state 7Li nuclear magnetic resonance. J Electrochem Soc 2017;164:A3403–9. https://doi.org/10.1149/2.1921713jes.

[120] Schweikert N, Hofmann A, Schulz M, Scheuermann M, Boles ST, Hanemann T, et al. Suppressed lithium dendrite growth in lithium batteries using ionic liquid electrolytes: Investigation by electrochemical impedance spectroscopy, scanning electron microscopy, and in situ 7Li nuclear magnetic resonance spectroscopy. J Power Sources 2013;228:237–43. https://doi.org/10.1016/j.jpowsour.2012.11.124.

[121] Gotoh K, Izuka M, Arai J, Okada Y, Sugiyama T, Takeda K, et al. In situ 7Li nuclear magnetic resonance study of the relaxation effect in practical lithium ion batteries. Carbon N Y 2014;79:380–7. https://doi.org/10.1016/j.carbon.2014.07.080.

[122] Ota H, Sakata Y, Wang X, Sasahara J, Yasukawa E. Characterization of Lithium Electrode in Lithium Imides/Ethylene Carbonate and Cyclic Ether Electrolytes II. Surface Chemistry. J Electrochem Soc 2004;151. https://doi.org/10.1149/1.1644137.

[123] Zheng T, Dahn J. Effect of turbostratic disorder on the staging phase diagram of lithium-intercalated graphitic carbon hosts. Phys Rev B - Condens Matter Mater Phys 1996;53:3061–71. https://doi.org/10.1103/PhysRevB.53.3061.

[124] Wandt J, Jakes P, Granwehr J, Eichel RA, Gasteiger HA. Quantitative and time-resolved detection of lithium plating on graphite anodes in lithium ion batteries. Mater Today 2018;21:231–40. https://doi.org/10.1016/j.mattod.2017.11.001.

[125] Niemöller A, Jakes P, Eichel RA, Granwehr J. EPR Imaging of Metallic Lithium and its Application to Dendrite Localisation in. Battery Separators. Sci Rep 2018;8:1–7. https://doi.org/10.1038/s41598-018-32112-y.

[126] Sathiya M, Leriche JB, Salager E, Gourier D, Tarascon JM, Vezin H. Electron paramagnetic resonance imaging for real-time monitoring of Li-ion batteries. Nat Commun 2015;6:1–7. https://doi.org/10.1038/ncomms7276.

[127] Wandt J, Marino C, Gasteiger HA, Jakes P, Eichel RA, Granwehr J. Operando electron paramagnetic resonance spectroscopy-formation of mossy lithium on

lithium anodes during charge-discharge cycling. Energy Environ Sci 2015;8:1358–67. https://doi.org/10.1039/c4ee02730b.
[128] Luo K, Yorgancioglu M, Keller D. Scanning force microscopy at -25°C. Ultramicroscopy 1993;50:147–55. https://doi.org/10.1016/0304-3991(93)90005-I.
[129] Morigaki KI, Ohta A. Analysis of the surface of lithium in organic electrolyte by atomic force microscopy, Fourier transform infrared spectroscopy and scanning auger electron microscopy. J Power Sources 1998;76:159–66. https://doi.org/10.1016/S0378-7753(98)00151-7.
[130] Mogi R, Inaba M, Iriyama Y, Abe T, Ogumi Z. In situ atomic force microscopy study on lithium deposition on nickel substrates at elevated temperatures. J Electrochem Soc 2002;149:0–5. https://doi.org/10.1149/1.1454138.
[131] Aurbach D, Cohen Y. The application of atomic force microscopy for the study of Li deposition processes. J Electrochem Soc 1996;143:3525–32. https://doi.org/10.1149/1.1837248.
[132] Shen C, Hu G, Cheong LZ, Huang S, Zhang JG, Wang D. Direct Observation of the Growth of Lithium Dendrites on Graphite Anodes by Operando EC-AFM. Small Methods 2018;2:1–7. https://doi.org/10.1002/smtd.201700298.
[133] Yang Y, Liu X, Dai Z, Yuan F, Bando Y, Golberg D, et al. In Situ Electrochemistry of Rechargeable Battery Materials: Status Report and Perspectives. Adv Mater 2017;29:1–22. https://doi.org/10.1002/adma.201606922.
[134] Cohen YS, Cohen Y, Aurbach D. Micromorphological studies of lithium electrodes in alkyl carbonate solutions using in situ atomic force microscopy. J Phys Chem B 2000;104:12282–91. https://doi.org/10.1021/jp002526b.
[135] Aurbach D, Markovsky B, Weissman I, Levi E, Ein-Eli Y. On the correlation between surface chemistry and performance of graphite negative electrodes for Li ion batteries. Electrochim Acta 1999;45:67–86. https://doi.org/10.1016/S0013-4686(99)00194-2.
[136] Castro L, Dedryvère R, Ledeuil JB, Bréger J, Tessier C, Gonbeau D. Aging mechanisms of LiFePO 4 //graphite cells studied by XPS: Redox reaction and electrodeelectrolyte interfaces. J Electrochem Soc 2012;159:357–63. https://doi.org/10.1149/2.024204jes.
[137] Aurbach D, Weissman I, Schechter A, Cohen H. X-ray photoelectron spectroscopy studies of lithium surfaces prepared in several important electrolyte solutions. A comparison with previous studies by fourier transform infrared spectroscopy. Langmuir 1996;12:3991–4007.
[138] Wenzel S, Leichtweiss T, Krüger D, Sann J, Janek J. Interphase formation on lithium solid electrolytes - An in situ approach to study interfacial reactions by photoelectron spectroscopy. Solid State Ionics 2015;278:98–105. https://doi.org/10.1016/j.ssi.2015.06.001.
[139] Harilal SS, Allain JP, Hassanein A, Hendricks MR, Nieto-Perez M. Reactivity of lithium exposed graphite surface. Appl Surf Sci 2009;255:8539–43. https://doi.org/10.1016/j.apsusc.2009.06.009.
[140] Wood V. X-ray tomography for battery research and development. Nat Rev Mater 2018;3:293–5. https://doi.org/10.1038/s41578-018-0053-4.
[141] Pietsch P, Wood V. X-Ray Tomography for Lithium Ion Battery Research: A Practical Guide. Annu Rev Mater Res 2017;47:451–79. https://doi.org/10.1146/annurev-matsci-070616-123957.
[142] Sun F, He X, Jiang X, Osenberg M, Li J, Zhou D, et al. Advancing knowledge of electrochemically generated lithium microstructure and performance decay of lithium ion battery by synchrotron X-ray tomography. Mater Today 2019;27:21–32. https://doi.org/10.1016/j.mattod.2018.11.003.
[143] Waldmann T, Scurtu R-G, Richter K. Wohlfahrt-Mehrens M. 18650 vs. 21700 Li-ion cells – A direct comparison of electrochemical, thermal, and geometrical properties. J Power Sources 2020;472:228614. https://doi.org/10.1016/j.jpowsour.2020.228614.
[144] Vanpeene V, Villanova J, King A, Lestriez B, Maire E, Roué L. Dynamics of the Morphological Degradation of Si-Based Anodes for Li-Ion Batteries Characterized by In Situ Synchrotron X-Ray Tomography. Adv Energy Mater 2019;9:1–13. https://doi.org/10.1002/aenm.201803947.
[145] Eastwood DS, Bayley PM, Chang HJ, Taiwo OO, Vila-Comamala J, Brett DJL, et al. Three-dimensional characterization of electrodeposited lithium microstructures using synchrotron X-ray phase contrast imaging. Chem Commun 2015;51:266–8. https://doi.org/10.1039/c4cc03187c.
[146] Harry KJ, Hallinan DT, Parkinson DY, MacDowell AA, Balsara NP. Detection of subsurface structures underneath dendrites formed on cycled lithium metal electrodes. Nat Mater 2014;13:69–73. https://doi.org/10.1038/nmat3793.
[147] An SJ, Li J, Daniel C, Mohanty D, Nagpure S, Wood DL. The state of understanding of the lithium-ion-battery graphite solid electrolyte interphase (SEI) and its relationship to formation cycling. Carbon N Y 2016;105:52–76. https://doi.org/10.1016/j.carbon.2016.04.008.
[148] Morigaki K. Analysis of the interface between lithium and organic electrolyte solution. J Power Sources 2002;104:13–23. https://doi.org/https://doi.org/10.1016/S0378-7753(01)00871-0.
[149] Krämer Y, Birkenmaier C, Feinauer J, Hintennach A, Bender CL, Meiler M, et al. A New Method for Quantitative Marking of Deposited Lithium by Chemical Treatment on Graphite Anodes in Lithium-Ion Cells. Chem - A Eur J 2015;21:6062–5. https://doi.org/10.1002/chem.201406606.
[150] Ellis LD, Buteau S, Hames SG, Thompson LM, Hall DS, Dahn JR. A New Method for Determining the Concentration of Electrolyte Components in Lithium-Ion Cells. Using Fourier Transform Infrared Spectroscopy and Machine Learning 2018;165:256–62. https://doi.org/10.1149/2.0861802jes.
[151] Burba CM, Frech R. In situ transmission FTIR spectroelectrochemistry: A new technique for studying lithium batteries. Electrochim Acta 2006;52:780–5. https://doi.org/10.1016/j.electacta.2006.06.007.
[152] Fan J, Tan S. Studies on charging lithium-ion cells at low temperatures. J Electrochem Soc 2006;153. https://doi.org/10.1149/1.2190029.
[153] Petzl M, Danzer MA. Nondestructive detection, characterization, and quantification of lithium plating in commercial lithium-ion batteries. J Power Sources 2014;254:80–7. https://doi.org/10.1016/j.jpowsour.2013.12.060.
[154] Schindler S, Bauer M, Petzl M, Danzer MA. Voltage relaxation and impedance spectroscopy as in-operando methods for the detection of lithium plating on graphitic anodes in commercial lithium-ion cells. J Power Sources 2016;304:170–80. https://doi.org/10.1016/j.jpowsour.2015.11.044.
[155] Zinth V, Von Lüders C, Hofmann M, Hattendorff J, Buchberger I, Erhard S, et al. Lithium plating in lithium-ion batteries at sub-ambient temperatures investigated by in situ neutron diffraction. J Power Sources 2014;271:152–9. https://doi.org/10.1016/j.jpowsour.2014.07.168.
[156] Koleti UR, Dinh TQ, Marco J. A new on-line method for lithium plating detection in lithium-ion batteries. J Power Sources 2020;451:227798. https://doi.org/10.1016/j.jpowsour.2020.227798.
[157] Smart MC, Ratnakumar B V, Wbitcanack L, Chin K, Rodriguez M, Surampudi S. Performance Characteristics of Lithium Ion Cells at Low Temperatures. Proc Annu Batter Conf Appl Adv 2002:41–6. https://doi.org/10.1109/BCAA.2002.986366. 2002-Janua.
[158] Jansen AN, Dees DW, Abraham DP, Amine K, Henriksen GL. Low-temperature study of lithium-ion cells using a LiySn micro-reference electrode. J Power Sources 2007;174:373–9. https://doi.org/10.1016/j.jpowsour.2007.06.235.
[159] Abraham DP, Poppen SD, Jansen AN, Liu J, Dees DW. Application of a lithium-tin reference electrode to determine electrode contributions to impedance rise in high-power lithium-ion cells. Electrochim Acta 2004;49:4763–75. https://doi.org/10.1016/j.electacta.2004.05.040.
[160] Hoshi Y, Narita Y, Honda K, Ohtaki T, Shitanda I, Itagaki M. Optimization of reference electrode position in a three-electrode cell for impedance measurements in lithium-ion rechargeable battery by finite element method. J Power Sources 2015;288:168–75. https://doi.org/10.1016/j.jpowsour.2015.04.065.
[161] Nara H, Mukoyama D, Yokoshima T, Momma T, Osaka T. Impedance analysis with transmission line model for reaction distribution in a pouch type lithium-ion battery by using micro reference electrode. J Electrochem Soc 2016;163:A434–41. https://doi.org/10.1149/2.0341603jes.
[162] McTurk E, Birkl CR, Roberts MR, Howey DA, Bruce PG. Minimally invasive insertion of reference electrodes into commercial lithium-ion pouch cells. ECS Electrochem Lett 2015;4:A145–7. https://doi.org/10.1149/2.0081512eel.
[163] Somerville L, Ferrari S, Lain MJ, McGordon A, Jennings P, Bhagat R. An in-situ reference electrode insertion method for commercial 18650-type cells. Batteries 2018;4:1–11. https://doi.org/10.3390/batteries4020018.
[164] La Mantia F, Wessells CD, Deshazer HD, Cui Y. Reliable reference electrodes for lithium-ion batteries. Electrochem Commun 2013;31:141–4. https://doi.org/10.1016/j.elecom.2013.03.015.
[165] Dollé M, Orsini F, Gozdz AS, Tarascon JM. Development of Reliable Three-Electrode Impedance Measurements in Plastic Li-Ion Batteries. J Electrochem Soc 2001;148:851–7. https://doi.org/10.1149/1.1381071.
[166] Pastor-Fernández C, Widanage WD, Chouchelamane GH, Marco J. A SoH diagnosis and prognosis method to identify and quantify degradation modes in Li-ion batteries using the IC/DV technique. IET Conf Publ 2016;2016:1–6. https://doi.org/10.1049/cp.2016.0966.
[167] Han X, Ouyang M, Lu L, Li J, Zheng Y, Li Z. A comparative study of commercial lithium ion battery cycle life in electrical vehicle: Aging mechanism identification. J Power Sources 2014;251:38–54. https://doi.org/10.1016/j.jpowsour.2013.11.029.
[168] Bard AJ, Faulkner LR. Fundamentals and Applications. vol. 30. 1980. https://doi.org/10.1146/annurev.matsci.30.1.117.
[169] Smith AJ, Burns JC, Trussler S, Dahn JR. Precision measurements of the Coulombic efficiency of lithium-ion batteries and of electrode materials for lithium-ion batteries. J Electrochem Soc 2010;157:196–202. https://doi.org/10.1149/1.3268129.
[170] Burns JC, Stevens DA, Dahn JR. In-situ detection of lithium plating using high precision coulometry. J Electrochem Soc 2015;162:A959–64. https://doi.org/10.1149/2.0621506jes.
[171] Liu Y, Hanai K, Yang J, Imanishi N, Hirano A, Takeda Y. Morphology-stable silicon-based composite for Li-intercalation 2004;168:61–8. https://doi.org/10.1016/j.ssi.2004.01.031.
[172] Smith AJ, Burns JC, Dahn JR. A high precision study of the coulombic efficiency of Li-Ion batteries. Electrochem Solid-State Lett 2010;13:177–9. https://doi.org/10.1149/1.3487637.
[173] Shi F, Pei A, Boyle DT, Xie J, Yu X, Zhang X, et al. Lithium metal stripping beneath the solid electrolyte interphase. Proc Natl Acad Sci U S A 2018;115:8529–34. https://doi.org/10.1073/pnas.1806878115.
[174] Stevens DA, Ying RY, Fathi R, Reimers JN, Harlow JE, Dahn JR. Using high precision coulometry measurements to compare the degradation mechanisms of NMC/LMO and NMC-only automotive scale pouch cells. J Electrochem Soc 2014;161:1364–70. https://doi.org/10.1149/2.0971409jes.
[175] Osaka T, Momma T, Nishimura K, Taiima T. In situ Observation and Evaluation of Electrodeposited Lithium by Means of Optical Microscopy with Alternating Current Impedance Spectroscopy. J Electrochem Soc 1993;140:2745–8. https://doi.org/10.1149/1.2220903.
[176] Downie LE, Krause LJ, Burns JC, Jensen LD, Chevrier VL, Dahn JR. In situ detection of lithium plating on graphite electrodes by electrochemical calorimetry. J Electrochem Soc 2013;160:588–94. https://doi.org/10.1149/2.049304jes.

[177] Wang CM, Li X, Wang Z, Xu W, Liu J, Gao F, et al. In situ TEM investigation of congruent phase transition and structural evolution of nanostructured silicon/carbon anode for lithium ion batteries. Nano Lett 2012;12:1624–32. https://doi.org/10.1021/nl204559u.
[178] Sacci RL, Dudney NJ, More KL, Parent LR, Arslan I, Browning ND, et al. Direct visualization of initial SEI morphology and growth kinetics during lithium deposition by in situ electrochemical transmission electron microscopy. Chem Commun 2014;50:2104–7. https://doi.org/10.1039/c3cc49029g.
[179] Bhattacharyya R, Key B, Chen H, Best AS, Hollenkamp AF, Grey CP. In situ NMR observation of the formation of metallic lithium microstructures in lithium batteries. Nat Mater 2010;9:504–10. https://doi.org/10.1038/nmat2764.
[180] Cheng H, Zhu CB, Lu M, Yang Y. In situ micro-FTIR study of the solid-solid interface between lithium electrode and polymer electrolytes. J Power Sources 2007;174:1027–31. https://doi.org/10.1016/j.jpowsour.2007.06.213.
[181] Takahara H, Kojyo A, Kodama K, Nakamura T, Shono K, Kobayashi Y, et al. Depth profiling of graphite electrode in lithium ion battery using glow discharge optical emission spectroscopy with small quantities of hydrogen or oxygen addition to argon. J Anal At Spectrom 2014;29:95–104. https://doi.org/10.1039/c3ja50183c.
[182] Schweikert N, Hahn H, Indris S. Cycling behaviour of Li/Li4Ti5O12 cells studied by electrochemical impedance spectroscopy. Phys Chem Chem Phys 2011;13:6234–40. https://doi.org/10.1039/c0cp01889a.
[183] Fernández Pulido Y, Blanco C, Anseán D, García VM, Ferrero F, Valledor M. Determination of suitable parameters for battery analysis by Electrochemical Impedance Spectroscopy. Meas J Int Meas Confed 2017;106:1–11. https://doi.org/10.1016/j.measurement.2017.04.022.
[184] Al Nazer R, Cattin V, Granjon P, Montaru M, Ranieri M. Broadband identification of battery electrical impedance for HEVs. IEEE Trans Veh Technol 2013;62:2896–905. https://doi.org/10.1109/TVT.2013.2254140.
[185] Bitzer B, Gruhle A. A new method for detecting lithium plating by measuring the cell thickness. J Power Sources 2014;262:297–302. https://doi.org/10.1016/j.jpowsour.2014.03.142.
[186] Bauer M, Wachtler M, Stöwe H, Persson JV, Danzer MA. Understanding the dilation and dilation relaxation behavior of graphite-based lithium-ion cells. J Power Sources 2016;317:93–102. https://doi.org/10.1016/j.jpowsour.2016.03.078.
[187] Grimsmann F, Gerbert T, Brauchle F, Gruhle A, Parisi J, Knipper M. Determining the maximum charging currents of lithium-ion cells for small charge quantities. J Power Sources 2017;365:12–6. https://doi.org/10.1016/j.jpowsour.2017.08.044.
[188] Liu QQ, Xiong DJ, Petibon R, Du CY, Dahn JR. Gas Evolution during Unwanted Lithium Plating in Li-Ion Cells with EC-Based or EC-Free Electrolytes. J OfThe Electrochem Soc 2016;163:A3010–5. https://doi.org/10.1149/2.0711614jes.
[189] Bommier C, Chang W, Li J, Biswas S, Davies G, Nanda J, et al. Operando Acoustic Monitoring of SEI Formation and Long-Term Cycling in NMC /SiGr Composite Pouch Cells Operando Acoustic Monitoring of SEI Formation and Long-Term Cycling in NMC / SiGr Composite Pouch Cells 2020. https://doi.org/10.1149/1945-7111/ab68d6.
[190] Davies G, Soc JE, Davies G, Knehr KW, Van Tassell B, Hodson T, et al. State of Charge and State of Health Estimation Using Electrochemical Acoustic Time of Flight Analysis. J OfThe Electrochem Soc 2017;164:A2746–55. https://doi.org/10.1149/2.1411712jes.
[191] Gold L, Bach T, Virsik W, Schmitt A, Müller J, Staab TEM, et al. Probing lithium-ion batteries ' state-of-charge using ultrasonic transmission e Concept and laboratory testing. J Power Sources 2017;343:536–44. https://doi.org/10.1016/j.jpowsour.2017.01.090.
[192] Hsieh AG, Bhadra S, Hertzberg BJ, Gjeltema PJ, Goy A, Fleischer JW, et al. Environmental Science Electrochemical-acoustic time of flight : in operando correlation of physical dynamics with battery charge and health † 2015:1569–77. https://doi.org/10.1039/c5ee00111k.
[193] Wu Y, Wang Y, Yung WKC, Pecht M. Ultrasonic Health Monitoring of Lithium-Ion Batteries. Electron 2019;8. https://doi.org/doi:10.3390/electronics8070751.
[194] Bommier C, Williams M, Chang W, Lu Y, Yeung J, Davies G, et al. In Operando Acoustic Detection of Lithium Metal Plating in Commercial LiCoO2/Graphite Pouch Cells. Cell Reports Phys Sci 2020;1:100035. https://doi.org/10.1016/j.xcrp.2020.100035.
[195] Konz ZM, McShane EJ, McCloskey BD. Detecting the Onset of Lithium Plating and Monitoring Fast Charging Performance with Voltage Relaxation. ACS Energy Lett 2020;5:1750–7. https://doi.org/10.1021/acsenergylett.0c00831.
[196] Belt JR, Bernardi DM, Utgikar V. Development and Use of a lithium-metal reference electrode in aging studies of lithium-ion batteries. J Electrochem Soc 2014;161:1116–26. https://doi.org/10.1149/2.062406jes.
[197] Raccichini R, Amores M, Hinds G. Critical review of the use of reference electrodes in li-ion batteries: A diagnostic perspective. Batteries 2019;5:1–24. https://doi.org/10.3390/batteries5010012.
[198] Ge H, Huang J, Zhang J, Li Z. Temperature-adaptive alternating current preheating of lithium-ion batteries with lithium deposition prevention. J Electrochem Soc 2016;163:A290–9. https://doi.org/10.1149/2.0961602jes.
[199] Harting N, Wolff N, Krewer U. Identification of Lithium Plating in Lithium-Ion Batteries using Nonlinear Frequency Response Analysis (NFRA). Electrochim Acta 2018;281:378–85. https://doi.org/10.1016/j.electacta.2018.05.139.
[200] Pastor-Fernández C, Yu TF, Widanage WD, Marco J. Critical review of non-invasive diagnosis techniques for quantification of degradation modes in lithium-ion batteries. Renew Sustain Energy Rev 2019;109:138–59. https://doi.org/10.1016/j.rser.2019.03.060.
[201] Berecibar M, Omar N, Garmendia M, Villarreal I, Van Den Bossche P, Van Mierlo J, et al. SOH Estimation and Prediction for NMC Cells Based on Degradation Mechanism Detection. In: 2015 IEEE Veh Power Propuls Conf VPPC 2015 - Proc; 2015. https://doi.org/10.1109/VPPC.2015.7353020.
[202] Lin X, Hao X, Ivanco A, Liu Z, Jia W. Physics-based and control-oriented modeling of diffusion-induced stress in Li-ion batteries. J Electrochem Soc 2018;165:A2255–66. https://doi.org/10.1149/2.0971810jes.
[203] Tomasov M, Kajanova M, Bracinik P, Motyka D. Overview of battery models for sustainable power and transport applications. Transp Res Procedia 2019;40:548–55. https://doi.org/10.1016/j.trpro.2019.07.079.
[204] Doyle M, Fuller T, Newman J. Modeling of galvanostatic charge and discharge of the lithium/polymer/insertion cell. J Electrochem Soc 1993;140:1526–33. https://doi.org/10.1149/1.2221597.
[205] Lin X. Real-Time Prediction of Anode Potential in Li-Ion Batteries Using Long Short-Term Neural Networks for Lithium Plating Prevention. J Electrochem Soc 2019;166:A1893–904. https://doi.org/10.1149/2.0621910jes.
[206] Tippmann S, Walper D, Balboa L, Spier B, Bessler WG. Low-temperature charging of lithium-ion cells part I: Electrochemical modeling and experimental investigation of degradation behavior. J Power Sources 2014;252:305–16. https://doi.org/10.1016/j.jpowsour.2013.12.022.
[207] Tang M, Albertus P, Newman J. Two-dimensional modeling of lithium deposition during cell charging. J Electrochem Soc 2009;156. https://doi.org/10.1149/1.3095513.
[208] Boovaragavan V, Harinipriya S, Subramanian VR. Towards real-time (milliseconds) parameter estimation of lithium-ion batteries using reformulated physics-based models. J Power Sources 2008;183:361–5. https://doi.org/10.1016/j.jpowsour.2008.04.077.
[209] Perkins RD, Randall AV, Zhang X, Plett GL. Controls oriented reduced order modeling of lithium deposition on overcharge. J Power Sources 2012;209:318–25. https://doi.org/10.1016/j.jpowsour.2012.03.003.
[210] Yang XG, Leng Y, Zhang G, Ge S, Wang CY. Modeling of lithium plating induced aging of lithium-ion batteries: Transition from linear to nonlinear aging. J Power Sources 2017;360:28–40. https://doi.org/10.1016/j.jpowsour.2017.05.110.
[211] Zhang SS. Reformulation of Electrolyte for Enhanced Fast-Charge Capability of Li-Ion Battery. J Electrochem Soc 2020;167:060527. https://doi.org/10.1149/1945-7111/ab84fd.
[212] Purushothaman BK, Landau U. Rapid charging of lithium-ion batteries using pulsed currents. J Electrochem Soc 2006;153. https://doi.org/10.1149/1.2161580.
[213] Cheng Q, Yuge R, Nakahara K, Tamura N, Miyamoto S. KOH etched graphite for fast chargeable lithium-ion batteries. J Power Sources 2015;284:258–63. https://doi.org/10.1016/j.jpowsour.2015.03.036.
[214] Liu Y, Zhu Y, Cui Y. Challenges and opportunities towards fast-charging battery materials. Nat Energy 2019;4:540–50. https://doi.org/10.1038/s41560-019-0405-3.
[215] Habedank JB, Kriegler J, Zaeh MF. Enhanced Fast Charging and Reduced Lithium-Plating by Laser-Structured Anodes for Lithium-Ion Batteries. J Electrochem Soc 2019;166:A3940–9. https://doi.org/10.1149/2.1241915jes.
[216] Park G, Gunawardhana N, Nakamura H, Lee YS, Yoshio M. The study of electrochemical properties and lithium deposition of graphite at low temperature. J Power Sources 2012;199:293–9. https://doi.org/10.1016/j.jpowsour.2011.10.058.
[217] Kim N, Chae S, Ma J, Ko M, Cho J. Fast-charging high-energy lithium-ion batteries via implantation of amorphous silicon nanolayer in edge-plane activated graphite anodes. Nat Commun 2017;8. https://doi.org/10.1038/s41467-017-00973-y.
[218] Kraft L, Habedank JB, Frank A, Rheinfeld A, Jossen A. Modeling and Simulation of Pore Morphology Modifications using Laser-Structured Graphite Anodes in Lithium-Ion Batteries. J Electrochem Soc 2020;167:013506. https://doi.org/10.1149/2.0062001jes.
[219] Logan ER, Tonita EM, Gering KL, Li J, Ma X, Beaulieu LY, et al. A Study of the Physical Properties of Li-Ion Battery Electrolytes Containing Esters. J Electrochem Soc 2018;165:A21–30. https://doi.org/10.1149/2.0271802jes.
[220] Ma X, Arumugam RS, Ma L, Logan E, Tonita E, Xia J, et al. A Study of Three Ester Co-Solvents in Lithium-Ion Cells. J Electrochem Soc 2017;164:A3556–62. https://doi.org/10.1149/2.0411714jes.
[221] Hall DS, Eldesoky A, Logan ER, Tonita EM, Ma X, Dahn JR. Exploring Classes of Co-Solvents for Fast-Charging Lithium-Ion Cells. J Electrochem Soc 2018;165:A2365–73. https://doi.org/10.1149/2.1351810jes.
[222] Diederichsen KM, McShane EJ, McCloskey BD. Promising Routes to a High Li+ Transference Number Electrolyte for Lithium Ion Batteries. ACS Energy Lett 2017;2:2563–75. https://doi.org/10.1021/acsenergylett.7b00792.
[223] Popovic J, Höfler D, Melchior JP, Münchinger A, List B, Maier J. High Lithium Transference Number Electrolytes Containing Tetratriflylpropene's Lithium Salt. J Phys Chem Lett 2018;9:5116–20. https://doi.org/10.1021/acs.jpclett.8b01846.
[224] Berhaut CL, Porion P, Timperman L, Schmidt G, Lemordant D, Anouti M. LiTDI as electrolyte salt for Li-ion batteries: Transport properties in EC/DMC. Electrochim Acta 2015;180:778–87. https://doi.org/10.1016/j.electacta.2015.08.165.
[225] Fong KD, Self J, Diederichsen KM, Wood BM, McCloskey BD, Persson KA. Ion Transport and the True Transference Number in Nonaqueous Polyelectrolyte Solutions for Lithium Ion Batteries. ACS Cent Sci 2019;5:1250–60. https://doi.org/10.1021/acscentsci.9b00406.
[226] Buss HG, Chan SY, Lynd NA, McCloskey BD. Nonaqueous Polyelectrolyte Solutions as Liquid Electrolytes with High Lithium Ion Transference Number and Conductivity. ACS Energy Lett 2017;2:481–7. https://doi.org/10.1021/acsenergylett.6b00724.

[227] Du Z, Wood DL, Belharouak I. Enabling fast charging of high energy density Li-ion cells with high lithium ion transport electrolytes. Electrochem Commun 2019; 103:109–13. https://doi.org/10.1016/j.elecom.2019.04.013.
[228] Liu QQ, Petibon R, Du CY, Dahn JR. Effects of electrolyte additives and solvents on unwanted lithium plating in lithium-ion cells. J Electrochem Soc 2017;164: A1173–83. https://doi.org/10.1149/2.1081706jes.
[229] Liu QQ, Ma L, Du CY, Dahn JR. Effects of the LiPO2F2 additive on unwanted lithium plating in lithium-ion cells. Electrochim Acta 2018;263:237–48. https://doi.org/10.1016/j.electacta.2018.01.058.
[230] Jones J-P, Smart MC, Krause FC, Bugga R V. The Effect of Electrolyte Additives upon Lithium Plating during Low Temperature Charging of Graphite-LiNiCoAlO 2 Lithium-Ion Three Electrode Cells. J Electrochem Soc 2020;167:020536. https://doi.org/10.1149/1945-7111/ab6bc2.
[231] Colclasure AM, Dunlop AR, Trask SE, Polzin BJ, Jansen AN, Smith K. Requirements for Enabling Extreme Fast Charging of High Energy Density Li-Ion Cells while Avoiding Lithium Plating. J Electrochem Soc 2019;166:A1412–24. https://doi.org/10.1149/2.0451908jes.
[232] Liu H, Zhang S, Zhu Q, Cao B, Zhang P, Sun N, et al. Fluffy carbon-coated red phosphorus as a highly stable and high-rate anode for lithium-ion batteries. J Mater Chem A 2019;7:11205–13. https://doi.org/10.1039/c9ta02030f.
[233] Kim CS, Jeong KM, Kim K, Yi CW. Effects of capacity ratios between anode and cathode on electrochemical properties for lithium polymer batteries. Electrochim Acta 2015;155:431–6. https://doi.org/10.1016/j.electacta.2014.12.005.
[234] Banguero E, Correcher A, Pérez-Navarro Á, Morant F, Aristizabal A. A review on battery charging and discharging control strategies: Application to renewable energy systems. Energies 2018;11:1–15. https://doi.org/10.3390/en11041021.
[235] Gao Y, Member S, Zhang XI, Member S, Cheng Q. Classification and Review of the Charging Strategies for Commercial Lithium-Ion Batteries. IEEE Access 2019;7: 43511–24. https://doi.org/10.1109/ACCESS.2019.2906117.
[236] Arabsalmanabadi B, Tashakor N, Javadi A, Al-Haddad K. Charging Techniques in Lithium-ion Battery Charger: Review and New Solution. IEEE 2018. https://doi.org/10.1109/IECON.2018.8591173.
[237] Howell David, Boyd Steven, Cunningham Brian, Samm Gillard LS. Enabling Fast Charging : A Technology Gap Assessment. US Dept Energy; 2017. p. 83.
[238] Eberman K, Gomadam PM, Jain G, Scott E. Material and design options for avoiding lithium-plating during charging. ECS Trans 2010;25:47–58. https://doi.org/10.1149/1.3414003. p.
[239] Choi SS, Lim HS. Factors that affect cycle-life and possible degradation mechanisms of a Li-ion cell based on. LiCoO 2 2002;111:130–6.
[240] Zhang SS, Xu K, Jow TR. Study of the charging process of a LiCoO2-based Li-ion battery. J Power Sources 2006;160:1349–54. https://doi.org/10.1016/j.jpowsour.2006.02.087.
[241] Anseán D, González M, Viera JC, García VM, Blanco C, Valledor M. Fast charging technique for high power lithium iron phosphate batteries : A cycle life analysis. J Power Sources 2013;239:9–15. https://doi.org/10.1016/j.jpowsour.2013.03.044.
[242] Luo Y, Wang S. Search for an Optimal Multistage Charging Pattern for Lithium-Ion Batteries Using the Taguchi Approach. In: TENCON 2009 - 2009 IEEE Reg 10 Conf; 2009. p. 1–5. https://doi.org/10.1109/TENCON.2009.5395823.
[243] Zhang SS. The effect of the charging protocol on the cycle life of a Li-ion battery. J Power Sources 2006;161:1385–91. https://doi.org/10.1016/j.jpowsour.2006.06.040.
[244] Amanor-Boadu JM, Guiseppi-Elie A, Sánchez-Sinencio E. The impact of pulse charging parameters on the life cycle of lithium-ion polymer batteries. Energies 2018;11:1–15. https://doi.org/10.3390/en11082162.
[245] Hasan MF, Chen C, Shaffer CE, Mukherjee PP. Analysis of the Implications of Rapid Charging on Lithium-Ion Battery Performance 2015;162:1382–95. https://doi.org/10.1149/2.0871507jes.
[246] Aryanfar A, Brooks D, Merinov B V, Goddard WA, Colussi AJ, Hoffmann MR. Dynamics of Lithium Dendrite Growth and Inhibition : Pulse Charging. J Phys Chem Lett 2014;5:1721–6.
[247] Notten PHL, Op JHG, Beek JRG Van. Boostcharging Li-ion batteries : A challenging new charging concept 2005;145:89–94. https://doi.org/10.1016/j.jpowsour.2004.12.038.
[248] Mussa AS, Klett M, Behm M, Lindbergh G, Lindström RW. Fast-charging to a partial state of charge in lithium-ion batteries: A comparative ageing study. J Energy Storage 2017;13:325–33. https://doi.org/10.1016/j.est.2017.07.004.
[249] Li W, Erickson EM, Manthiram A. High-nickel layered oxide cathodes for lithium-based automotive batteries. Nat Energy 2020;12. https://doi.org/10.1038/s41560-019-0513-0.
[250] Lemon C, Booklet L, S U. OWNER'S MANUAL For your safety, read carefully and keep in this vehicle. 2010.
[251] Tu H, Feng H, Srdic S, Lukic S. Extreme Fast Charging of Electric Vehicles: A Technology Overview. IEEE Trans Transp Electrif 2019;5:861–78. https://doi.org/10.1109/TTE.2019.2958709.
[252] Tesla increases Model S and X Supercharging rate to 225 kW - Electrek n.d. https://electrek.co/2020/06/24/tesla-model-s-x-supercharging-rate-increase-225-kw/(accessed July 19, 2020).
[253] Porsche installs first 350 kW ultra-rapids in Berlin - Zap-Map 2020. https://www.zap-map.com/porsche-installs-first-350-kw-ultra-rapids-in-berlin/(accessed July 19, 2020).
[254] The charging process: Quick, comfortable, intelligent and universal 2020. https://newsroom.porsche.com/en/products/taycan/charging-18558.html (accessed July 19, 2020).
[255] XCEL : eXtreme Fast Charge Cell Evaluation of Lithium-ion Batteries Report Period : July – September 2019. 2019.
[256] Hayes JG, Goodarzi AG. Electric Powertrain: Energy Systems, Power Electronics and Drives for Hybrid, Electric and Fuel Cell Vehicles. Wiley; 2018.
[257] Tanim TR, Shirk MG, Bewley RL, Dufek EJ, Liaw BY. Fast charge implications: Pack and cell analysis and comparison. J Power Sources 2018;381:56–65. https://doi.org/10.1016/j.jpowsour.2018.01.091.
[258] Zou C, Hu X, Wei Z. Electrochemical Estimation and Control for Lithium-Ion Battery Health-Aware Fast Charging. IEEE Trans Ind Electron 2018;65:6635–45. https://doi.org/10.1109/TIE.2017.2772154.
[259] Song M, Choe SY. Fast and safe charging method suppressing side reaction and lithium deposition reaction in lithium ion battery. J Power Sources 2019;436: 226835. https://doi.org/10.1016/j.jpowsour.2019.226835.
[260] Chu Z, Feng X, Lu L, Li J, Han X, Ouyang M. Non-destructive fast charging algorithm of lithium-ion batteries based on the control-oriented electrochemical model. Appl Energy 2017;204:1240–50. https://doi.org/10.1016/j.apenergy.2017.03.111.
[261] Lin X, Hao X, Liu Z, Jia W. Health conscious fast charging of Li-ion batteries via a single particle model with aging mechanisms. J Power Sources 2018;400:305–16. https://doi.org/10.1016/j.jpowsour.2018.08.030.
[262] Spingler FB, Wittmann W, Sturm J, Rieger B, Jossen A. Optimum fast charging of lithium-ion pouch cells based on local volume expansion criteria. J Power Sources 2018;393:152–60. https://doi.org/10.1016/j.jpowsour.2018.04.095.
[263] Zhao H, Wang L, Chen Z, He X. Challenges of Fast Charging for Electric Vehicles and the Role of Red Phosphorus as Anode Material : Review 2019. https://doi.org/10.3390/en12203897.
[264] Shevtsov S, Chang S. ScienceDirect Modeling of vibration energy harvesting system with power PZT stack loaded on Li-Ion battery. Int J Hydrogen Energy 2016;41:12618–25. https://doi.org/10.1016/j.ijhydene.2016.03.183.
[265] Dubarry M, Baure G. Perspective on commercial Li-ion battery testing, best practices for simple and effective protocols. Electron 2020;9. https://doi.org/10.3390/electronics9010152.
[266] Taylor J, Barai A, Ashwin TR, Guo Y, Amor-Segan M, Marco J. An insight into the errors and uncertainty of the lithium-ion battery characterisation experiments. J Energy Storage 2019;24:100761. https://doi.org/10.1016/j.est.2019.100761.
[267] Zhang L. applied sciences Effects of Vibration on the Electrical Performance of Lithium-Ion Cells Based on Mathematical Statistics 2017. https://doi.org/10.3390/app7080802.
[268] Michael J, Marco J, Henri G, Sylvie J, Williams D. Multi-axis vibration durability testing of lithium ion 18650 NCA cylindrical cells. J Energy Storage 2018;15: 103–23. https://doi.org/10.1016/j.est.2017.11.006.
[269] Somerville L, Hooper JM, Marco J, Mcgordon A, Lyness C, Walker M, et al. Impact of Vibration on the Surface Film of Lithium-Ion Cells. Energies 2017;10:1–12. https://doi.org/10.3390/en10060741.
[270] Schmidt JP, Arnold S, Loges A, Werner D, Wetzel T, Ivers-Tiffée E. Measurement of the internal cell temperature via impedance: Evaluation and application of a new method. J Power Sources 2013;243:110–7. https://doi.org/10.1016/j.jpowsour.2013.06.013.
[271] Ojo O, Lang H, Kim Y, Hu X, Mu B, Lin X. A Neural Network Based Method for Thermal Fault Detection in Lithium-Ion Batteries. IEEE Trans Ind Electron 2021; 68:4068–78. https://doi.org/10.1109/TIE.2020.2984980.
[272] Li Y, Feng X, Ren D, Ouyang M, Lu L, Han X. Thermal Runaway Triggered by Plated Lithium on the Anode after Fast Charging. ACS Appl Mater Interfaces 2019; 11:46839–50. https://doi.org/10.1021/acsami.9b16589.
[273] Carter R, Klein EJ, Kingston TA, Love CT. Detection of Lithium Plating During Thermally Transient Charging of Li-Ion Batteries. Front Energy Res 2019;7:1–12. https://doi.org/10.3389/fenrg.2019.00144.
[274] Dubarry M, Beck D. Big data training data for artificial intelligence-based Li-ion diagnosis and prognosis. J Power Sources 2020;479:228806. https://doi.org/10.1016/j.jpowsour.2020.228806.
[275] Rynne O, Dubarry M, Molson C, Lepage D, Prébé A, Aymé-Perrot D, et al. Designs of experiments for beginners-A quick start guide for application to electrode formulation. Batteries 2019;5. https://doi.org/10.3390/batteries5040072.

Xianke Lin received the BS degree from Zhejiang University, Hangzhou, China, in 2009, and the Ph.D. degree in mechanical engineering from the University of Michigan, Ann Arbor, MI, USA, in 2014. He has extensive industrial experience with Fiat Chrysler Automobiles, Auburn Hills, MI, USA, Mercedes-Benz Research & Development North America, Detroit, MI, USA, and General Motors of Canada, Oshawa, ON, Canada. He is currently an Assistant Professor with the Department of Automotive and Mechatronics Engineering, Ontario Tech University, Oshawa, Canada. His research activities have concentrated on hybrid powertrain design and control strategy optimization, multiscale/multiphysics modeling, and optimization of energy storage systems.

Kavian Khosravinia received the BS degree in automotive engineering from Azad University of Khomeinishahr, Iran in 2012. And Master of Science in Automotive Engineering in University Putra Malaysia in 2018. He is currently pursuing the Ph.D. degree in automotive engineering at Ontario Tech University. His research interests include battery degradation modeling and fast charging technologies.

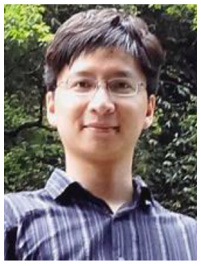

Xiaosong Hu received the Ph.D. degree in automotive engineering from Beijing Institute of Technology, China, in 2012. He did scientific research and completed the Ph.D. dissertation in Automotive Research Center at the University of Michigan, Ann Arbor, USA, between 2010 and 2012. He is currently a Professor at the State Key Laboratory of Mechanical Transmissions and at the Department of Automotive Engineering, Chongqing University, Chongqing, China. He was a postdoctoral researcher at the Department of Civil and Environmental Engineering, University of California, Berkeley, USA, between 2014 and 2015, as well as at the Swedish Hybrid Vehicle Center and the Department of Signals and Systems at Chalmers University of Technology, Gothenburg, Sweden, between 2012 and 2014. He was also a visiting postdoctoral researcher in the Institute for Dynamic systems and Control at Swiss Federal Institute of Technology, Zurich, Switzerland, in 2014. His research interests include battery management technologies and modeling and controls of electrified vehicles. He has been a recipient of several prestigious awards/honors, including SAE Ralph Teetor Educational Award in 2019, Emerging Sustainability Leaders Award in 2016, EU Marie Currie Fellowship in 2015, ASME DSCD Energy Systems Best Paper Award in 2015, and Beijing Best Ph.D. Dissertation Award in 2013.

Ju Li received the BS degree in Physics from the University of Science and Technology of China in 1994, and the Ph.D. degree in nuclear engineering from the Massachusetts Institute of Technology, USA, in 2000. He is currently the Battelle Energy Alliance Professor of Nuclear Science and Engineering at Massachusetts Institute of Technology. He has received TMS Robert Lansing Hardy Award and MRS Outstanding Young Investigator Award. A highly cited expert in his field, he is also a Fellow of the Materials Research Society and American Physical Society.

Wei Lu received his Ph.D. from the Mechanical and Aerospace Engineering Department, Princeton University, and joined the faculty of Mechanical Engineering Department, the University of Michigan in 2001. He received his BS from Tsinghua University, China. His research interests include energy storage and electrochemistry; simulation of nano/microstructure evolution; mechanics in nano/micro systems; advanced manufacturing; mechanical properties and performance of advanced materials and relation to microstructures. Prof. Lu was the recipient of many prestigious awards including the CAREER award by the US National Science Foundation, the Robert J. McGrattan Award by the American Society of Mechanical Engineers, Elected Fellow of the American Society of Mechanical Engineers, Robert M. Caddell Memorial Research Achievement Award, Faculty Recognition Award, Department Achievement Award, Distinguished Professor Award, Novelis and College of Engineering, Ted Kennedy Family Faculty Team Excellence Award, CoE George J. Huebner, Jr. Research Excellence Award, and the Gustus L Larson Memorial Award by the American Society of Mechanical Engineers. He was invited to the National Academies Keck Futures Initiative Conference multiple times.